

SANDIA REPORT

SAND2004-1163
Unlimited Release
Printed March 2004

Optimization of the Lead Probe Neutron Detector

Alan J. Nelson, Carlos L. Ruiz, Gary W. Cooper, James K. Franklin, Lee Ziegler

Prepared by
Sandia National Laboratories
Albuquerque, New Mexico 87185 and Livermore, California 94550

Sandia is a multiprogram laboratory operated by Sandia Corporation, a Lockheed Martin Company, for the United States Department of Energy's National Nuclear Security Administration under Contract DE-AC04-94AL85000.

Approved for public release; further dissemination unlimited.



Issued by Sandia National Laboratories, operated for the United States Department of Energy by Sandia Corporation.

NOTICE: This report was prepared as an account of work sponsored by an agency of the United States Government. Neither the United States Government, nor any agency thereof, nor any of their employees, nor any of their contractors, subcontractors, or their employees, make any warranty, express or implied, or assume any legal liability or responsibility for the accuracy, completeness, or usefulness of any information, apparatus, product, or process disclosed, or represent that its use would not infringe privately owned rights. Reference herein to any specific commercial product, process, or service by trade name, trademark, manufacturer, or otherwise, does not necessarily constitute or imply its endorsement, recommendation, or favoring by the United States Government, any agency thereof, or any of their contractors or subcontractors. The views and opinions expressed herein do not necessarily state or reflect those of the United States Government, any agency thereof, or any of their contractors.

Printed in the United States of America. This report has been reproduced directly from the best available copy.

Available to DOE and DOE contractors from

U.S. Department of Energy
Office of Scientific and Technical Information
P.O. Box 62
Oak Ridge, TN 37831

Telephone: (865)576-8401
Facsimile: (865)576-5728
E-Mail: reports@adonis.osti.gov
Online ordering: <http://www.doe.gov/bridge>

Available to the public from

U.S. Department of Commerce
National Technical Information Service
5285 Port Royal Rd
Springfield, VA 22161

Telephone: (800)553-6847
Facsimile: (703)605-6900
E-Mail: orders@ntis.fedworld.gov
Online order: <http://www.ntis.gov/help/ordermethods.asp?loc=7-4-0#online>



OPTIMIZATION OF THE LEAD PROBE NEUTRON DETECTOR

Alan J. Nelson, Carlos L. Ruiz, and Gary W. Cooper
Diagnostics and Target Physics
Sandia National Laboratories
P.O. Box 5800
Albuquerque, NM 87185-1196

James K. Franklin,
Ktech Corporation
Albuquerque, NM 87185

Lee Ziegler
Bechtel/Nevada
Las Vegas, NV 89030

ABSTRACT

The lead probe neutron detector was originally designed by Spencer and Jacobs in 1965[§]. The detector is based on lead activation due to the following neutron scattering reactions: $^{207}\text{Pb}(n, n')^{207\text{m}}\text{Pb}$ and $^{208}\text{Pb}(n, 2n)^{207\text{m}}\text{Pb}$. Delayed gammas from the metastable state of $^{207\text{m}}\text{Pb}$ are counted using a plastic scintillator. The half-life of $^{207\text{m}}\text{Pb}$ is 0.8 seconds. In the work reported here, MCNP[†] was used to optimize the efficiency of the lead probe by suitably modifying the original geometry. A prototype detector was then built and tested.

A “layer cake” design was investigated in which thin (< 5 mm) layers of lead were sandwiched between thicker (~ 1 – 2 cm) layers of scintillator. An optimized “layer cake” design had Figures of Merit (derived from the code) which were a factor of 3 greater than the original lead probe for DD neutrons, and a factor of 4 greater for DT neutrons, while containing 30% less lead.

A smaller scale, “proof of principle” prototype was built by Bechtel/Nevada to verify the code results. Its response to DD neutrons was measured using the DD dense plasma focus at Texas A&M and it conformed to the predicted performance. A voltage and discriminator sweep was performed to determine optimum sensitivity settings. It was determined that a calibration operating point could be obtained using a ^{133}Ba “bolt” as is the case with the original lead probe.

[§] Spencer, C. E., and Jacobs, E. L., “The lead activation technique for high energy neutron measurement,” IEEE Transactions on Nuclear Science, NS-12, 407 (1965).

[†] Seagraves, D. T., editor, “Practical MCNP for the Health Physicist, Rad Engineer, & Medical Physicist,” Version 4C, Los Alamos National Laboratory, (February 2000).

ACKNOWLEDGEMENTS

This work was originally done by Alan Nelson as a thesis in partial fulfillment of the requirements for the Degree of Master of Science in Nuclear Engineering at the University of New Mexico. It was prepared under the direction of Dr. Gary Cooper, faculty advisor, and Dr. Carlos Ruiz of Sandia National Laboratories. The authors would like to acknowledge Dr. Ray Leeper and Dr. Tom Mehlhorn for providing Sandia National Laboratory support and funding. Also, special thanks go to Dr. Chris Hagen, Steve Molnar, Brent Davis and Irene Garcia of Bechtel/Nevada for constructing and testing the prototype lead “layer cake” neutron detector. Additional thanks go to Dr. Bruce Freeman of Texas A&M University for the availability of the 2.45 MeV DD dense plasma focus neutron calibration source.

TABLE OF CONTENTS

LIST OF FIGURES	7
LIST OF TABLES	9
CHAPTER 1	11
Introduction	11
CHAPTER 2	15
Monte Carlo Modeling	15
Tallies	18
Efficiency	29
CHAPTER 3	32
DT Neutrons	32
CHAPTER 4	37
The Prototype	37
CHAPTER 5	41
Experimental Results	41
Dense Plasma Focus	41
“Face On” Configuration	46
“Edge On” Configuration	48
$1/R^2$ Measurements	50
Calibration	52
Chapter 6	57
Summary	57
Future Work	58

References.....	61
Appendices.....	64
Appendix A.....	65
MCNP Code Listing of Original Lead Probe	65
Part 1: F4 Neutron Tally	65
Part 2: F8 Counts Tally and F6 Energy Deposited Tally	71
MCNP Code Listing of Optimized Layer Cake	77
Part 3: F4 Neutron Tally	77
Part 4: F8 Counts Tally and F6 Energy Deposited Tally	90
Appendix B.....	97
DD Neutron Attenuation in 0.2 cm and 0.3 cm Cases	97
Appendix C.....	101
Layer Cake Prototype Sensitivity Data	101
Appendix D.....	103
Hamamatsu Photomultiplier Tube R1250 Data	103
Appendix E.....	107
BC-400 Scintillator Data	107
Distribution	110

LIST OF FIGURES

Figure 1. Cross-sectional view of the Original Lead Probe	12
Figure 2. Original Lead Probe Modeled with MCNP	15
Figure 3. Lead Probe Divided into Concentric Cylinders (Face Shown)	16
Figure 4. Cross Section Curves for $^{207}\text{Pb}(n, n')^{207\text{m}}\text{Pb}$ and $^{208}\text{Pb}(n, 2n)^{207\text{m}}\text{Pb}$	17
Figure 5. Variation of Neutron Detection Efficiency vs Thickness of Lead Sheath	19
Figure 6. MCNP results of Normalized Figure of Merit vs Lead Thickness compared to Original Lead Probe with 9% Calibration Uncertainty	20
Figure 7. MCNP Model of 8 layers of Scintillator 1 cm thick with 8 layers of lead	22
Figure 8. F4 Tally, F8 Tally and Figure of Merit as a Function of Lead Layer Thickness, for Constant Lead Mass and Scintillator Thickness	23
Figure 9. Radius of Detector vs Lead Layer Thickness for Constant Lead Mass and Scintillator Thickness	24
Figure 10. Normalized Figure of Merit vs Scintillator Thickness for 0.3 cm and 0.2 cm lead layer cases	25
Figure 11. Layer Cake Prototype with 9 layers of lead, 8 layers of scintillator	38
Figure 12. Plate and O-ring on Layer Cake to couple to 12.7 cm (5 in) diameter	39
Figure 13. Completed Layer Cake Detector Assembly: Lead/Scintillator Section Coupled to 12.7 cm (5 in) Hamamatsu Photomultiplier Tube	39
Figure 14. Block Diagram of Layer Cake Prototype Neutron Detector	40
Figure 15. Dense Plasma Focus at Texas A&M; typical neutron yield is $\sim 3.5 \times 10^{10}$ neutrons (based on indium activation) in 100 ns (FWHM); center is marked with yellow tape for alignment purposes.	41

Figure 16. Layer Cake placed on thin metal table (to minimize neutron scattering) on stacked cinderblocks; at this height the detector was aligned to center of DPF	42
Figure 17. Layer Cake with Original Lead Probe beneath it; another lead probe	43
Figure 18. Raw Data taken with Layer Cake on Typical Shot on DPF	44
Figure 19. A Least Squares Fit Performed on Data in Figure 17 to Determine $A(0)$, the Relative Initial Activity per unit Time of the Lead	45
Figure 20. Layer Cake Sensitivity as a Function of Photomultiplier Tube Bias	46
Figure 21. Layer Cake in “Edge On” Configuration to Source	48
Figure 22. Layer Cake Experimental Data, MCNP Calculations and $1/R^2$ Behavior.....	52
Figure 23. Barium Bolt Placed in center of Layer Cake perpendicular to edges of lead and scintillator.....	55
Figure 24. Fixing a position for a Barium Bolt on the Layer Cake in the form of a nut being either epoxied or welded to housing	56

LIST OF TABLES

Table I. $^{207}\text{Pb}(n, n')^{207\text{m}}\text{Pb}$ and $^{208}\text{Pb}(n, 2n)^{207\text{m}}\text{Pb}$ Cross Sections	16
Table II. Mean Free Paths of Gammas and Neutrons in Lead and Scintillator	21
Table III. Lead Layer Thickness vs F4 & F8 Tallies and FOM for Constant Lead Mass of 17.1 kg (37.7 lbs).....	23
Table IV. Comparison between the Original Lead Probe and 0.2 cm and 0.3 cm lead cases	26
Table V. Neutron Reactions per Layer for the 0.2 cm and 0.3 cm lead layer cases	27
Table VI. F8 Tallies for the 0.2 cm and 0.3 cm lead layer cases	28
Table VII. F6 Tallies, Energy Deposited and Efficiencies of Original Lead Probe, and 0.2 cm and 0.3 cm Lead Layer Cases.....	30
Table VIII. Comparison between the Original Lead Probe and 0.2 cm and 0.3 cm lead cases for DT Neutrons (14 MeV)	33
Table IX. Mean Free Paths of 14 MeV neutrons in Lead and Scintillator	34
Table X. Neutron Reactions per Layer for the 0.2 cm and 0.3 cm lead layer cases for DT Neutrons	34
Table XI. F8 Tallies for the 0.2 cm and 0.3 cm lead layer cases for DT Neutrons	35
Table XII. Experimental Data of Layer Cake “Face On” & Original Lead Probe	47
Table XIII. Modeled Layer Cake “Face On” & OLP at 198.12 cm (78 in) from Point Source	47
Table XIV. Experimental Data of Layer Cake “Edge On” & Original Lead Probe	49
Table XV. Modeled Layer Cake “Edge On” & OLP at 198.12 cm (78 in) from Point Source	49

Table XVI. Comparison of Experimental and Modeled Data of the Layer Cake “Face On” to “Edge On” at 198.12 cm (78 in) from Point Source	50
Table XVII. Comparison of Experimental and Calculated Data at 121.92 cm (48 in), 198.12 cm (78 in) and 259.08 cm (102 in).....	51
Table XVIII. Comparison between Original Lead Probe, “Comparable Case” and Optimized Case for DD neutrons	59
Table XIX. Determination of Volumetric Gamma Source Values for Lead Layers	90
Table XX. 0.2 cm Lead Case: F4 Tallies with Scintillator Removed Compared with F4 Tallies with Scintillator Present	97
Table XXI. 0.3 cm Lead Case: F4 Tallies with Scintillator Removed Compared with F4 Tallies with Scintillator Present	98
Table XXII. 0.2 cm Lead Case without Scintillator Compared with 0.3 cm Lead Case without Scintillator	99
Table XXIII. Layer Cake Prototype Sensitivity (in Counts/Incident Neutron) as a Function of Photomultiplier Tube Bias And Discriminator Setting.....	101
Table XXIV. Layer Cake Prototype Sensitivity (in Incident Neutrons/Count) as a Function of Photomultiplier Tube Bias And Discriminator Setting.....	102

CHAPTER 1

Introduction

The lead activation technique has been utilized to measure the yield of pulsed neutron sources for the past 40 years (Ruby and Rechen 1962). It is based on the neutron reactions of $^{207}\text{Pb}(n, n')^{207\text{m}}\text{Pb}$ and $^{208}\text{Pb}(n, 2n)^{207\text{m}}\text{Pb}$ in which delayed gammas from the metastable state of $^{207\text{m}}\text{Pb}$ are counted in a plastic scintillator. The half-life of $^{207\text{m}}\text{Pb}$ is 0.8 seconds. Spencer and Jacobs developed a detector based on this technique in 1965 and called it the “lead probe,” which became a laboratory standard at Sandia National Laboratories for measuring DT neutrons produced via the following Deuterium-Tritium reaction (Spencer and Jacobs 1965):



There are many advantages to using the lead probe for measuring DT neutrons: it has a high sensitivity (1 count per 255 incident neutrons), a low yield detection level of 10^6 neutrons into 4π per pulse, an energy threshold of 1.6 MeV and an accuracy of 10 percent (Spencer and Jacobs 1965). The data is obtained in real time, approximately 3 seconds, and if multi-channel scaling is used, the half-life can be verified to insure the counts represent the “true” signal. A cross-sectional view of the lead probe is shown in Figure 1.

For applications on Sandia National Laboratories’ Z machine (Matzen 1997 and Spielman 1995), where Inertial Confinement Fusion (ICF) experiments are performed using deuterium filled capsules, a detector is needed to measure neutron yields from the reaction:



This detector should have as high a sensitivity as possible to measure the lowest possible

neutron yields. Unfortunately, the lead probe was designed for measuring DT neutrons, and was determined not to be useful for DD pulsed neutron sources which yield less than 2×10^7 neutrons into 4π per pulse (Ruby and Rechen 1967). Therefore, an idea was born that became the subject of this thesis: could one optimize the lead probe in such a way as to increase its sensitivity in detecting DD neutrons without simply increasing the mass of lead? An idea similar to this was thought of by my mentor at Sandia, Dr. Carlos Ruiz,

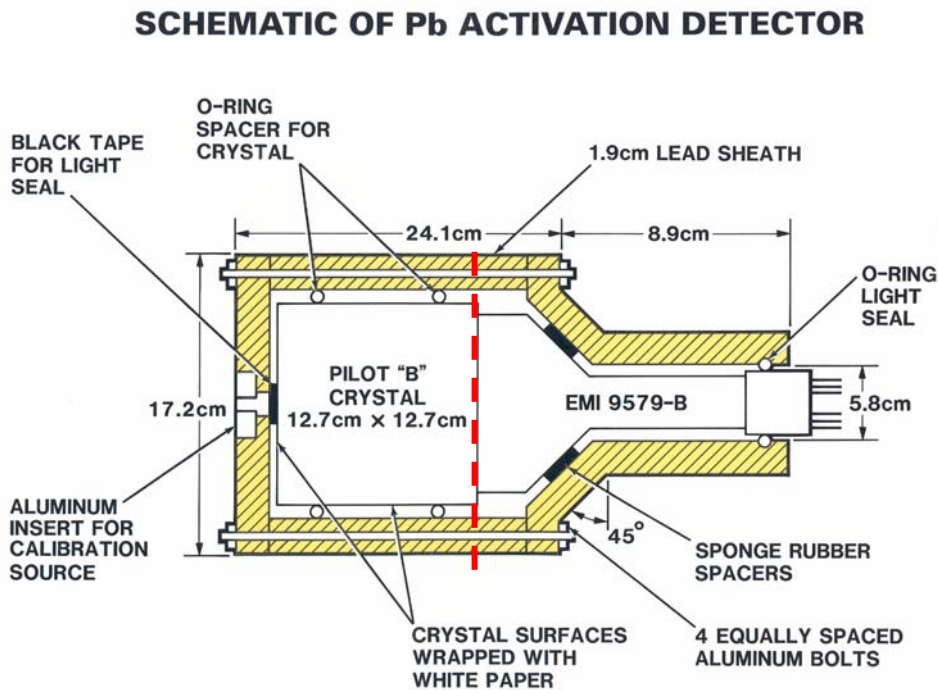


Figure 1. Cross-sectional view of the Original Lead Probe

twenty years ago – that perhaps one could change the geometry of the lead probe by interchanging slices of lead and scintillator to increase its performance. This idea, coupled with the desire to maintain (or reduce, if possible) the overall weight of the detector, became the subject of this thesis.

There was one neutron detector in the literature which was comprised of layers. It consisted of beryllium and scintillator and was based on beryllium activation via the following neutron reaction: ${}^9\text{Be}(n, \alpha){}^6\text{He}$ (Rowland 1984). The ${}^6\text{He}$ decays by beta emission; the beta particle is stopped in the scintillator. It was designed analytically for DT neutrons (14 MeV). A prototype was built and tested. However, until now, no one had tried to design a “layer cake” detector with lead for DD neutrons.

The first step was to model the standard lead probe using MCNP (Monte Carlo Neutron Photon) transport code, version 4C (Seagraves 2000), and then investigate alternative geometries via modeling in an attempt to increase the lead probe’s efficiency. MCNP is a very versatile and powerful transport code, and can model virtually any kind of geometry imaginable. The original designers of the lead probe relied solely on empirical methods. A great advantage of MCNP is that one can vary the geometry of a design many times without having to physically reproduce each change in the laboratory. This saves considerable expense at not having to build and calibrate intermediate designs along the way.

This work presents just such a scenario. MCNP was used to vary the geometry of the prototype – a “layer cake” design was investigated in which layers of scintillator were sandwiched between layers of lead. “Tallies” were generated by the code – a neutron tally denoted the number of neutron reactions per cm^3 of ${}^{207\text{m}}\text{Pb}$ in the lead. A “counts” tally represented pulses generated in the scintillator by the delayed gammas from ${}^{207\text{m}}\text{Pb}$, and an “energy deposited tally” denoted the total amount of energy those gammas deposited in the scintillator. A Figure of Merit was derived from the product of the neutron tally, the counts tally, and the volume of the lead in cm^3 . This gave a point of comparison between different designs modeled with the same code.

Different geometries of the layer cake were run in which varying widths of lead and scintillator were investigated and compared with the original. It was observed that the mean free path of the gammas were extremely short (~ 0.9 cm) in lead compared with that of scintillator (~ 11.7 cm). A layer cake design was investigated in which thin (< 5 mm) layers of lead were sandwiched between thicker ($\sim 1 - 2$ cm) layers of scintillator. The resulting optimized layer cake detector had 8 layers of lead 0.2 cm thick and 8 layers of scintillator 1.1 cm thick, was 30 cm in diameter, and had the same overall weight as the original lead probe. This produced Figures of Merit which were a factor of 3 greater than the original lead probe for DD neutrons, and a factor of 4 greater for DT neutrons.

To verify the code results, a smaller scale, “proof of principle” prototype was then built by Bechtel/Nevada comprising 8 layers of scintillator 1.5875 cm ($5/8$ ”) thick, and 9 layers of lead 0.225 cm (0.0886 in) thick. The particular widths were chosen because they consisted of materials in hand. This geometry was modeled using MCNP and its response to DD neutrons was measured using the DD dense plasma focus neutron source at Texas A&M (Freeman 2001). A voltage and discriminator sweep were performed to determine optimum settings during operation. Conclusions are presented which verify the code results.

CHAPTER 2

Monte Carlo Modeling

As a starting point, the original lead probe was modeled with MCNP. (The MCNP input deck used is presented in Appendix A, as well as the input deck for the final, optimized layer cake design.) It consisted of 37 cells and 16 surfaces. A diagram of the model is shown in Figure 2. It should be noted that the lead probe was modeled from the face of the detector to the back edge of scintillator, and included the surrounding lead sheath (note the dashed red line in Figures 1 and 2). The photomultiplier tube was not included or necessary. The code took into account the neutrons interacting with the lead and scintillator, the gammas produced in the lead from neutron activation, the energy the gammas deposited in the scintillator and the counts produced.

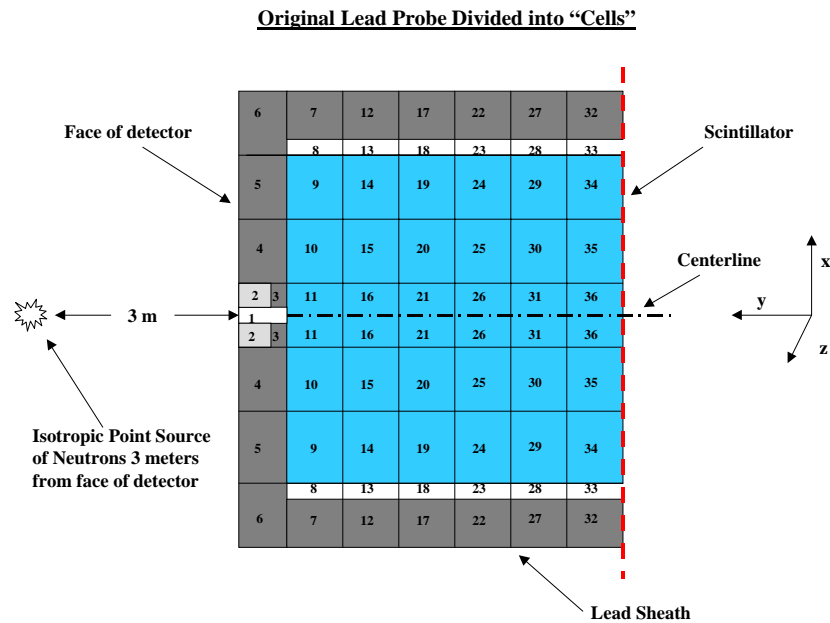


Figure 2. Original Lead Probe Modeled with MCNP

The model was divided into concentric cylinders about the centerline (see Figure

3). Initially, a point source of DD neutrons (2.45 MeV) was placed 3 meters from the

Face of Original Lead Probe Modeled with MCNP

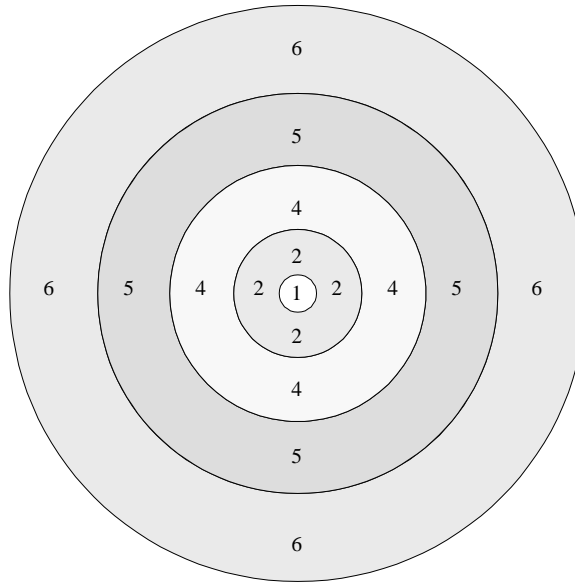


Figure 3. Lead Probe Divided into Concentric Cylinders (Face Shown)

“face” of the lead probe to simulate the distance from a fielded lead probe on the lid of the Z machine to the wire array. Cross sections were input into the code, and were the same as those used by Spencer and Jacobs (Shunk, Wagner and Hemmendinger 1962). The values of the cross sections used are shown in Table I below.

Table I.

$^{207}\text{Pb}(n, n')^{207\text{m}}\text{Pb}$ and $^{208}\text{Pb}(n, 2n)^{207\text{m}}\text{Pb}$ Cross Sections

E_n (MeV)	σ_{207} (mb)	σ_{208} (mb)	E_n (MeV)	σ_{207} (mb)	σ_{208} (mb)
1.8	15.6	...	8.0	905.0	1.8
2.2	68.7	...	9.0	948.8	4.5
3.0	202.4	...	10.0	655.9	173.7
4.0	400.3	...	11.0	476.5	504.2
5.0	749.5	...	14.0	215.7	1313.5
6.0	859.1	...			

Other values of cross sections were found for both reactions (www.nndc.bnl.gov, IAEA 1987) – however, to first order this is a comparison of the layer cake to the lead probe and therefore, as long as the same values were input into each model, an accurate comparison could be made. It was therefore decided to use the original cross sections that Spencer and Jacobs used. A plot of those cross sections are shown in Figure 4.

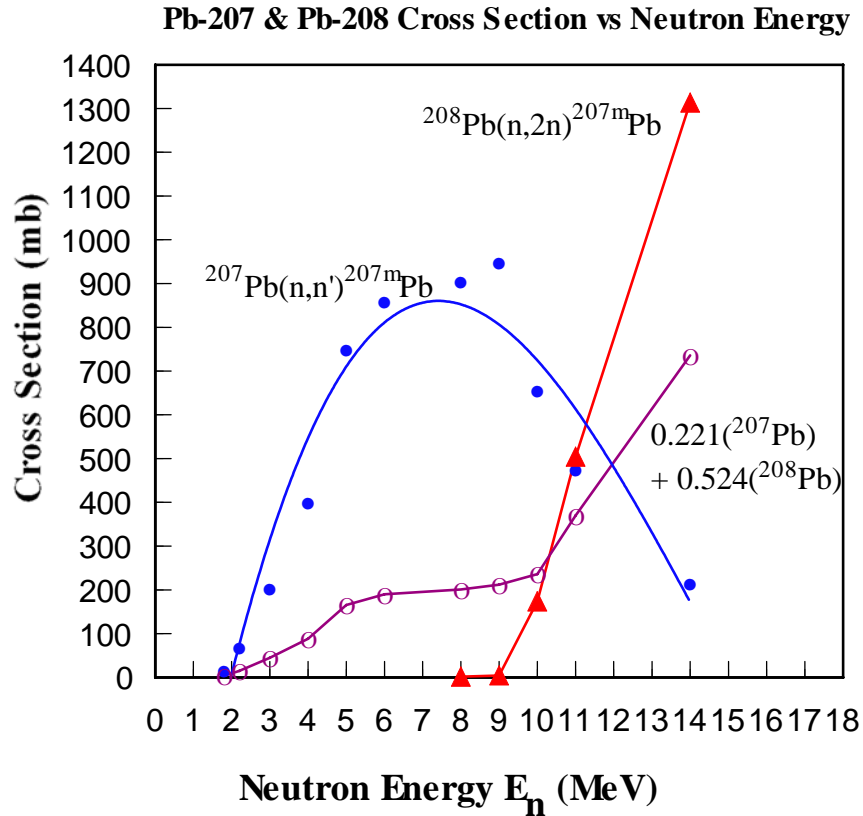


Figure 4. Cross Section Curves for $^{207}\text{Pb}(n, n')^{207m}\text{Pb}$ and $^{208}\text{Pb}(n, 2n)^{207m}\text{Pb}$

The cross sections for the production of ^{207m}Pb are shown for ^{207}Pb (blue curve) and ^{208}Pb (red curve). However, due to the isotopic abundance of both isotopes (natural Lead is comprised of 22.1% and 52.4% of ^{207}Pb and ^{208}Pb , respectively), the purple plot shows the effective cross sections that were used in the calculations. As can be seen, at DD neutron energies (2.45 MeV) the values of the effective cross sections are small

(~ 26.9 mb), while at DT neutron energies (14 MeV) they are a factor of 27 greater (~ 735.9 mb), which makes this particular activation technique more suited for DT pulsed neutron sources. (DT neutrons are discussed in Chapter 3.) However, as will be shown, it can be used successfully for DD pulsed neutron sources as well.

Tallies

The tallies used in the calculations consisted of one neutron tally and two photon tallies. The neutron tally was F4 Cell Fluence in units of $\#/\text{cm}^2$. The effective cross sections (discussed above, and converted to cm^2) as well as the atomic density of lead ($3.296\text{E}10^{22}$ atoms/ cm^3) were folded into the code as a multiplier to the F4 tally. This was necessary to convert the F4 tally into units of neutron reactions/ cm^3 . Thus, fluence ($\#/\text{cm}^2$) times cross section (cm^2) times atomic density (atoms/ cm^3) yield reactions/ cm^3 .

Once this first stage was completed, a second modeling step involved treating the lead in the detector as a volumetric gamma source. The delayed gammas from the metastable state of $^{207\text{m}}\text{Pb}$ have energies of 0.5697 MeV and 1.0636 MeV, with corresponding branching ratios of 52.5% and 47.5%. These values were input into the code, and the gamma case was run. This produced the photon tallies in the scintillator: F6 Energy Deposition (MeV/gm) and F8 Pulse Height (Counts).

A Figure of Merit was derived as the product of the F4 tally (neutron reactions/ cm^3), the F8 tally (counts in the scintillator) and the volume of the lead in cm^3 . The resulting units of the Figure of Merit were: (neutron reactions in the lead) x (counts in the scintillator).

Run times for each case (neutron and photon) were determined by the statistics produced in the output. Due to the fact that the geometry of the design was relatively

simple, long run times were unnecessary. To obtain statistics less than ten percent with a DD point source at 3 meters a run time of 5 minutes was sufficient for the neutron case, which produced ~10 million particle histories. Three minutes was more than adequate for the gamma case, which produced ~ 800,000 particle histories.

Early on, verification was needed to ensure that the output of the code was similar to the actual performance of the original lead probe. Spencer and Jacobs had produced a plot of the relative neutron sensitivity versus thickness of the lead sheath for the original lead probe. They had done this empirically by running four cases in which four different lead sheaths were analyzed, each having a thickness of 1.27 cm, 1.905 cm, 2.54 cm and 3.175cm ($\frac{1}{2}$ ", $\frac{3}{4}$ ", 1", and 1 $\frac{1}{4}$ ") respectively. Their results are shown in Figure 5.

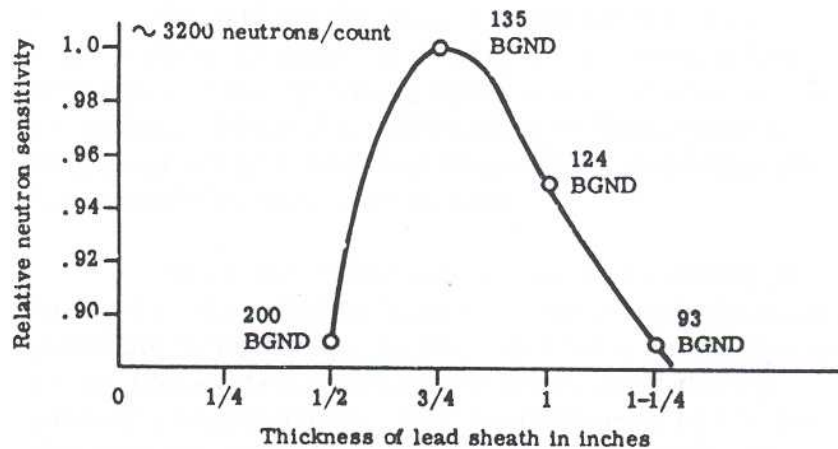


Figure 5. Variation of Neutron Detection Efficiency vs Thickness of Lead Sheath

In an effort to reproduce their data, several cases were run with MCNP in which the thickness of the lead sheath was increased from 1.27 cm to 3.175 cm ($\frac{1}{2}$ " to 1 $\frac{1}{4}$ "), while keeping the volume of the scintillator constant. The results are plotted in Figure 6 and compared with Spencer & Jacobs plot of the original lead probe (Fig. 5) with its 9%

calibration uncertainty (Burns 2003). This good agreement between their data and the MCNP results instilled confidence that other geometries could be modeled that would correctly predict the relative performance of a new detector with respect to the standard lead probe.

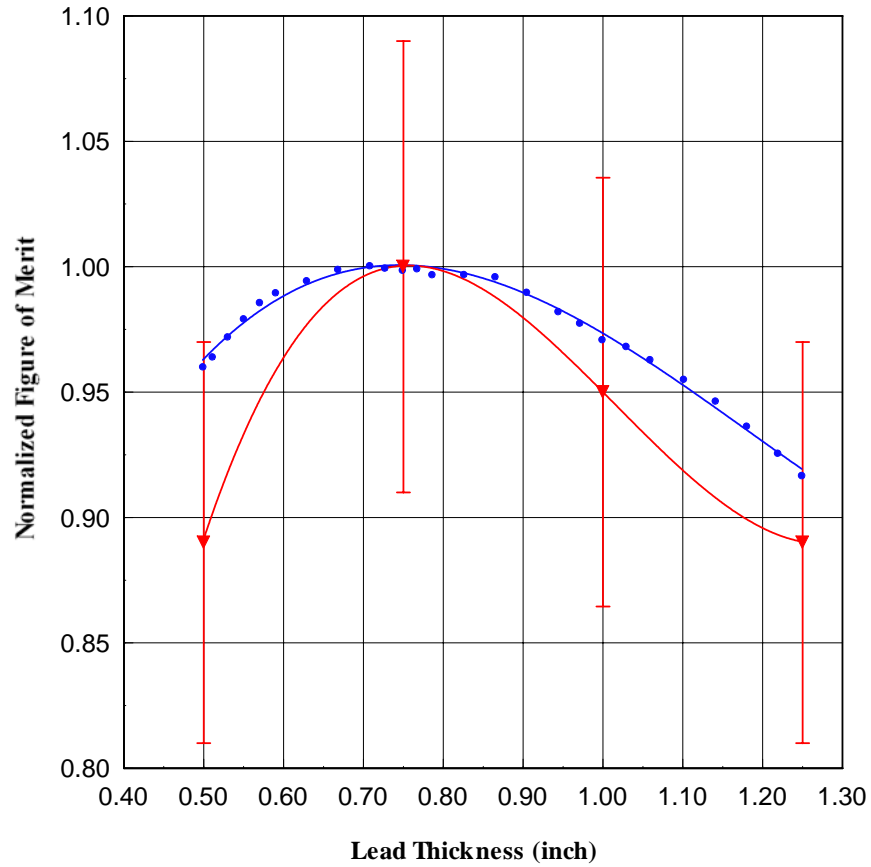


Figure 6. MCNP results of Normalized Figure of Merit vs Lead Thickness compared to Original Lead Probe with 9% Calibration Uncertainty

While running MCNP, it was observed that the delayed gammas from ^{207}mPb had extremely short mean free paths in the lead compared to their mean free paths in the scintillator. However, the mean free paths of the neutrons in the lead were only slightly larger than their mean free paths in the scintillator, as shown below in Table II.

Table II.

Mean Free Paths of Gammas and Neutrons in Lead and Scintillator

	<u>Lead</u>	<u>Scintillator</u>
Gammas	~ 0.9 cm	~ 11.7 cm
Neutrons	~ 4.0 cm	~ 3.5 cm

This presented an interesting problem: the gammas would rather stop in the lead than in the scintillator, and to a lesser degree, the neutrons would rather stop in the scintillator than in the lead. This was the exact opposite of what was desired. However, the most obvious dissimilarity in the table above are the gamma mean free paths, which differ by more than an order of magnitude in the lead and scintillator. This then was the crux upon which the design criteria would be based – if the lead layers were not thin enough, self attenuation would dominate, and the resulting gamma interactions (F8 tally) in the scintillator would decrease. It was therefore decided that the lead layers in any subsequent design would be less than 0.9 cm to maximize gamma output.

An analysis was performed in which 8 layers of lead of a given mass of 17.1 kg (37.7 lbs) were alternated with 8 layers of scintillator with a constant thickness of 1 cm (0.394 in). A diagram of the model is shown in Figure 7. Note that the layers of lead are labeled as “Front Face, A, B, C,” etc., through layer “G”; the layers of scintillator are labeled “1” through “8.” Six different cases were analyzed, from 0.6 cm (0.236 in) lead layers to 0.1 cm (0.0394 in) lead layers, with a corresponding increase in radius for the progressively thinner layers of lead to maintain a constant mass of 17.1 kg (37.7 lbs). A point source was placed 3 meters from the face of the detector in each case. F4 and F8

tallies were generated and a Figure of Merit was calculated for each run. The results are in Table III below.

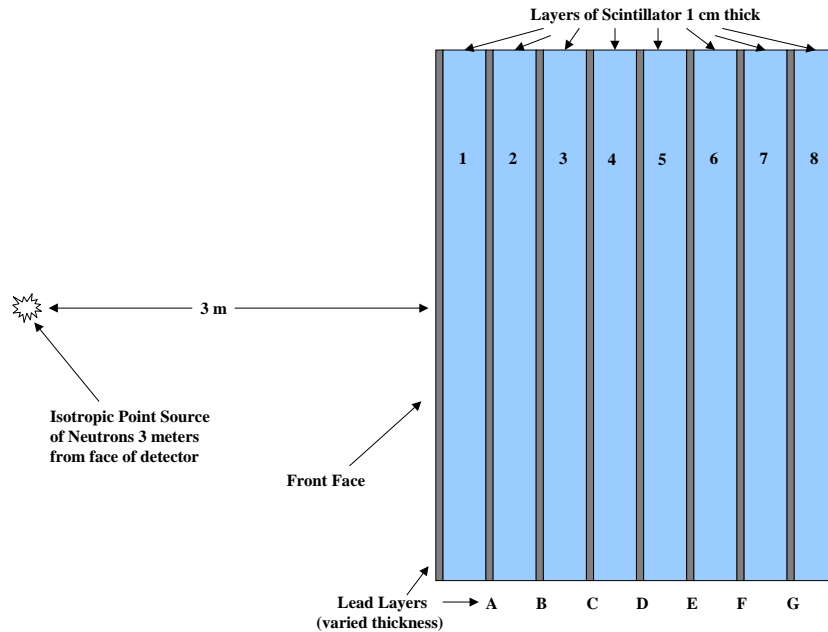


Figure 7. MCNP Model of 8 layers of Scintillator 1 cm thick with 8 layers of lead

As can be seen in Table III, the F4 tallies increase by a modest 7.2 % from a thickness of 0.6 cm (0.236 in) to 0.1 cm (0.0394 in), whereas the largest increases are seen in the F8 tallies and the Figure of Merit. The F8 tallies increase by 187 % from 0.6 cm to 0.1 cm. This is due to two factors: (1) the lead layers are decreasing in thickness, thereby allowing more gammas to escape the lead, and (2) the radius of the detector is increasing, so that more scintillator mass is present to detect the gammas. The Figure of Merit increases by 208 % from 0.6 cm to 0.1 cm – this is primarily due to the increase in the F8 tally. Figure 8 below plots the F4 tally, the F8 tally and the Figure of Merit as a function of lead layer thickness.

Table III.

Lead Layer Thickness vs F4 & F8 Tallies and FOM

for Constant Lead Mass of 17.1 kg (37.7 lbs)

<u>Lead Thickness</u> (cm)	<u>F4 Tally</u> (n reactions/cm ³)	<u>F8 Tally</u> (counts)	<u>Radius</u> (cm)	<u>Figure of Merit</u> (reactions x counts)
0.6	4.72524E-10	0.109192	10	7.7803E-08
0.5	4.84888E-10	0.126695	10.95	9.2635E-08
0.4	4.94024E-10	0.149670	12.25	11.1498E-08
0.3	5.01351E-10	0.183041	14.14	13.8379E-08
0.2	5.01628E-10	0.232290	17.32	17.5707E-08
0.1	5.06483E-10	0.313412	24.49	23.9365E-08

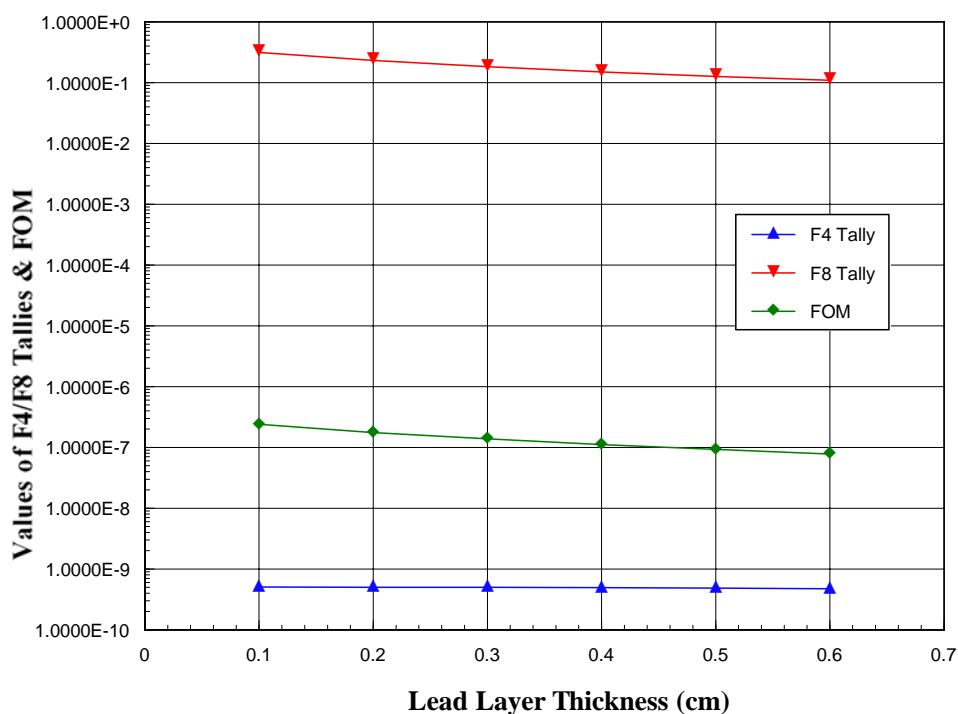


Figure 8. F4 Tally, F8 Tally and Figure of Merit as a Function of Lead Layer Thickness, for Constant Lead Mass and Scintillator Thickness

Figure 9 displays the radius of the detector as a function of the lead layer thickness for the runs described in Table III. What do these figures (8 & 9) reveal? That thinner is better and wider is better for the lead layers. Theoretically, one could keep making the lead layers thinner and wider for a constant lead mass and constant scintillator thickness and the Figure of Merit would steadily increase. However size limitations play a role in practical use, and one must decide how large a detector can ultimately be. For this design, it was decided that a maximum radius of 15 cm (5.9 in) be used for the optimum detector design, giving it a diameter of 30 cm (~1 ft). Anything larger was considered impractical for one person to carry and field by themselves.

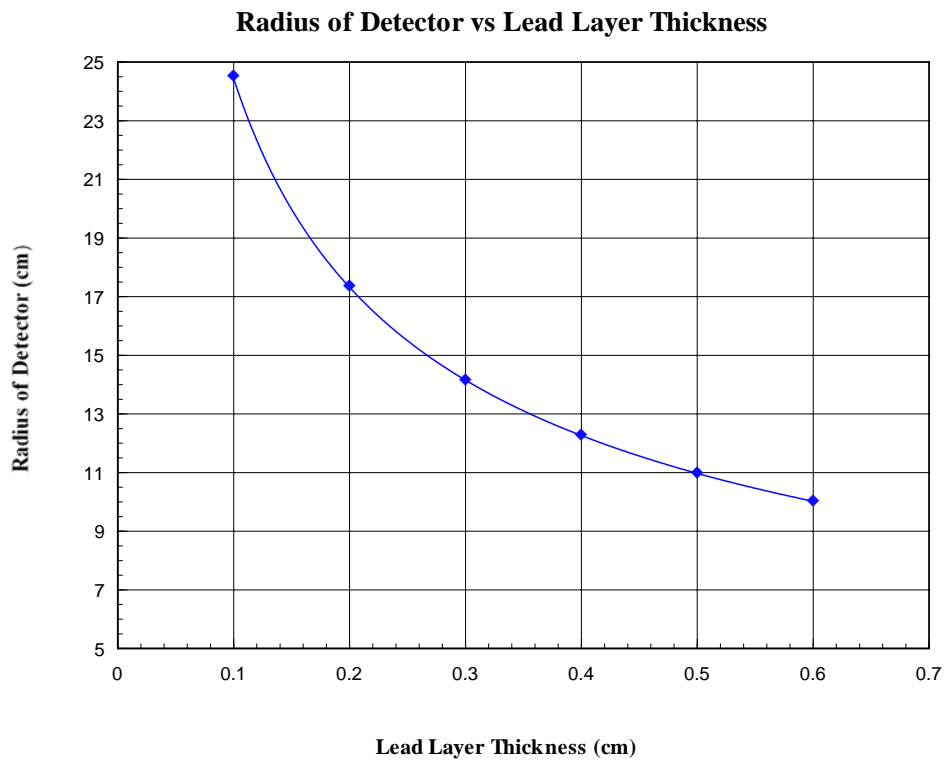


Figure 9. Radius of Detector vs Lead Layer Thickness for Constant Lead Mass and Scintillator Thickness

In looking at Figure 9, the values of lead layer thickness above and below a radius

of 15 cm (5.9 in) are 0.2 cm (0.0787 in) and 0.3 cm (0.118 in), respectively. A series of runs were performed on both these values in which the scintillator thickness was varied, keeping the lead layer thickness and radius constant, in order to find the thickness of scintillator which would optimize the Figure of Merit for each case. The results for both the 0.3 cm and 0.2 cm lead layer cases are shown in Figure 10 below.

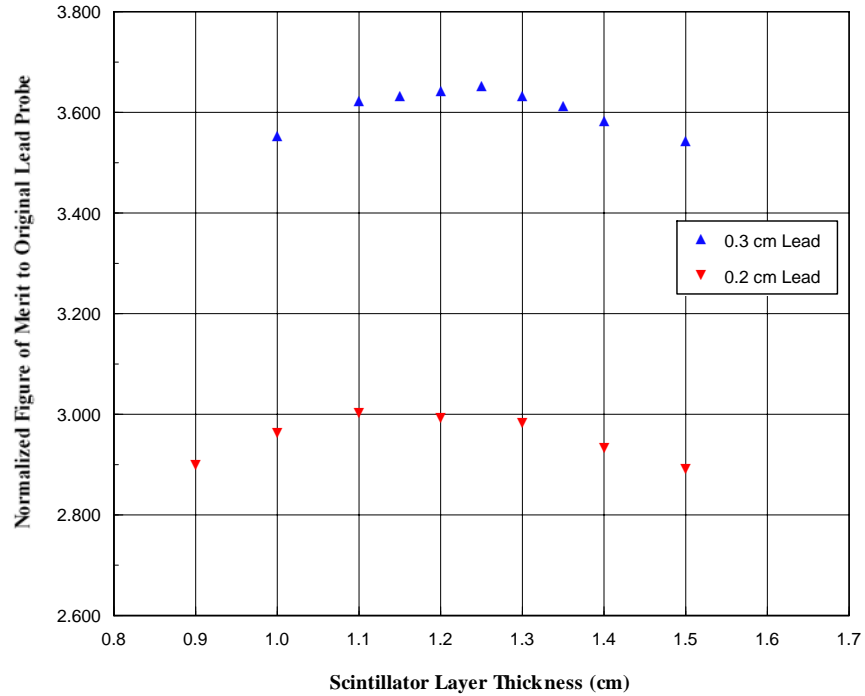


Figure 10. Normalized Figure of Merit vs Scintillator Thickness for 0.3 cm and 0.2 cm lead layer cases

As can be seen in Figure 10, the thickness of scintillator found which would optimize the Figure of Merit in the 0.3 cm lead case was 1.25 cm. This resulted in a Figure of Merit of 3.66 in comparison to the original lead probe. In the 0.2 cm lead case, the thickness of scintillator was found to be 1.1 cm. This optimized the Figure of Merit to a value of 3.0 in comparison to the original lead probe.

The values of the F4 tally, the F8 tally, mass of lead, scintillator, total mass and Figure of Merit are listed in Table IV below for the original lead probe and both the 0.2cm (0.0787 in) and 0.3 cm (0.118 in) lead layer cases, each at their optimized thickness of scintillator. Note that the values in parentheses are normalized to the corresponding values of the original lead probe. As can be seen, the values of the F4 tally drop 4.7% for the 0.2 cm lead case and 11.5% for the 0.3 cm lead case. However, the F8 tallies increase dramatically – 344% for the 0.2 cm case and 290% for the 0.3 cm case.

Table IV.

Comparison between the Original Lead Probe and 0.2 cm and 0.3 cm lead cases

	F4 Tally (reactions/cm³)	F8 Tally (counts)	Mass of Lead	Mass of Plastic	Total Mass	Figure of Merit (reactions x counts)
Original Lead Probe	5.1145E-10 (1.0)	0.053917 (1.0)	18.14 kg (40 lbs)	1.66 kg (3.66 lbs)	19.80 kg (43.66 lbs)	4.41E-08 (1.0)
0.2 cm Lead, 1.1 cm Scintillator	4.8742E-10 (0.953)	0.239599 (4.44)	12.83 kg (28.28 lbs)	6.42 kg (14.15 lbs)	19.25 kg (42.43 lbs)	13.21E-08 (3.0)
0.3 cm Lead, 1.25 cm Scintillator	4.5264E-10 (0.885)	0.210382 (3.90)	19.24 kg (42.42 lbs)	7.29 kg (16.08 lbs)	26.53 kg (58.48 lbs)	16.15E-08 (3.66)

It is interesting to note in Table IV that the 0.3 cm lead case has 50% more lead than the 0.2 cm lead case, (19.24 kg vs 12.83 kg), but it has 14% fewer counts in the scintillator (0.210832 vs 0.239599). This is due to the fact that the lead layers are 0.1 cm thinner in the 0.2 cm case than in the 0.3 cm case, allowing less self attenuation in the lead, thereby letting more gammas out into the scintillator, and will be shown below. (The mean free paths of gammas in lead are 0.9 cm; see Table II, p. 11.) A comparison of F4 tallies (reactions/cm³) times the volume of each layer (cm³/layer) yielding neutron reactions per layer for both the 0.2 cm and 0.3 cm cases are shown in Table V below.

Table V.

Neutron Reactions per Layer for the 0.2 cm and 0.3 cm lead layer cases

<u>Lead Layers</u>	<u>0.2 cm Lead Layers</u> Neutron Reactions per Layer (x 10 ⁻⁸) (n reactions/cm ³) x (cm ³ /layer)	<u>0.3 cm Lead Layers</u> Neutron Reactions per Layer (x 10 ⁻⁸) (n reactions/cm ³) x (cm ³ /layer)
Front Face	12.30 (100%)	18.95 (100%)
Layer "A"	10.33 (84%)	15.33 (81%)
Layer "B"	8.66 (70%)	12.22 (64%)
Layer "C"	7.05 (57%)	9.59 (51%)
Layer "D"	5.60 (46%)	7.27 (38%)
Layer "E"	4.71 (38%)	5.89 (31%)
Layer "F"	3.67 (30%)	4.38 (23%)
Layer "G"	2.80 (23%)	3.16 (17%)

In looking at Table V, the 0.3 cm lead case has more neutron reactions per layer than the 0.2 cm lead case. (It has thicker layers of lead, and hence more volume per layer.) However, in looking at the values in parenthesis (which are normalized to the front face value in each case), despite being higher, the neutron reactions/layer for the 0.3

cm case fall off slightly faster from the front face to the last layer (“G”). This seems to indicate, that for the 0.3 cm case, with its thicker layers of scintillator 1.25 cm thick, that more neutron attenuation is occurring as the neutrons travel through to the back layers than in the 0.2 cm case. However, neutron attenuation through the layers of scintillator would be more pronounced if the thickness of scintillator approached the neutron mean free path in scintillator (3.5 cm, Table II, p. 11). (See Appendix B for DD neutron attenuation in 0.2 cm and 0.3 cm cases).

From Table V, it is shown that the 0.3 cm case has more neutron reactions per layer. Thus, more ^{207}Pb atoms are being activated and producing delayed gammas in the 0.3 cm lead case. But are they reaching the scintillator to produce counts? A comparison of F8 tallies for the 0.2 cm and 0.3 cm lead layer cases are shown in Table VI below.

Table VI.

F8 Tallies for the 0.2 cm and 0.3 cm lead layer cases

<u>Scintillator Layers</u>	<u>0.2 cm Lead Layers</u> <u>F8 Tallies</u> (Counts in Scintillator)	<u>0.3 cm Lead Layers</u> <u>F8 Tallies</u> (Counts in Scintillator)
Layer 1	0.044364 (> 2%)	0.043284
Layer 2	0.045144 (> 7%)	0.041991
Layer 3	0.041888 (> 12%)	0.037237
Layer 4	0.037103 (> 18%)	0.031344
Layer 5	0.031769 (> 25%)	0.025365
Layer 6	0.025703 (> 29%)	0.019901
Layer 7	0.020006 (> 36%)	0.014687
Layer 8	0.012889 (> 46%)	0.008815

In Table VI, for every layer of scintillator the F8 tallies are greater in the 0.2 cm lead case than in the 0.3 cm lead case, due to the reasons mentioned above. Namely, that

(1) the lead layers are thinner in the 0.2 cm lead case (0.2 cm vs 0.3 cm), allowing less self attenuation to occur so that more gammas exit the lead. And (2) to a lesser degree, the layers of scintillator are thinner in the 0.2 cm lead case (1.1 cm vs 1.25 cm), thereby attenuating fewer neutrons throughout the detector.

Efficiency

The other photon tally generated by the code was the F6 tally, in units of MeV/gm, *per source particle* (or gamma). The total energy deposited (MeV) in the scintillator was found by multiplying the total mass of scintillator (in grams) by the F6 tally, and also by the number of source particles, or gammas, in the run. The total energy emitted by the lead in the form of gammas, was the number of source gammas multiplied by the weighted average energy of each gamma ray, or 0.8 MeV. The efficiency was then found by dividing the total amount of energy deposited in the detector by the total amount of energy emitted in gamma rays. (And since the number of source gammas was in both the numerator and denominator, simply dividing the energy deposited by 0.8 MeV calculated the efficiency as well.) Table VII lists the efficiency for the original lead probe, the 0.2 cm lead layer case and 0.3 cm lead layer case as well as the energy deposited in each case for both DD and DT neutrons.

Once more, just as the F8 tallies in Table VI are higher for the 0.2 cm lead case, so are the F6 tallies in Table VII. Despite the fact that the 0.3 cm case has more mass of scintillator than the 0.2 cm case (7.29 kg vs 6.42 kg), or (16.08 lbs vs 14.15 lbs), it has a lower F6 tally. The 0.3 cm case has more neutron reactions/layer (as shown in Table V), but its thicker lead layers contribute to more self attenuation, so fewer gammas exit the

lead. The net result is less energy is deposited in the scintillator, producing a lower value for efficiency, both for DD and for DT neutrons.

Table VII.

**F6 Tallies, Energy Deposited and Efficiencies of Original Lead Probe,
and 0.2 cm and 0.3 cm Lead Layer Cases**

	<u>F6 Tally</u> <u>(MeV/gm)</u>	<u>Mass of</u> <u>Scintillator</u>	<u>Energy</u> <u>Deposited</u> (MeV)	<u>Efficiency (%)</u> <u>DD Neutrons</u>	<u>Efficiency (%)</u> <u>DT Neutrons</u>
OLP	1.21191E-05	1.66054 kg (3.66 lbs)	0.020124	2.52	2.58
0.2 cm Pb	1.24744E-05	6.41940 kg (14.15 lbs)	0.080078	10.01	10.31
0.3 cm Pb	9.63972E-06	7.29 kg (16.08 lbs)	0.070320	8.79	9.14

As can be seen, the differences in efficiency between DT neutrons and DD neutrons vary by only 2 – 4%, indicating that despite the increase in neutron energy (from 2.45 MeV to 14.1 MeV), similar processes are occurring in the DT case. More will be discussed about DT neutrons in Chapter 3.

A final comparison between the 0.2 cm lead case and the 0.3 cm lead case was to look at the overall mass of lead and scintillator in each case and compare those values

with the mass of lead and scintillator in the original lead probe (Table IV). In looking at the total mass of each case, the overall mass of the original lead probe comprising the lead face, lead sheath and block of scintillator is 19.8 kg (43.66 lbs). This value was taken as an upper bound in weight – any new design, however configured, would have to weigh in at that weight or be less than that weight. The 0.3 cm lead case with 1.25 cm layers of scintillator has an overall mass of 26.53 kg (58.48 lbs) making it prohibitively heavy, despite its Figure of Merit being a factor of 3.66 higher than the original lead probe. The 0.2 cm lead case with 1.1 cm layers of scintillator has an overall mass of 19.24 kg (42.42 lbs), which is just under the original lead probe's overall weight of 19.8 kg (43.66 lbs). This configuration, then, was chosen as the optimum design, with its higher F4 and F8 tallies due to its thinner layers of both scintillator and lead, and having a Figure of Merit 3 times greater than the original lead probe.

CHAPTER 3

DT Neutrons

Since the original lead probe was designed to measure pulsed DT neutron sources (14 MeV), it was only fitting that an analysis be carried out with both the 0.2 cm (0.0787 in) and 0.3 cm (0.118 in) lead cases above to determine how they performed in comparison. As shown in Figure 4, the effective cross sections at DT neutron energies are a factor of 27 greater (~735.9 mb) than those at DD neutron energies (~26.9 mb). This is primarily due to the threshold reaction $^{208}\text{Pb}(n, 2n)^{207\text{m}}\text{Pb}$ which occurs for neutron energies above about 8 MeV (Spencer & Jacobs, 1965); this threshold value was further analyzed to be 7.38 MeV (Ruby and Rechen, 1967). As is shown in Figure 4, the cross section for the $^{207}\text{Pb}(n, n')^{207\text{m}}\text{Pb}$ decreases as one increases in neutron energy above 8 MeV, while the $^{208}\text{Pb}(n, 2n)^{207\text{m}}\text{Pb}$ reaction cross section increases more than a factor of two between 11 MeV (504.2 mb) and 14 MeV (1313.5 mb).

MCNP was used to model a point source of DT neutrons placed 3 meters away from the face of the original lead probe. The neutron case was run for five minutes (generating ~ 10 million particle histories) and the $^{207\text{m}}\text{Pb}$ production was calculated (F4 tally). The lead in the detector was then treated as a volumetric gamma source in which a photon case was run that generated a counts tally (F8) in the scintillator from the ~800,000 particle histories generated. The values of the F4 tally, the F8 tally, mass of lead, scintillator, total mass and Figure of Merit are listed in Table VIII. The values in parentheses are normalized to the corresponding values of the original lead probe.

Again, the F8 tallies increase dramatically – 347% for the 0.2 cm lead case and 295% for the 0.3 cm lead case. And, once again, the 0.3 cm case has 50% more lead than

Table VIII.**Comparison between the Original Lead Probe and 0.2 cm and 0.3 cm lead cases****For DT Neutrons (14 MeV)**

	F4 Tally (reactions/cm³)	F8 Tally (Counts)	Mass of Lead	Mass of Plastic	Total Mass	Figure of Merit (reactions x counts)
Original Lead Probe	1.3697E-08 (1.0)	0.055367 (1.0)	18.14 kg (40 lbs)	1.66 kg (3.66 lbs)	19.80 kg (43.66 lbs)	1.21E-06 (1.0)
0.2 cm Lead, 1.1 cm Scintillator	1.7325E-08 (1.26)	0.247316 (4.47)	12.83 kg (28.28 lbs)	6.42 kg (14.15 lbs)	19.25 kg (42.43 lbs)	4.85E-06 (4.0)
0.3 cm Lead, 1.25 cm Scintillator	1.6347E-08 (1.19)	0.218956 (3.95)	19.24 kg (42.42 lbs)	7.29 kg (16.08 lbs)	26.53 kg (58.48 lbs)	6.08E-06 (5.0)

the 0.2 cm case, but it has 13% fewer counts in the scintillator. This is due to the reasons mentioned above for DD neutrons – the lead layers are 1 mm thinner in the 0.2 cm case than in the 0.3 cm case, which allow less self attenuation to occur so that more gammas exit the lead. And in contrast to the DD case, DT neutrons have more advantageous mean free paths as shown in Table IX below. The mean free paths of 14 MeV neutrons in lead are actually shorter than they are in the scintillator, which is what is desired (as opposed to the DD neutron case, Table II).

Table IX.

Mean Free Paths of 14 MeV neutrons in Lead and Scintillator

	<u>Lead</u>	<u>Scintillator</u>
DT Neutrons	~ 5.2 cm	~ 7.5 cm

A comparison of neutron reactions per layer for both the 0.2 cm and 0.3 cm cases are shown in Table X below. Note that the reactions/layer for DT neutrons are over an order of magnitude greater than the reactions/layer for DD neutrons (Table V). This is due to the higher cross section of the $^{208}\text{Pb}(n, 2n)^{207\text{m}}\text{Pb}$ reaction (Figure 4), and well as the beneficial mean free paths of 14 MeV neutrons in lead and scintillator.

Table X.

Neutron Reactions per Layer for the 0.2 cm and 0.3 cm lead layer cases

For DT Neutrons

<u>Lead Layers</u>	<u>0.2 cm Lead Layers</u> Neutron Reactions per Layer (x 10 ⁻⁶) (n reactions/cm ³) x (cm ³ /layer)	<u>0.3 cm Lead Layers</u> Neutron Reactions per Layer (x 10 ⁻⁶) (n reactions/cm ³) x (cm ³ /layer)
Front Face	3.13 (100%)	4.70 (100%)
Layer “A”	2.94 (94%)	4.33 (92%)
Layer “B”	2.73 (87%)	3.96 (84%)
Layer “C”	2.54 (81%)	3.65 (78%)
Layer “D”	2.32 (74%)	3.22 (69%)
Layer “E”	2.20 (70%)	2.93 (62%)
Layer “F”	1.96 (63%)	2.64 (56%)
Layer “G”	1.78 (57%)	2.30 (49%)

As was seen for DD neutrons, the neutron reactions/layer for the 0.3 cm case fall off slightly faster from the front face to the last layer (“G”), indicating that more neutron attenuation is occurring in the 0.3 cm case than in the 0.2 cm case. Also, since the 0.3 cm lead case has more neutron reactions per layer than the 0.2 cm lead case, more ^{207}Pb atoms are being activated and producing delayed gammas. To see if these gammas are reaching the scintillator and being counted, a comparison of F8 tallies (Counts) for the 0.2 cm and 0.3 cm lead layer cases are shown in Table XI below.

Table XI.

F8 Tallies for the 0.2 cm and 0.3 cm lead layer cases

For DT Neutrons

<u>Scintillator Layers</u>	<u>0.2 cm Lead Layers</u> <u>F8 Tallies</u> (Counts in Scintillator)	<u>0.3 cm Lead Layers</u> <u>F8 Tallies</u> (Counts in Scintillator)
Layer 1	0.036472 (> 7%)	0.034032
Layer 2	0.040178 (> 9%)	0.036667
Layer 3	0.039946 (> 12%)	0.035492
Layer 4	0.038090 (> 14%)	0.033180
Layer 5	0.036043 (> 18%)	0.030532
Layer 6	0.032212 (> 21%)	0.026605
Layer 7	0.026501 (> 22%)	0.021678
Layer 8	0.017346 (> 29%)	0.013424

As was also seen for DD neutrons, for every layer of scintillator the F8 tallies are greater in the 0.2 cm lead case than in the 0.3 cm lead case, due to the reasons mentioned above. Namely, that (1) the lead layers are thinner in the 0.2 cm lead case (0.2 cm vs 0.3 cm), allowing less self attenuation to occur so that more gammas exit the lead which produces a higher F8 tally (Table VIII). And (2) to a lesser degree, the layers of

scintillator are thinner in the 0.2 cm lead case (1.1 cm vs 1.25 cm) or (0.433 in vs 0.492 in), thereby attenuating less neutrons throughout the detector. Overall this produces a Figure of Merit which is a factor of 4 greater than the original lead probe for the 0.2 cm case, and a Figure of Merit which is a factor of 5 greater than the original lead probe for the 0.3 cm case (Table VIII). However, due to weight considerations, the 0.3 cm case is considered prohibitively heavy with its total mass of 26.53 kg (58.48 lbs). The 0.2 cm case is chosen again as the optimized design with its weight of 19.25 kg (42.43 lbs).

CHAPTER 4

The Prototype

The analysis up to this point had provided the optimum “layer cake” design parameters: 0.2 cm lead thickness and 1.1 cm scintillator thickness, with a radius of 15 cm. The overall mass of this model was 19.25 kg (42.43 lbs), which was just under the original lead probe’s mass of 19.80 kg (43.66 lbs), and it produced a Figure of Merit which was a factor of 3 greater than that of the original lead probe for DD neutrons. It was now necessary to build a “proof of principle” prototype, test it experimentally, and compare the experimental results with the code predictions.

A meeting at Bechtel/Nevada in Las Vegas was held to discuss the design of such a prototype. In order to minimize cost, it was decided that the prototype was to be built out of materials at hand and its size reduced. Also, instead of a cylindrical configuration which would require additional machining, a square configuration was chosen instead. The scintillator that was available at Bechtel was in 1.5875 cm (5/8”) sheets. This dimension was not the 1.1 cm (0.433 in) optimized thickness that the code specified; however, once the prototype was built it was modeled with the code to its exact dimensions and the results of the code were compared with experimental data.

In order to reduce background and provide some shielding, it was decided that the prototype have 9 layers of lead and only 8 layers of scintillator; in this way, lead layers would be on each exterior side. Also, it was decided that the size of each layer would be approximately 15.24 cm (6 in) square – the final dimensions were 15.47 cm x 15.37 cm (6.092” x 6.052”). The lead layers were between 2.2 – 2.3 mm (0.0866 – 0.0906 in) thick. For modeling purposes, a thickness of 2.25 mm (0.0886 in) was chosen. The

layers of scintillator were 1.5875 cm (5/8”), and were comprised of BC-400, a general purpose scintillator, equivalent to NE-102. (More specifications of BC-400 can be found in Appendix D.) A photograph of the completed prototype in a steel housing is shown in Figure 11 below.

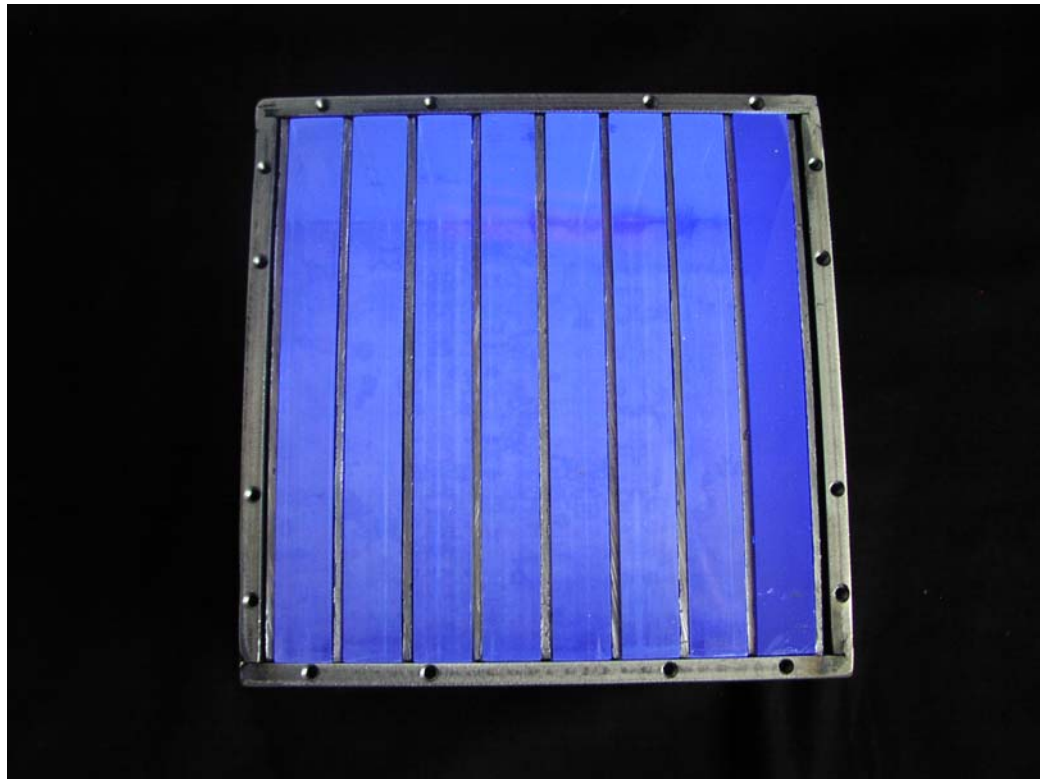


Figure 11. Layer Cake Prototype with 9 layers of lead, 8 layers of scintillator

Encased in a steel housing

In order to reduce costs still further, a light guide was deemed unnecessary; instead a 12.7 cm (5 in) Hamamatsu photomultiplier tube was coupled directly to the edge on view via a plate and o-ring as shown in Figure 12. The completed detector assembly with the lead/scintillator section coupled to the photomultiplier tube is shown in Figure 13 below. Specifications on the Hamamatsu R1250 photomultiplier tube can be seen in Appendix C.

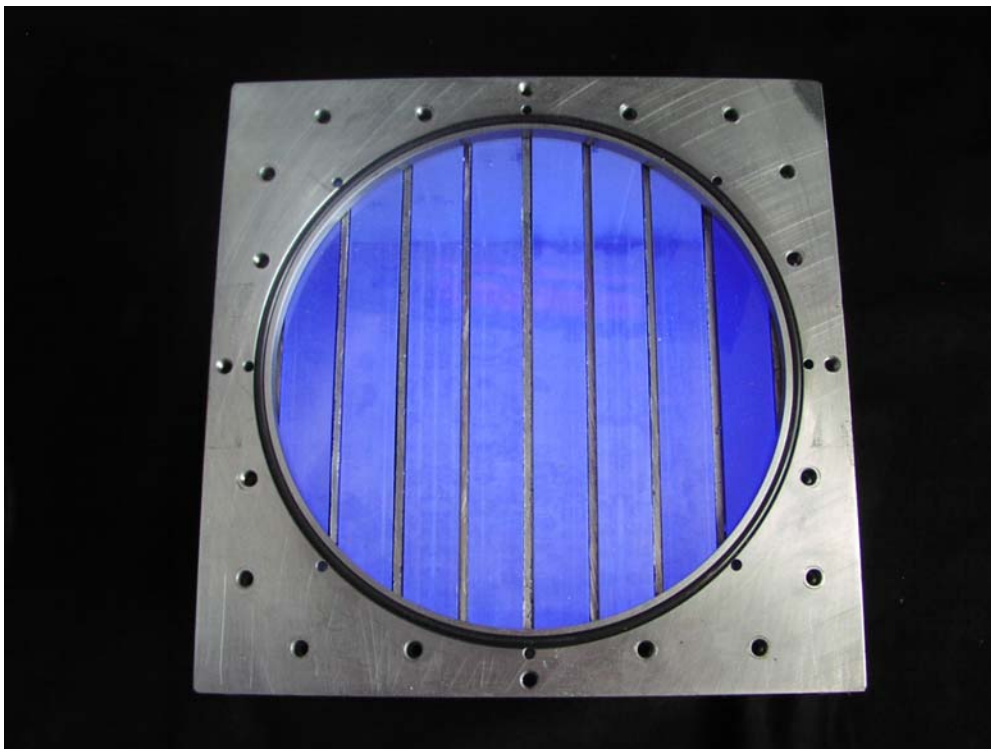


Figure 12. Plate and O-ring on Layer Cake to couple to 12.7 cm (5 in) diameter

Hamamatsu Photomultiplier tube

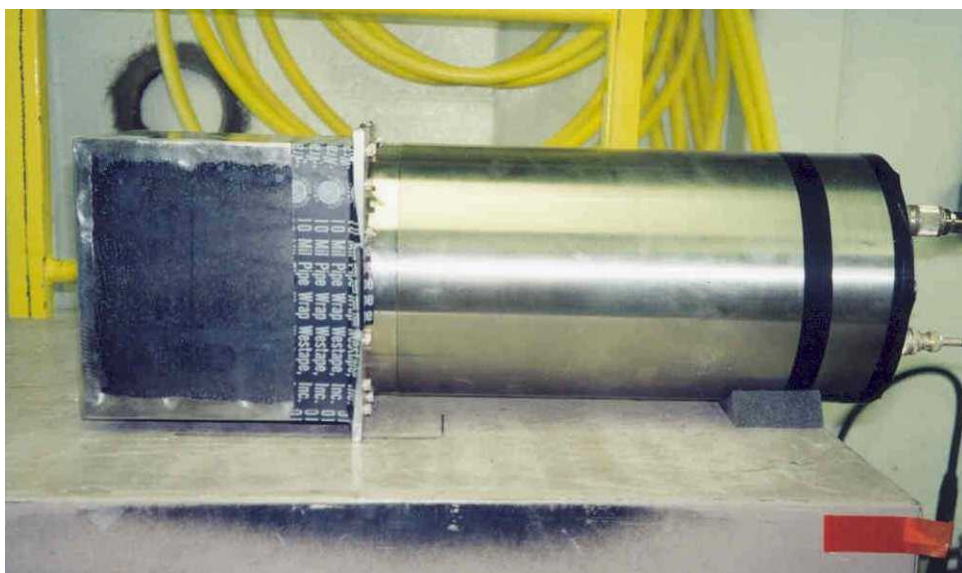


Figure 13. Completed Layer Cake Detector Assembly: Lead/Scintillator Section

Coupled to 12.7 cm (5 in) Hamamatsu Photomultiplier Tube

A block diagram of the layer cake prototype detector is shown in Figure 14. It consists of the layer cake, a photomultiplier tube and divider chain, a high voltage power supply, a constant fraction discriminator and multi-channel scaler.

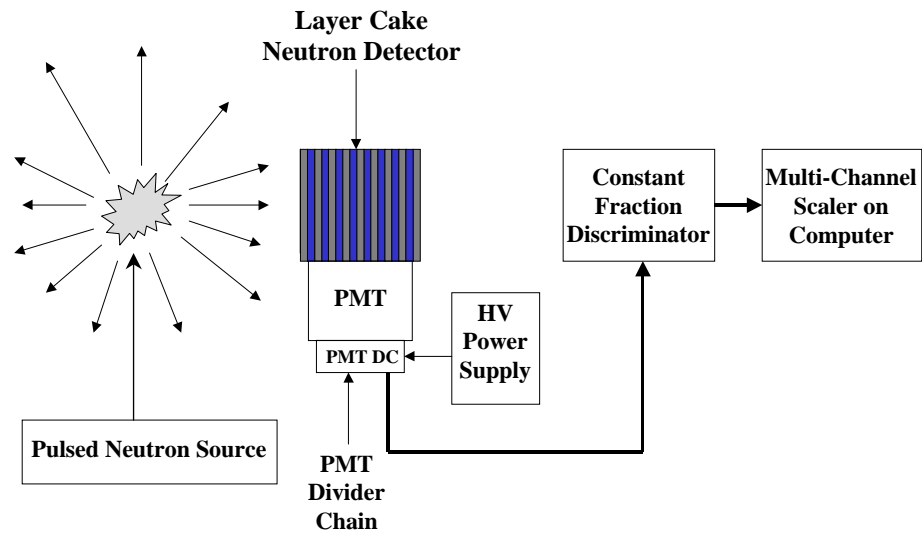


Figure 14. Block Diagram of Layer Cake Prototype Neutron Detector

CHAPTER 5

Experimental Results

Dense Plasma Focus

The neutron source used to calibrate the layer cake prototype was the 480-kJ, 60kV, capacitor driven DD dense plasma focus operated by Dr. Bruce Freeman at Texas A&M University Riverside campus (Freeman 2001). The typical neutron yield for this machine is $\sim 3.5 \times 10^{10}$ neutrons (based on indium activation, discussed below) in 100 ns

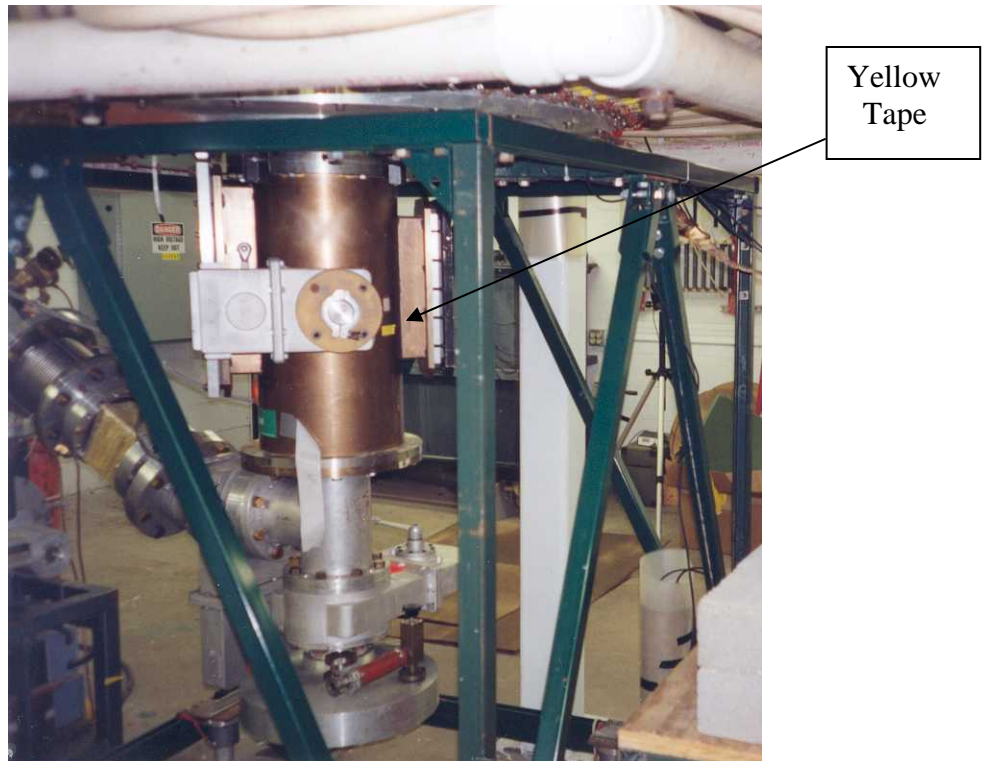


Figure 15. Dense Plasma Focus at Texas A&M; typical neutron yield is $\sim 3.5 \times 10^{10}$ neutrons (based on indium activation) in 100 ns (FWHM); center is marked with yellow tape for alignment purposes.

(FWHM). The DPF is shown in Figure 15 (note the small piece of yellow tape on the chamber wall – this denotes the center of the dense plasma focus).

The layer cake was placed on a thin metal table (to minimize neutron scattering) which stood on stacked cinderblocks as shown in Figure 16. This permitted the center of the face of the detector to be 129.54 cm (51 in) above the floor; the center of the dense plasma focus was determined to be 131.45 cm (51 $\frac{3}{4}$ in) (i.e., marked with yellow tape in Fig. 15).



Figure 16. Layer Cake placed on thin metal table (to minimize neutron scattering) on stacked cinderblocks; at this height the detector was aligned to center of DPF

Also, for $1/R^2$ measurements the table could be rolled towards or away from the DPF on the cinderblocks, depending on the measurement that was desired. Figure 17 shows the layer cake and the original lead probe beneath it while another lead probe from

Bechtel rests on a nearby table. They are all facing the DPF, approximately 1.83 m (6 ft) away.

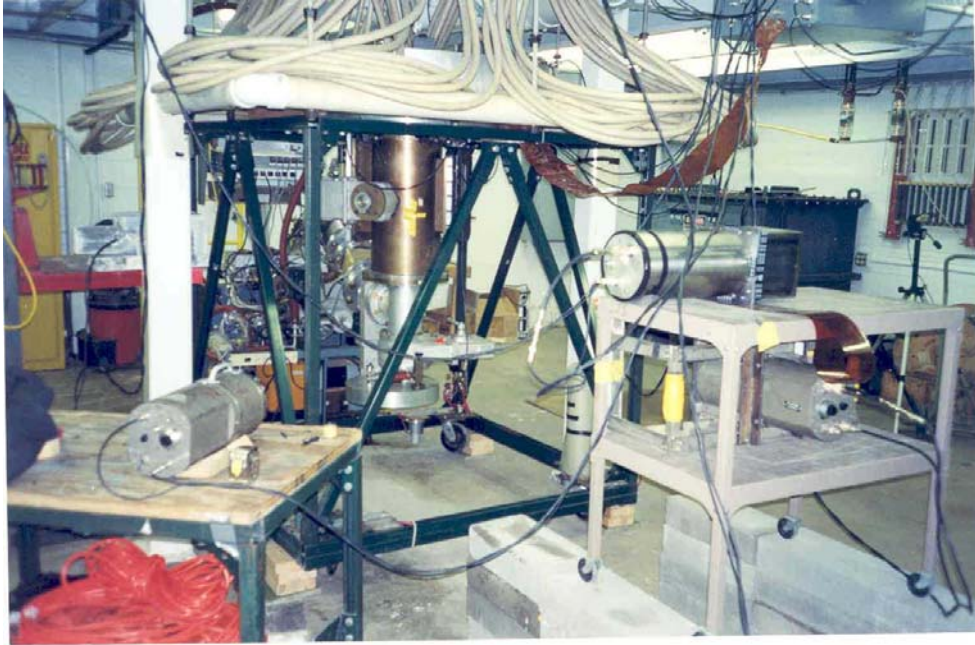


Figure 17. Layer Cake with Original Lead Probe beneath it; another lead probe from Bechtel rests on a table nearby. All are facing the Dense Plasma Focus.

A series of shots were performed with the layer cake at 3 different distances from the chamber wall of the DPF: 243.84 cm (8 ft), 182.88 cm (6 ft) and 106.68cm (42 in). It was noted that the center of the DPF was 15.24 cm (6 in) within the chamber – this was taken into account in the calculations. DD neutron yields were found using activation of nominally 50 gram (1.76 oz) indium samples via the following inelastic neutron scattering reaction: $^{115}\text{In}(n,n')^{115\text{m}}\text{In}$; its threshold is 336 keV (Cooper and Ruiz 2001). The yields were then mass-corrected, and the number of incident neutrons on the face of the detector were calculated.

The data from each shot were taken with a multi-channel scaler. A decay curve of

a typical shot is shown in Figure 18, before any analysis was performed. Note the areas of background, the long lived component and the x-ray peak which accompany the neutron pulse. This raw data must be manipulated before a 0.8 second half life can emerge.

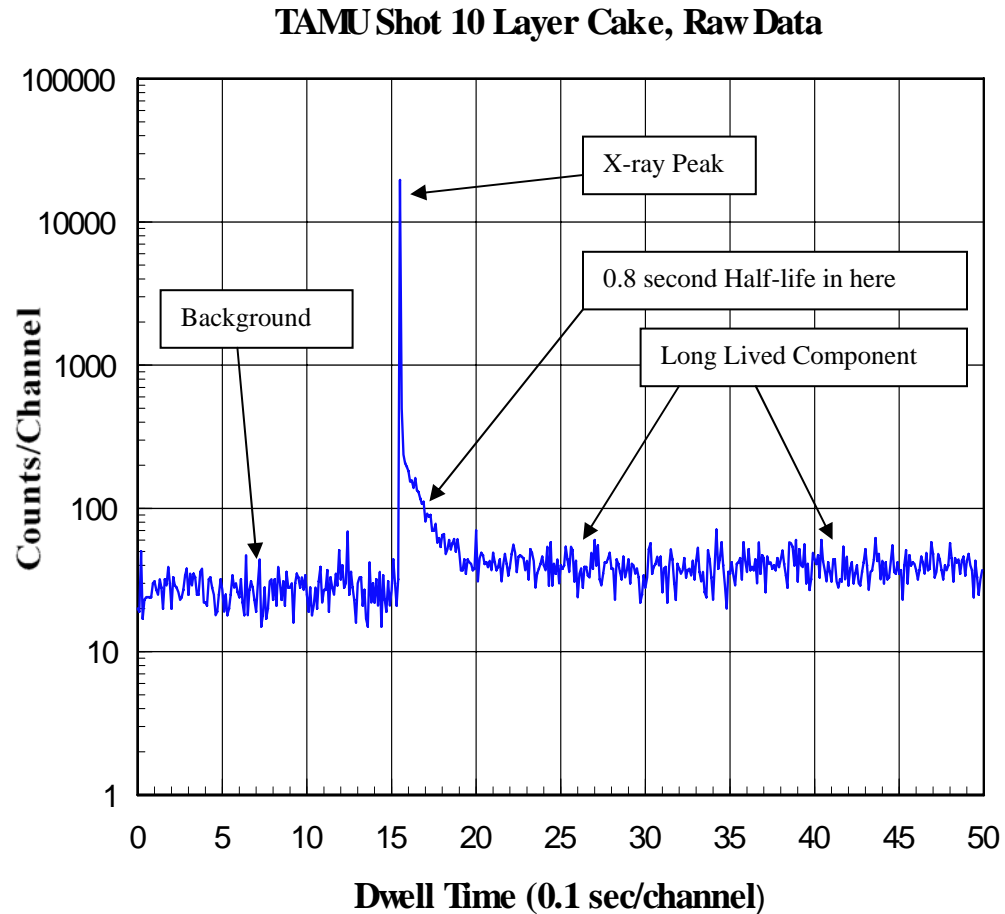
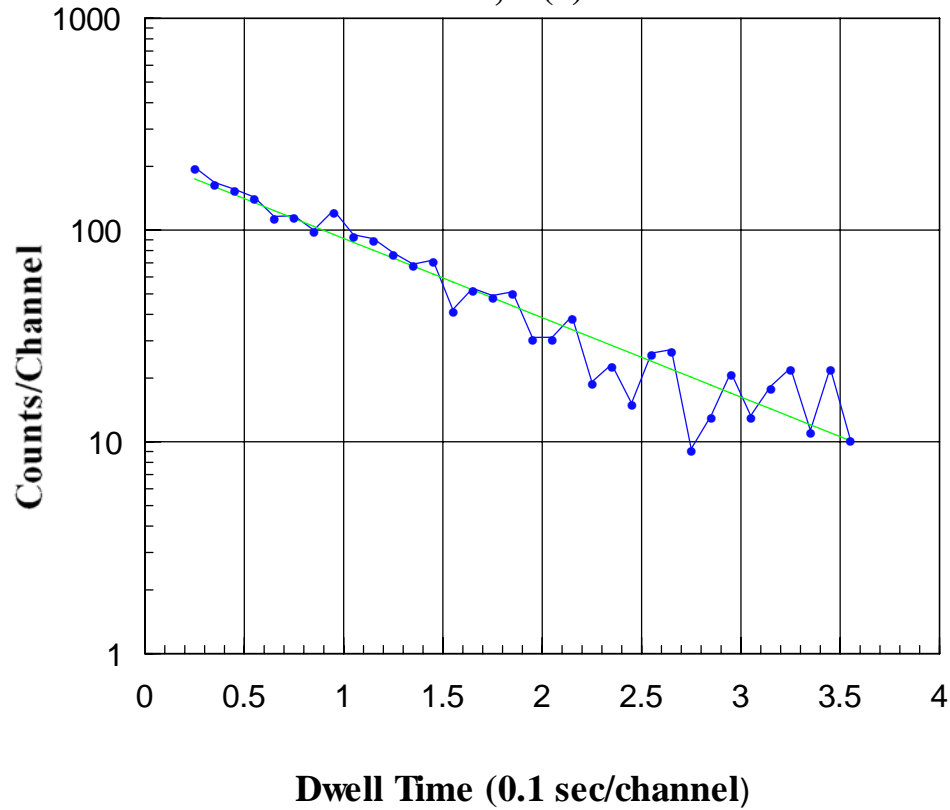


Figure 18. Raw Data taken with Layer Cake on Typical Shot on DPF

Once the background is subtracted, the long lived component is found and subtracted, the x-ray data is removed and a time correction is performed, a least squares fit is performed to determine the initial count rate, $A(0)$, and the corresponding total number of counts, $N(0)$, which is directly proportional to the number of neutrons that interacted with the lead. A plot of a least squares fit that was performed for the raw data

in Figure 18 is shown below in Figure 19.

**TAMU Shot 10 Layer Cake, 259.08 cm (102''), Face On, -2400V, -50mV,
Half Life = 0.80 sec, $A(0) = 216.7$ Counts/0.1 sec**



**Figure 19. A Least Squares Fit Performed on Data in Figure 17 to Determine $A(0)$,
the Relative Initial Activity per unit Time of the Lead**

The sensitivity was then determined by dividing the total counts, $N(0)$, by the number of incident neutrons. A voltage sweep and discriminator sweep were performed to determine optimum sensitivity settings. A plot of the sensitivity as a function of photomultiplier tube bias and discriminator setting can be seen in Figure 20. (Note: the values of sensitivity vs tube bias and discriminator setting can be seen in table form in Appendix C.)

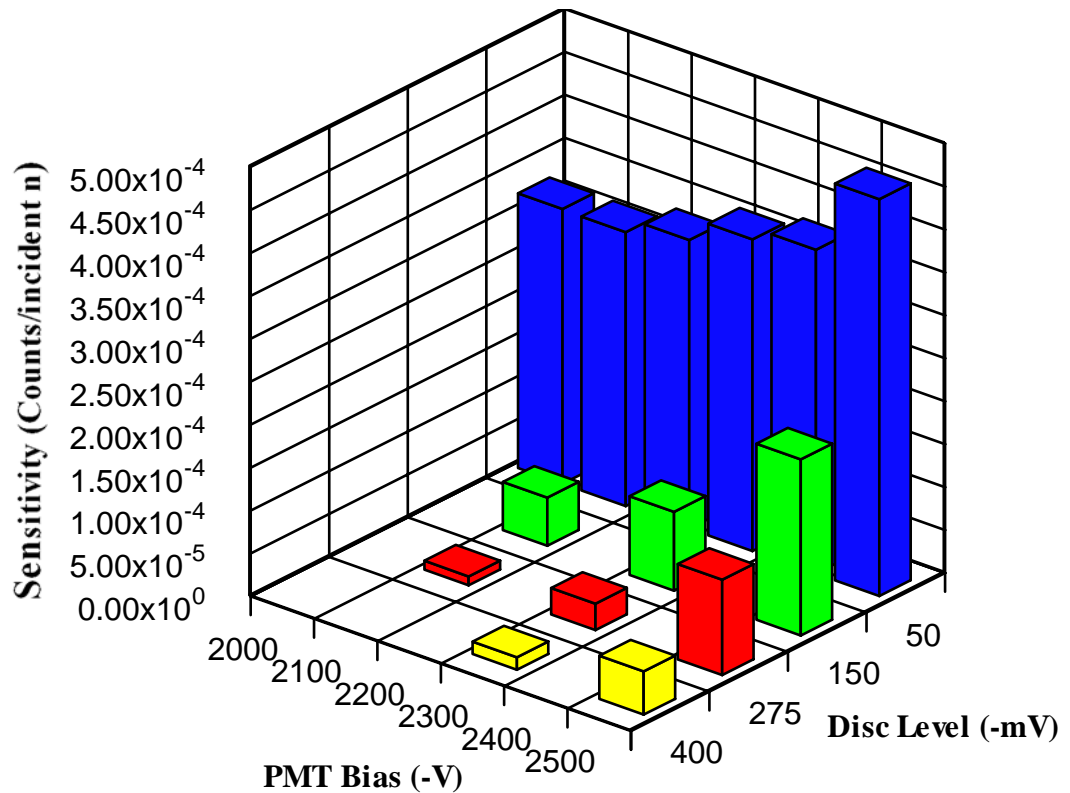


Figure 20. Layer Cake Sensitivity as a Function of Photomultiplier Tube Bias
And Discriminator Setting

“Face On” Configuration

An operating voltage of -2200 Volts and a discriminator setting of -50 mVolts (the lowest) was chosen as reasonable for operation of the layer cake. This produced a sensitivity of ~ 3000 incident neutrons/count, which approximated Sandia’s lead probe sensitivity of ~ 2635 neutrons/count (from data taken at TAMU’s DPF, May 2003). At these settings it was then compared with the original lead probe at a total distance of 198.12 cm (78”) from the center of the DPF in a “face on” configuration (i.e., the face of the detector was placed toward the source as shown in Figure 7).

After fielding the detectors at Texas A&M, the prototype layer cake, as it was built by Bechtel – 0.225 cm (0.0886 in) lead layers, 1.59 cm (5/8”) scintillator layers, was modeled with MCNP with a point source of DD neutrons at exactly the same distance 198.12 cm (78 in). The run times for each case (layer cake and original lead probe) were equal, both for the first run (which generated a neutron tally) and the second run (which produced a counts tally). The results of the experimental and modeled data of the layer cake compared with the original lead probe are shown in Tables XII and XIII below.

Table XII.

Experimental Data of Layer Cake “Face On” & Original Lead Probe

<u>Detector</u>	<u>Distance</u>	<u>Shot #</u>	<u>A(0) Counts/0.1 sec</u>	<u>LC/OLP</u>
Layer Cake	198.12 cm	27	142.1	142.1/198.6 = <u>0.715509</u>
Orig. Lead Probe	198.12 cm	27	198.6	
Layer Cake	198.12 cm	28	231.6	231.6/321.4 = <u>0.720597</u>
Orig. Lead Probe	198.12 cm	28	321.4	

Ave. Ratio of Layer Cake “Face On” to Original Lead Probe:

$$(0.715509 + 0.720597)/2 = \underline{0.72} \quad \leftarrow \text{Measured Value}$$

Table XIII.

Modeled Layer Cake “Face On” & OLP at 198.12 cm (78 in) from Point Source

<u>Detector</u>	<u>F4 Tally</u> (n reactions/cm ³)	<u>F8 Tally</u> (Counts)	<u>Mass of Lead</u>	<u>FOM</u> (reactions x counts)
Layer Cake	7.8786E-10	0.226469	5.46 kg 12.04 (lbs)	8.5907E-08
Orig. Lead Probe	11.4083E-10	0.053722	18.14 kg 40 (lbs)	9.8036E-08

From Table XIII above, the ratio of Figures of Merit of the Layer Cake
“Face On” to Original Lead Probe:

$$(8.5907)/(9.8036) = \underline{0.88} \leftarrow \text{Calculated Value}$$

“Edge On” Configuration

Another comparison was made of the Layer Cake to the Original Lead Probe comprising a different geometry – the detector was turned such that the “edge-on” view was facing the source as shown in Figure 21 below. It was placed at the same distance of 198.12 cm (78”) as was the “face on” evaluation above. Unfortunately, due to time restrictions, only one shot was allowed for a comparison. The experimental data of the Layer Cake in an “edge-on” configuration compared with the Original Lead Probe can be seen in Table XIV below. The modeled data are presented in Table XV.

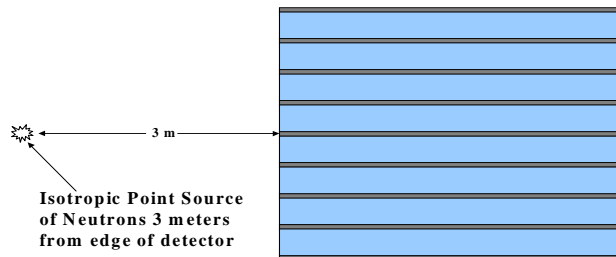


Figure 21. Layer Cake in “Edge On” Configuration to Source

Table XIV.

Experimental Data of Layer Cake “Edge On” & Original Lead Probe

<u>Detector</u>	<u>Distance</u>	<u>Shot #</u>	<u>A(0) Counts/0.1 sec</u>	<u>LC/OLP</u>
Layer Cake	198.12 cm	29	174.8	174.8/257.8 = <u>0.678045</u>
Orig. Lead Probe	198.12 cm	29	257.8	

Ratio of Layer Cake “Edge On” to Original Lead Probe:

0.68 ← Measured Value

Table XV.

Modeled Layer Cake “Edge On” & OLP at 198.12 cm (78 in) from Point Source

<u>Detector</u>	<u>F4 Tally</u> (n reactions/cm ³)	<u>F8 Tally</u> (Counts)	<u>Mass of Lead (lbs)</u>	<u>FOM</u> (reactions x counts)
Layer Cake	6.8945E-10	0.240990	5.46 kg (12.04 lbs)	7.9999E-08
Orig. Lead Probe	11.4083E-10	0.053722	18.14 kg (40 lbs)	9.8036E-08

From Table XV above, the ratio of Figures of Merit of “Edge On” Layer Cake to Original Lead Probe:

$(7.9999)/(9.8036) = \underline{0.82}$ ← Calculated Value

A summary of the comparisons of the experimental data to the modeled data of the “face on” and “edge on” configurations are shown in Table XVI below. The modeled values (0.88 and 0.82) are approximately 20% – 22% higher than the experimental values (0.72 and 0.68), but this is not surprising. The MCNP model is considered an “ideal” detector, which assumes that all the pulses in the scintillator are counted, etc., and is not subject to background or various bias and discriminator settings that an actual detector is

subject to. However, what is interesting, are the ratios between the modeled values and the measured ones for the same configurations. The modeled evaluation of the “face on” to “edge on” layer cake is within 1% of the measured “face on” to “edge on” layer cake (1.07 vs 1.06). These results indicate that the code results are valid.

Table XVI.

Comparison of Experimental and Modeled Data of the Layer Cake

“Face On” to “Edge On” at 198.12 cm (78 in) from Point Source

<u>Case</u>	<u>Layer Cake</u> <u>Face On/Edge On</u>
Modeled	$0.88/0.82 = \underline{1.07}$
Measured	$0.72/0.68 = \underline{1.06}$

1/R² Measurements

In the three positions mentioned above, namely, 121.92 cm (48 in), 198.12 cm (78 in) and 259.08 cm (102 in) from the DPF, 1/R² measurements were performed with the Layer Cake in the “face on” configuration. A(0) – the initial count rate – was found using a least squares fit to the data. The neutron yields were determined from indium activation (Cooper and Ruiz, 2001) and mass-corrected. The values of A(0) were then normalized using the mass-corrected neutron yields. Figures of Merit were produced from the code at each position and multiplied by a constant to compare with the

experimental data. The data – both experimental and calculated – are listed in Table XVII.

Table XVII.

Comparison of Experimental and Calculated Data at 121.92 cm (48 in), 198.12 cm (78 in) and 259.08 cm (102 in)

<u>Distance</u>	<u>Shot #</u>	<u>A(0)</u> <u>Counts/0.1sec</u>	<u>Mass-Corrected</u> <u>Neutron yields</u>	<u>Norm</u> <u>A(0)</u>	<u>FOM</u> <u>x 10⁻⁸</u>	<u>FOM x K</u>
121.92 cm (48 in)	26	434.1	1.46×10^{10}	627.4	21.77	593.9
198.12 cm (78 in)	27	141.0	1.35×10^{10}	220.4	8.59	234.4
”	28	209.9	1.902×10^{10}	232.9	“	“
”	24	218.7	2.01×10^{10}	229.6	“	“
”	25	191.8	1.59×10^{10}	254.5	“	“
259.08 cm (102 in)	5	172.2	2.11×10^{10}	172.2	5.23	142.6
”	6	162.8	1.98×10^{10}	173.5	“	“

The values of A(0) were normalized to the highest mass-corrected neutron yield of 2.11×10^{10} on shot #5 at a distance of 259.08 cm (102 in). Averages were taken at 198.12 cm (78 in) and 259.08 cm (102 in); their values were 234.4 and 172.9 respectively. The constant K was derived from the average value at 198.12 cm, or 78 in (234.4) divided by the Figure of Merit produced by the code at that distance (8.59×10^{-8}):

$$K = (234.4)/(8.59 \times 10^{-8}) = 2.73 \times 10^9.$$

The last column in Table XVII lists the Figures of Merit multiplied by the constant K.

The experimental data (i.e., the normalized values of A(0)), the Figures of Merit multiplied by the constant K, and $1/R^2$ values are plotted in Figure 22. Note: the $1/R^2$ values were derived for the data at distances of 121.92 cm (48 in) and 259.08 cm (102 in), using the average normalized A(0) for 198.12 cm (78 in) of 234.4, as follows:

$1/R^2$ at 121.92 cm: $(198.12)^2/(121.92)^2 * (234.4) = \underline{619.0}$, and,

$1/R^2$ at 259.08 cm: $(198.12)^2/(259.08)^2 * (234.4) = \underline{137.1}$

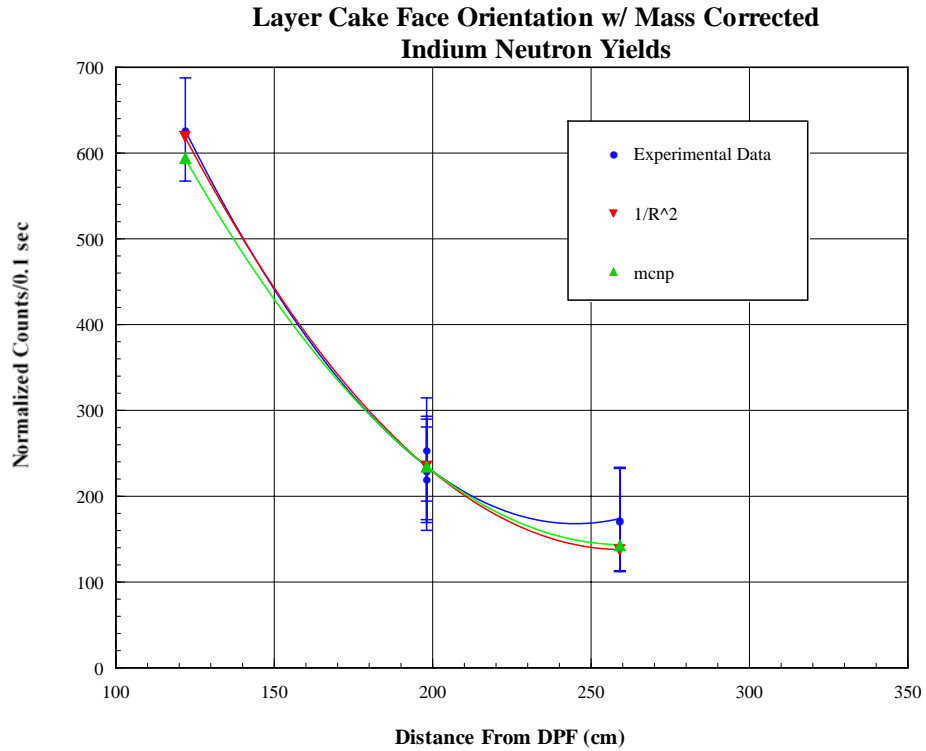


Figure 22. Layer Cake Experimental Data, MCNP Calculations and $1/R^2$ Behavior

The experimental data can be seen to compare well with both the $1/R^2$ behavior (red) and the MCNP calculations (green) – their values fall within the experimental data's standard error bars (blue) of ± 63.3 counts/0.1 sec.

Calibration

As seen in Figure 20, the sensitivity of the layer cake neutron detector can be adjusted by photomultiplier tube bias as well as pulse height discriminator level. The amplifier gain in the electronics can also be varied to adjust sensitivity. However, at the time of calibration against a known yield of pulsed neutrons (such as at Texas A&M, as

mentioned above) these parameters are determined before each pulse, and the system is calibrated by the number of delayed gamma counts in the scintillator. Thus, the neutron sensitivity of the detector is directly related to the gamma scintillation sensitivity. This relationship, then, provides a technique to reset the system gain to the level used during initial calibration.

By using a radioactive source placed at a predefined position on the detector at the time of calibration, the gamma counts in the scintillator can be recorded. Then the photomultiplier tube bias, as well as the pulse height discriminator level can be varied to attain the level of gamma scintillations produced during the primary calibration with a neutron source. In this way the same neutron sensitivity can be achieved when the detector is fielded elsewhere, regardless of the local background and relative settings of the photomultiplier tube bias and discriminator level, as well as any long cable lengths that may be required over which voltage drops could occur.

^{133}Ba was used as the radioactive source for the original lead probe (Spencer & Jacobs, 1965), due to its relatively long half life of 10.53 years and a gamma spectrum of photopeaks with energies below 0.4 MeV. It was produced by taking 20 to 30 microcuries of barium powder (evaporated from a solution), which was then placed in a drilled out bolt and sealed with epoxy. The bolt was then placed in the aluminum insert shown in Figure 1. The rigid mounting of the insert assured that the ^{133}Ba source would always be placed in the same position relative to the scintillator so that the sensitivity could be adjusted to the level determined at the time of calibration. Also, due to slight geometrical discrepancies in source mountings from lead probe to lead probe, a reference source from one probe would not necessarily produce the same ratio of gamma counts to

neutron sensitivity in the other. Therefore, it was determined that each lead probe be assigned a ^{133}Ba source at its primary calibration which would then be dedicated to that particular probe throughout its working life.

Initially at Texas A&M, before fielding the detector on neutron shots, it was necessary to determine whether the layer cake could be calibrated in the same fashion as the original lead probe, i.e., with a barium source in a predefined position. Due to the multiple layers of lead in the layer cake, it was unknown whether the low energy gammas from ^{133}Ba would penetrate enough of the scintillator to generate adequate counts to calibrate the detector. The original lead probe, on the other hand, has no lead layers to attenuate gammas; the entire mass of scintillator “sees” the barium source. Therefore, a barium bolt with an activity of 5.1 μCi from a lead probe belonging to Bechtel was placed on top of the Layer Cake in the center, perpendicular to the edges of lead and scintillator as seen in Figure 23.

The voltage applied to the detector at the time was -2000 volts, with the discriminator setting at -50 mV (the lowest). The dwell time was set on the multi-channel scaler to 2.367 sec. The average counts recorded from the barium bolt were ~ 3412 counts/sec. The barium bolt was then taken away and the average background recorded at the same settings was ~ 200 counts/sec. Since the ratio between source counts and background counts was large (~ 17) it was determined that a barium bolt similar to those used with lead probes could be used to calibrate the layer cake. Particularly if the bolt was placed in a fixed position (perhaps a nut could be epoxied or welded to the housing of the layer cake such that a barium bolt could be screwed into it, as shown in Figure 24.)

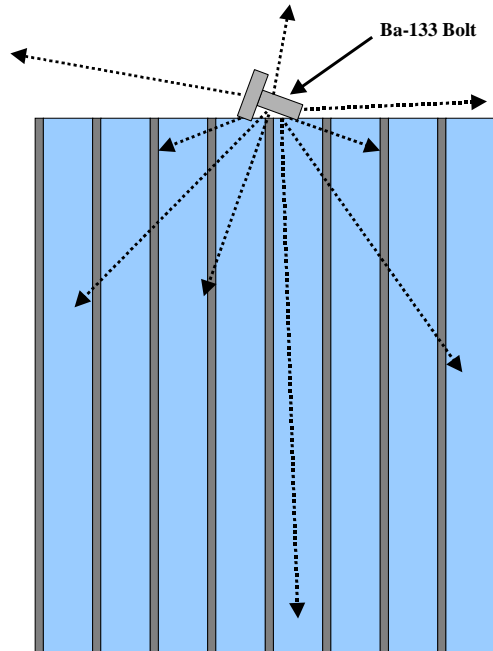


Figure 23. Barium Bolt Placed in center of Layer Cake perpendicular to edges of lead and scintillator.

Also, increasing the gain on the photomultiplier tube would also increase the ratio between source counts and background counts. The operating voltage (as was mentioned above) chosen for the layer cake was -2200 Volts; however, the Hamamatsu photomultiplier tube can be operated up to -3000 Volts (Appendix C). This voltage range is more than adequate for setting system gain to attain the level of gamma scintillations with a ^{133}Ba source to equate to those scintillations produced by neutron activation at the time of calibration.

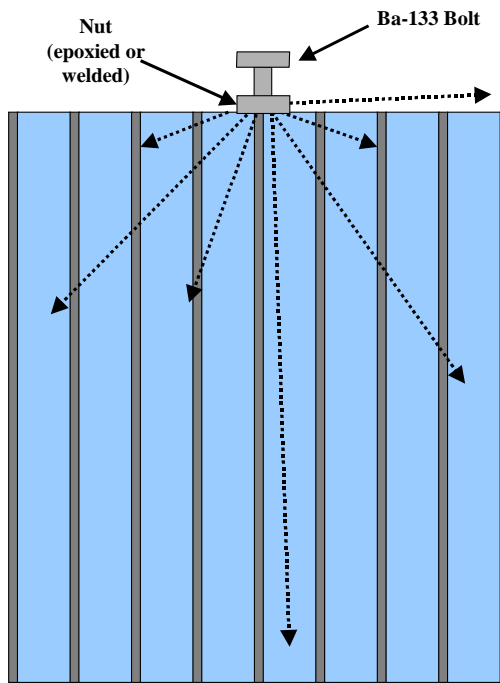


Figure 24. Fixing a position for a Barium Bolt on the Layer Cake in the form of a nut being either epoxied or welded to housing

Chapter 6

Summary

The lead probe neutron detector designed by Spencer and Jacobs in 1965 was optimized using a layer cake design in which thin, 2 mm (0.0787 in) layers of lead were sandwiched between thicker, 1.1 cm (0.433 in) layers of scintillator. The optimized layer cake was 30 cm (11.81 in) in diameter (which was considered the upper design limit on size), and had an equal number of lead and scintillator layers at 8 each. This produced an overall Figure of Merit which was a factor of 3 times greater than the original lead probe for DD neutrons (2.45 MeV) and a factor of 4 times greater for DT neutrons (14 MeV). It has slightly less overall mass – 19.25 kg vs 19.80 kg , (42.43lbs vs 43.66 lbs), and contained 30% less lead.

A smaller, “proof of principle” prototype was built by Bechtel/Nevada out of materials at hand and consisted of 9 layers of lead 0.225 cm (0.0886 in) thick and 8 layers of scintillator (BC-400), 1.5875 cm (5/8 in) thick and was approximately 15.24 cm (6 in) square. In order to reduce background and provide some shielding, it was decided that the prototype have lead layers on each exterior face. To further reduce costs, a light guide was not used; instead a 12.7 cm (5 in) Hamamatsu photomultiplier tube was coupled directly to the edge on view, in line with the layers of lead and scintillator.

The prototype was then calibrated using the 480-kJ, 60kV, capacitor driven DD dense plasma focus operated by Dr. Bruce Freeman at Texas A&M University Riverside campus. A series of shots were performed with the layer cake at 3 different distances from the chamber wall: 106.68 cm, 182.88 cm and 243.84 cm (42 in, 6 ft, and 8 ft). DD neutron yields were found using activation of (nominally) 50 gram (1.76 oz) samples of

indium which were mass corrected. The total number of incident neutrons on the face of the detector was found. A least squares fit was performed on the data to determine $A(0)$, the initial count rate. $N(0)$ – the total number of counts from $^{207\text{m}}\text{Pb}$ atoms (and therefore the number of neutrons which had interacted with the detector) was found. Sensitivity was determined from dividing $N(0)$ by the number of incident neutrons. A voltage and discriminator sweep was performed to determine optimum sensitivity settings.

The prototype was tested in both a “face on” and “edge on” configuration and compared well in each case with calculations (within 3% – 5%). $1/R^2$ measurements were performed at the three distances mentioned above. The calculations and $1/R^2$ behavior values fell within the experimental data’s standard error bars. It was determined that calibration could be accomplished with a standard ^{133}Ba bolt which is used to calibrate the original lead probe.

Future Work

It should be noted that this design process yielded two different pathways one could take. (1) A most efficient case in which the Figure of Merit is a factor of 3 greater than the original lead probe, but the overall weight is the same, or (2) a comparable case in which the performance is the same for a considerable decrease in lead (approximately 68% less lead). The former is advantageous in experiments in which one is attempting to measure marginal neutron yields. The latter is desirable in situations in which one is satisfied with the same sensitivity as the original lead probe, but does not want the added weight: 8.84 kg vs 18.14 kg (19.49 lbs vs 40 lbs). This latter case was discovered during the course of this work. It was analyzed with 11 layers of lead at 0.2 cm (0.0787 in) thick, and 10 layers of scintillator 1.27 cm (½ in) thick, with a face that was 15.24 cm (6

in) square. (Essentially, it has just a few more layers of lead and scintillator than the prototype that Bechtel/Nevada built, which was analyzed above.) This produced a Figure of Merit which approximated that of the original lead probe. MCNP code results of this “comparable case” are listed below in Table XVIII and compared with the original lead probe as well as the optimized layer cake design for DD neutrons.

Table XVIII.

Comparison between Original Lead Probe, “Comparable Case”
and Optimized Case for DD neutrons

	F4 Tally (reactions/cm³)	F8 Tally (Counts)	Mass of Lead	Mass of Plastic	Total Mass	Figure of Merit (reactns x cnts)
Original Lead Probe	5.1145E-10 (1.0)	0.053917 (1.0)	18.14 kg (40 lbs)	1.66 kg (3.66 lbs)	19.80 kg (43.66 lbs)	4.4112E-08 (1.0)
Comparable Case: 0.2 cm Lead, 1.27 cm Scintillator, 15.24 cm (6 in) Square	3.4507E-10 (0.675)	0.246082 (4.56)	5.80 kg (12.78 lbs)	3.04 kg (6.71 lbs)	8.84 kg (19.49 lbs)	4.3432E-08 (0.985)
Optimized Case: 0.2 cm Lead, 1.1 cm Scintillator	4.8742E-10 (0.953)	0.239599 (4.44)	12.83 kg (28.28 lbs)	6.42 kg (14.15 lbs)	19.25 kg (42.43 lbs)	13.2127E-08 (3.0)

The code used in this analysis was verified to simulate the actual performance of the lead probe (Figs. 5 & 6). The prototype layer cake that was built by Bechtel/Nevada

was compared, both with experimental data and modeled data with the original lead probe as well (Table XVI). Then perhaps the comparable case listed above could be considered by those who wish to have the same performance as the original lead probe, but with a 51% reduction in weight.

It also should be noted that, due to the modular design of the layer cake geometry, that the optimized case studied here is only one such solution. The discoveries made during the course of this work, that “thinner is better” could lead to further optimum designs. This could be especially true in looking at even thinner layers of lead in a layer cake design (1mm or less). Of course, those designs would also be constrained by the same parameters as those in this work, namely, overall size, mass of lead and total weight.

References

- ¹ Ruby, L., and Rechen, J. B., “A fast-neutron activation detector for 14-MeV pulsed neutron sources,” Nuclear Instruments and Methods, **15**, 74 (1962).
- ² Spencer, C. E., and Jacobs, E. L., “The lead activation technique for high energy neutron measurement,” IEEE Transactions on Nuclear Science, NS-12, 407 (1965).
- ³ Ibid.
- ⁴ Matzen, K., *Phys. Plasmas* **4**, 1519 (1997).
- ⁵ Spielman, R. B., *et al.*, *Proceedings of the 9th IEEE Pulse Power Conference*, Albuquerque, NM, edited by R. White and K. Prestwich (Institute of Electrical and Electronics Engineers, New York, 1995), p. 396.
- ⁶ Ruby, L., and Rechen, J. B., “Activation detectors for 2.50 MeV pulsed neutron sources,” Nuclear Instruments and Methods, **53**, 290 (1967).
- ⁷ Rowland, M. S., “A Novel Fast Neutron Counting System for Short Bursts,” Ph.D. Dissertation, University of New Mexico, 1984.

⁸ Freeman, B., “Plasma Focus: Research Reasons for Continuing Efforts,” invited paper in the 4th International Symposium on Fusion Research, Washington, DC, March 12-16, 2001.

⁹ Seagraves, D. T., editor, “Practical MCNP for the Health Physicist, Rad Engineer, & Medical Physicist,” Version 4C, Los Alamos National Laboratory, (February 2000).

¹⁰ Shunk, E. R., Wagner, R. T., and Hemmendinger, A., “ $\text{Pb}^{207}(\text{n}, \text{n}')\text{Pb}^{207\text{m}}$ and $\text{Pb}^{208}(\text{n}, 2\text{n})\text{Pb}^{207\text{m}}$ Cross Sections,” Bulletin of the American Physical Society, Series 2, **7**, No. 4, 334, April 1962.

¹¹ www.nndc.bnl.gov/nndcscr/testwww/endl7155.txt.

¹² Editors, International Atomic Energy Agency, Handbook on Nuclear Activation Data, Technical Reports Series No. 273, 409, Vienna, 1987.

¹³ Personal communication with Erskine J. T. “Bud” Burns, Project Leader, Primary Standards Laboratory, Sandia National Laboratories, April 24, 2003.

¹⁴ Spencer, C. E., and Jacobs, E. L., “The lead activation technique for high energy neutron measurement,” IEEE Transactions on Nuclear Science, NS-12, 407 (1965).

¹⁵ Ruby, L., and Rechen, J. B., “Activation detectors for 2.50 MeV pulsed neutron sources,” Nuclear Instruments and Methods, **53**, 290 (1967).

¹⁶ Freeman, B., “Plasma Focus: Research Reasons for Continuing Efforts,” invited paper in the 4th International Symposium on Fusion Research, Washington, DC, March 12-16, 2001.

¹⁷ Cooper, G. W., and Ruiz, C. L., “NIF total neutron yield diagnostic,” Review of Scientific Instruments, **72**, Number 1, 814 (2001).

¹⁸ Ibid.

¹⁹ Spencer, C. E., and Jacobs, E. L., “The lead activation technique for high energy neutron measurement,” IEEE Transactions on Nuclear Science, NS-12, 407 (1965).

Appendices

Appendix A

MCNP Code Listing of Original Lead Probe

Part 1: F4 Neutron Tally

```
lmcnp      version 4c      ld=01/20/00      06/04/02 11:11:49
*****
probid =    06/04/02 11:11:49
inp=xspsnal outp=xspsnalo

1-      Pb-207m photons into scintillator
2-      c      **** MCNP INPUT DECK FOR ORIGINAL LEAD PROBE ****
3-      c      ***** XSPSNAL -- POINT SOURCE ****
4-      c      ***** 5 MIN RUN *****
5-      c      **** THIS IS ORIGINAL MODEL OF LEAD PROBE ****
6-      c      ***** WITH ALUMINUM INSERT ****
7-      c      **** NOTE: USING SHUNK, WAGNER & HEMMENDINGER CROSS SECTIONS (1962)
8-      c      THAT SPENCER & JACOBS USED (1965) ****
9-      c      Looking at a monoenergetic (2.5 MeV) neutron source
10-     c      striking the lead
11-     1      0 1 -3 -10
12-     2      1 -2.7 1 -2 10 -11
13-     3      2 -11.34 2 -3 10 -11
14-     4      2 -11.34 1 -3 11 -12
15-     5      2 -11.34 1 -3 12 -13
16-     6      2 -11.34 1 -3 13 -15
17-     7      2 -11.34 3 -4 14 -15
18-     8      0 3 -4 13 -14
19-     9      3 -1.032 3 -4 12 -13
20-    10      3 -1.032 3 -4 11 -12
21-    11      3 -1.032 3 -4 -11
22-    12      2 -11.34 4 -5 14 -15
23-    13      0 4 -5 13 -14
24-    14      3 -1.032 4 -5 12 -13
25-    15      3 -1.032 4 -5 11 -12
26-    16      3 -1.032 4 -5 -11
27-    17      2 -11.34 5 -6 14 -15
28-    18      0 5 -6 13 -14
29-    19      3 -1.032 5 -6 12 -13
30-    20      3 -1.032 5 -6 11 -12
31-    21      3 -1.032 5 -6 -11
32-    22      2 -11.34 6 -7 14 -15
33-    23      0 6 -7 13 -14
34-    24      3 -1.032 6 -7 12 -13
35-    25      3 -1.032 6 -7 11 -12
36-    26      3 -1.032 6 -7 -11
37-    27      2 -11.34 7 -8 14 -15
38-    28      0 7 -8 13 -14
39-    29      3 -1.032 7 -8 12 -13
40-    30      3 -1.032 7 -8 11 -12
41-    31      3 -1.032 7 -8 -11
42-    32      2 -11.34 8 -9 14 -15
43-    33      0 8 -9 13 -14
44-    34      3 -1.032 8 -9 12 -13
45-    35      3 -1.032 8 -9 11 -12
46-    36      3 -1.032 8 -9 -11
47-    37      0 16 -1 -15      $ Cell between point source and face
48-    38      0 -16:15:9      $ Universe outside detector -- kill zone
49-
50-     1      py 0
51-     2      py 1.27
52-     3      py 1.905
53-     4      py 4.022
54-     5      py 6.139
55-     6      py 8.256
```

```

56-      7      py 10.373
57-      8      py 12.49
58-      9      py 14.607
59-     10      cy 0.3175
60-     11      cy 1.27
61-     12      cy 3.81
62-     13      cy 6.35
63-     14      cy 6.695
64-     15      cy 8.6
65-     16      py -300.1    $ Plane near point source
66-
67-      c      **** Point Source of 2.5 MeV neutrons ****
68-      c      **** 3 meters from face of detector ****
69-      mode   n
70-      sdef   par=1 erg=2.5 pos=0 -300 0
71-      c      Aluminum G-11
72-      m1     13027 1
73-      c      Lead G-23
74-      m2     82000.50c 1    $ <==== NOTE: USING NEUTRON LIBRARY VALUE
75-      c      Plastic
76-      m3     1001 1.1 6000 1
77-      imp:n   1 36r 0
78-      cut:n   10000 0
79-      c      Total F4 Tally
80-      f4:n    3 4 5 6 7 12 17 22 27 32 t
81-      e4      1.6 1.7 1.8 1.9 2.0 2.1 2.2 2.3 2.4 2.5
82-      em4     0 0.0001 3.448 6.055 9.531 13.008 16.484
83-             19.9605 23.4369 26.9133
84-      c      **** Front Face Tally (Except Cell 3) ****
85-      fl4:n   4 5 6 t
86-      el4     1.6 1.7 1.8 1.9 2.0 2.1 2.2 2.3 2.4 2.5
87-      eml4    0 0.0001 3.448 6.055 9.531 13.008 16.484
88-             19.9605 23.4369 26.9133
89-      ctme   5

```

Effective Cross Sections input into the code as multipliers to the F4 tally – in units of millibarns (Note: they will be converted to cm² later)

neutron activity in each cell
print table 126

average	cell	average	population	collisions	collisions	number	flux
track weight	weight	entering			* weight	weighted	weighted
(relative)		track mfp			(per history)	energy	energy
		(cm)					
1	1	3	3	0	0.0000E+00	4.6472E-03	
2.3516E+00		9.8729E-01	0.0000E+00				
2	2	78	68	16	1.4947E-06	1.1147E-02	
1.9778E+00		9.9599E-01	5.6032E+00				
3	3	71	62	8	7.4730E-07	7.3717E-03	
1.6509E+00		9.9103E-01	4.2130E+00				
4	4	591	513	309	2.8461E-05	8.1071E-03	
2.0167E+00		9.9341E-01	4.1704E+00				
5	5	1109	984	607	5.6431E-05	1.4260E-02	
2.1214E+00		9.9631E-01	4.2533E+00				
6	6	1320	1209	634	5.9049E-05	2.2163E-02	
2.2488E+00		9.9815E-01	4.2051E+00				
7	7	1049	932	486	4.5144E-05	1.3678E-02	
2.1192E+00		9.9767E-01	4.2397E+00				
8	8	448	392	0	0.0000E+00	8.8022E-03	
1.9805E+00		9.9577E-01	0.0000E+00				
9	9	1068	869	1206	1.0854E-04	3.0610E-03	
1.6342E+00		9.8974E-01	3.5134E+00				
10	10	658	478	845	7.5151E-05	1.8237E-03	
1.4733E+00		9.8214E-01	3.2587E+00				
11	11	126	106	138	1.2242E-05	1.3099E-03	
1.3311E+00		9.7747E-01	3.0451E+00				
12	12	922	824	477	4.4043E-05	5.6294E-03	
1.8751E+00		9.9381E-01	4.2402E+00				
13	13	489	412	0	0.0000E+00	4.4482E-03	
1.8047E+00		9.9113E-01	0.0000E+00				

14	14	990	756	1404	1.2559E-04	1.5403E-03	
1.3278E+00	9.8336E-01	3.0325E+00		1050	9.1521E-05	1.0671E-03	
15	15	643	459				
1.1381E+00	9.7320E-01	2.7379E+00		147	1.2798E-05	1.0908E-03	
16	16	127	101				
1.0865E+00	9.7475E-01	2.6471E+00		314	2.8939E-05	5.1567E-03	
17	17	680	615				
1.7632E+00	9.9286E-01	4.2217E+00		0	0.0000E+00	4.7925E-03	
18	18	384	338				
1.8890E+00	9.9303E-01	0.0000E+00		1201	1.0648E-04	1.3030E-03	
19	19	823	621				
1.2036E+00	9.8109E-01	2.8368E+00		1100	9.5934E-05	6.4436E-04	9.5028E-
20	20	527	375				
01	9.6810E-01	2.4053E+00		106	9.3406E-06	1.2756E-03	
21	21	87	71				
1.0914E+00	9.7083E-01	2.6846E+00		256	2.3631E-05	3.8949E-03	
22	22	548	489				
1.6385E+00	9.9118E-01	4.2468E+00		0	0.0000E+00	3.7364E-03	
23	23	350	301				
1.7812E+00	9.8872E-01	0.0000E+00		971	8.6269E-05	1.1133E-03	
24	24	610	481				
1.1604E+00	9.7911E-01	2.7617E+00		639	5.5589E-05	8.6176E-04	
25	25	371	266				
1.0068E+00	9.7111E-01	2.5243E+00		112	9.6740E-06	8.0344E-04	9.2089E-
26	26	70	62				
01	9.5913E-01	2.4394E+00		187	1.7144E-05	3.3804E-03	
27	27	393	352				
1.5451E+00	9.8752E-01	4.2649E+00		0	0.0000E+00	4.6232E-03	
28	28	243	208				
1.8786E+00	9.8846E-01	0.0000E+00		711	6.2506E-05	1.0740E-03	
29	29	425	342				
1.1384E+00	9.7705E-01	2.7247E+00		464	4.0191E-05	1.0150E-03	
30	30	282	212				
1.0196E+00	9.7414E-01	2.5622E+00		61	5.0300E-06	1.1952E-03	
31	31	57	48				
1.0507E+00	9.6377E-01	2.6576E+00		120	1.1023E-05	5.0877E-03	
32	32	258	242				
1.6292E+00	9.9213E-01	4.3163E+00		0	0.0000E+00	8.0697E-03	
33	33	179	160				
1.9308E+00	9.9660E-01	0.0000E+00		397	3.5681E-05	1.5742E-03	
34	34	280	245				
1.2660E+00	9.8599E-01	2.9428E+00		310	2.7766E-05	1.1117E-03	9.2707E-
35	35	181	150				
01	9.8446E-01	2.4356E+00		63	5.3185E-06	8.2764E-04	8.0772E-
36	36	38	32				
01	9.6288E-01	2.2428E+00		0	0.0000E+00	2.4691E+00	
37	37	10704063	10703567				
2.4999E+00	1.0000E+00	0.0000E+00					

total 10720541 10717345 14339 1.2817E-03
tally 4 nps = 10703567
tally type 4 track length estimate of particle flux.
tally for neutrons

this tally is modified by cm, em or tm cards.

volumes		cell:	3	4	5	6	7
12	17						
			3.01649E+00	7.72222E+01	1.54444E+02	2.01311E+02	1.93783E+02
1.93783E+02	1.93783E+02						
		cell:	22	27	32	total	
			1.93783E+02	1.93783E+02	1.93783E+02	1.59869E+03	

cell	3	energy		
		1.6000E+00	0.00000E+00	0.0000
		1.7000E+00	0.00000E+00	0.0000
		1.8000E+00	0.00000E+00	0.0000
		1.9000E+00	0.00000E+00	0.0000
		2.0000E+00	1.17384E-06	0.5920

Total Volume of Lead (cm³)

Total Mass of Lead:

**1,598.69 cm³ x 11.34 grams/cm³ = 18,129.14 grams
= 18.129 kg
= 40 lbs**

2.1000E+00	9.99652E-08	1.0000
2.2000E+00	0.00000E+00	0.0000
2.3000E+00	0.00000E+00	0.0000
2.4000E+00	0.00000E+00	0.0000
2.5000E+00	2.30247E-05	0.1697
total	2.42985E-05	0.1653

cell 4

energy		
1.6000E+00	0.00000E+00	0.0000
1.7000E+00	2.36615E-12	0.3189
1.8000E+00	2.53300E-08	0.5219
1.9000E+00	2.35333E-07	0.2882
2.0000E+00	2.28046E-07	0.3966
2.1000E+00	1.03298E-07	0.5817
2.2000E+00	7.38223E-09	1.0000
2.3000E+00	6.71325E-09	1.0000
2.4000E+00	3.31689E-07	0.6550
2.5000E+00	2.82430E-05	0.0528
total	2.91808E-05	0.0532

cell 5

energy		
1.6000E+00	0.00000E+00	0.0000
1.7000E+00	9.08009E-13	0.3547
1.8000E+00	3.74023E-08	0.4143
1.9000E+00	2.85379E-07	0.2107
2.0000E+00	1.94187E-07	0.2692
2.1000E+00	1.61271E-07	0.5731
2.2000E+00	1.13684E-08	1.0000
2.3000E+00	0.00000E+00	0.0000
2.4000E+00	1.73985E-07	0.4007
2.5000E+00	2.86738E-05	0.0374
total	2.95374E-05	0.0371

cell 6

energy		
1.6000E+00	0.00000E+00	0.0000
1.7000E+00	8.49739E-13	0.4199
1.8000E+00	1.08713E-08	0.5199
1.9000E+00	1.22854E-07	0.2274
2.0000E+00	1.37577E-07	0.2991
2.1000E+00	3.57402E-08	0.6451
2.2000E+00	5.64764E-08	0.5343
2.3000E+00	0.00000E+00	0.0000
2.4000E+00	1.42200E-07	0.4476
2.5000E+00	2.77079E-05	0.0328
total	2.82136E-05	0.0327

cell 7

energy		
1.6000E+00	0.00000E+00	0.0000
1.7000E+00	7.99460E-13	0.3715
1.8000E+00	2.32109E-08	0.4373
1.9000E+00	8.36041E-08	0.2926
2.0000E+00	2.13529E-07	0.2799
2.1000E+00	4.13070E-08	0.4823
2.2000E+00	9.21588E-08	0.4316
2.3000E+00	6.59892E-08	0.5549
2.4000E+00	2.16072E-07	0.3308
2.5000E+00	2.07155E-05	0.0405
total	2.14513E-05	0.0398

cell 12

energy		
1.6000E+00	0.00000E+00	0.0000
1.7000E+00	7.38961E-13	0.3793
1.8000E+00	2.23664E-08	0.5174
1.9000E+00	9.27075E-08	0.2669
2.0000E+00	1.08517E-07	0.2871
2.1000E+00	7.94962E-08	0.4182

2.2000E+00	5.34230E-08	0.5034
2.3000E+00	1.41854E-07	0.3783
2.4000E+00	2.90607E-07	0.2787
2.5000E+00	1.48222E-05	0.0480
total	1.56112E-05	0.0466

cell 17

energy		
1.6000E+00	0.00000E+00	0.0000
1.7000E+00	8.14344E-13	0.3648
1.8000E+00	6.77000E-09	0.5950
1.9000E+00	7.58634E-08	0.3243
2.0000E+00	8.35715E-08	0.3533
2.1000E+00	3.00552E-08	0.6693
2.2000E+00	1.08919E-07	0.4483
2.3000E+00	1.78733E-07	0.4174
2.4000E+00	2.63895E-07	0.2878
2.5000E+00	9.61198E-06	0.0597
total	1.03598E-05	0.0572

cell 22

energy		
1.6000E+00	0.00000E+00	0.0000
1.7000E+00	8.45323E-13	0.4138
1.8000E+00	2.29847E-08	0.3858
1.9000E+00	5.31890E-08	0.4282
2.0000E+00	5.36392E-08	0.4329
2.1000E+00	1.22919E-08	1.0000
2.2000E+00	3.49295E-08	0.7267
2.3000E+00	1.24378E-07	0.4519
2.4000E+00	2.90133E-07	0.3149
2.5000E+00	7.01597E-06	0.0714
total	7.60751E-06	0.0682

cell 27

energy		
1.6000E+00	0.00000E+00	0.0000
1.7000E+00	6.44374E-13	0.4581
1.8000E+00	1.51810E-08	0.4290
1.9000E+00	3.05121E-08	0.3983
2.0000E+00	9.31244E-08	0.3476
2.1000E+00	5.00328E-10	1.0000
2.2000E+00	4.74862E-08	0.6917
2.3000E+00	7.17633E-08	0.4942
2.4000E+00	1.88504E-07	0.3719
2.5000E+00	4.37446E-06	0.0854
total	4.82153E-06	0.0815

cell 32

energy		
1.6000E+00	0.00000E+00	0.0000
1.7000E+00	3.57477E-13	0.5332
1.8000E+00	2.42960E-08	0.4613
1.9000E+00	8.38207E-09	0.7593
2.0000E+00	4.82805E-08	0.4406
2.1000E+00	3.04844E-08	0.6399
2.2000E+00	3.90029E-08	0.5780
2.3000E+00	8.05038E-08	0.5177
2.4000E+00	7.19966E-08	0.4916
2.5000E+00	3.00561E-06	0.1023
total	3.30856E-06	0.0960

cell union total

energy		
1.6000E+00	0.00000E+00	0.0000
1.7000E+00	8.18103E-13	0.1936
1.8000E+00	2.01222E-08	0.2102
1.9000E+00	9.61358E-08	0.1345
2.0000E+00	1.22122E-07	0.1505
2.1000E+00	4.87904E-08	0.3002
2.2000E+00	5.41330E-08	0.2692

2.3000E+00 8.07155E-08 0.2285
 2.4000E+00 2.10884E-07 0.1594
 2.5000E+00 1.48845E-05 0.0284
total 1.55174E-05 0.0279

lanalysis of the results in the tally fluctuation chart bin (tfc) for tally 4 with nps
 = 10703567 print table 160

**Total F4 Tally, in units of millibarns/cm²
 (Fluence times cross section)**

tally 14 nps = 10703567
 tally type 4 track length estimate of particle flux.
 tally for neutrons

this tally is modified by cm, em or tm cards.

volumes

cell:	4	5	6	total
	7.72222E+01	1.54444E+02	2.01311E+02	4.32978E+02

cell 4
 energy
 1.6000E+00 0.00000E+00 0.0000
 1.7000E+00 2.36615E-12 0.3189
 1.8000E+00 2.53300E-08 0.5219
 1.9000E+00 2.35333E-07 0.2882
 2.0000E+00 2.28046E-07 0.3966
 2.1000E+00 1.03298E-07 0.5817
 2.2000E+00 7.38223E-09 1.0000
 2.3000E+00 6.71325E-09 1.0000
 2.4000E+00 3.31689E-07 0.6550
 2.5000E+00 2.82430E-05 0.0528
 total 2.91808E-05 0.0532

Converting F4 tally from millibarns/cm² to reactions/cm³:

(1.55174E-05 millibarns/cm²) x (10⁻²⁷ cm²/millibarns) x (3.296 x 10²² atoms/cm³, atomic density of lead)

→ 5.1145E-10 n reactions/cm³

cell 5
 energy
 1.6000E+00 0.00000E+00 0.0000
 1.7000E+00 9.08009E-13 0.3547
 1.8000E+00 3.74023E-08 0.4143
 1.9000E+00 2.85379E-07 0.2107
 2.0000E+00 1.94187E-07 0.2692
 2.1000E+00 1.61271E-07 0.5731
 2.2000E+00 1.13684E-08 1.0000
 2.3000E+00 0.00000E+00 0.0000
 2.4000E+00 1.73985E-07 0.4007
 2.5000E+00 2.86738E-05 0.0374
 total 2.95374E-05 0.0371

cell 6
 energy
 1.6000E+00 0.00000E+00 0.0000
 1.7000E+00 8.49739E-13 0.4199
 1.8000E+00 1.08713E-08 0.5199
 1.9000E+00 1.22854E-07 0.2274
 2.0000E+00 1.37577E-07 0.2991
 2.1000E+00 3.57402E-08 0.6451
 2.2000E+00 5.64764E-08 0.5343
 2.3000E+00 0.00000E+00 0.0000
 2.4000E+00 1.42200E-07 0.4476
 2.5000E+00 2.77079E-05 0.0328
 total 2.82136E-05 0.0327

cell union total
 energy
 1.6000E+00 0.00000E+00 0.0000
 1.7000E+00 1.14098E-12 0.2510
 1.8000E+00 2.29137E-08 0.3091
 1.9000E+00 2.00888E-07 0.1480
 2.0000E+00 1.73905E-07 0.2055
 2.1000E+00 9.25664E-08 0.5220
 2.2000E+00 3.16302E-08 0.4889
 2.3000E+00 1.19732E-09 1.0000
 2.4000E+00 1.87333E-07 0.3453

```

2.5000E+00  2.81479E-05 0.0248
total      2.88583E-05 0.0249
lanalysis of the results in the tally fluctuation chart bin (tfc) for tally 14 with nps
= 10703567 print table 160
*****
*****
dump no.    2 on file runtpe      nps = 10703567      coll =      14339      ctm =
5.00      nrn =      27465346

```

5 warning messages so far.

run terminated when it had used 5 minutes of computer time.

computer time = 5.02 minutes

```

mcnp      version 4c      01/20/00      06/04/02 11:16:50
probid = 06/04/02 11:11:49

```

MCNP Code Listing of Original Lead Probe

Part 2: F8 Counts Tally and F6 Energy Deposited Tally

```

lmcpn      version 4c      ld=01/20/00      06/04/02 15:20:02
*****
probid = 06/04/02 15:20:02
inp=xspsgal outp=xspsgalo

1-      Pb-207m photons into scintillator
2-      c      ***** New Cross Sections, Point Source 1 for Gammas *****
3-      c      **** XSPSGAL -- 5 MIN RUN TO COMPARE WITH XSPSG1 (1000 MIN RUN) ****
4-      c      ***** THIS IS THE ORIGINAL MODEL OF THE LEAD PROBE *****
5-      c      ***** WITH ALUMINUM INSERT *****
6-      c      **** This is a Redo because I want to run it again with
7-      c      **** an F4 Tally for Cells 4, 5 & 6 to use in normalizing
8-      c      **** all the lead; also used neutron library value ****
9-      c      **** ALSO DOING IT WITH USING SHUNK, WAGNER & HEMMENDINGER
10-     c      CROSS SECTIONS FOR PB-207 THAT SPENCER & JACOBS USED (1965) ****
11-     c      Looking at Energy Deposited (F6) and Interactions (F8)
12-     c      in Plastic Scintillator
13-     1      0 1 -3 -10
14-     2      1 -2.7 1 -2 10 -11
15-     3      2 -11.34 2 -3 10 -11
16-     4      2 -11.34 1 -3 11 -12
17-     5      2 -11.34 1 -3 12 -13
18-     6      2 -11.34 1 -3 13 -15
19-     7      2 -11.34 3 -4 14 -15
20-     8      0 3 -4 13 -14
21-     9      3 -1.032 3 -4 12 -13
22-     10     3 -1.032 3 -4 11 -12
23-     11     3 -1.032 3 -4 -11
24-     12     2 -11.34 4 -5 14 -15
25-     13     0 4 -5 13 -14
26-     14     3 -1.032 4 -5 12 -13
27-     15     3 -1.032 4 -5 11 -12
28-     16     3 -1.032 4 -5 -11
29-     17     2 -11.34 5 -6 14 -15
30-     18     0 5 -6 13 -14
31-     19     3 -1.032 5 -6 12 -13
32-     20     3 -1.032 5 -6 11 -12
33-     21     3 -1.032 5 -6 -11
34-     22     2 -11.34 6 -7 14 -15
35-     23     0 6 -7 13 -14
36-     24     3 -1.032 6 -7 12 -13

```

```

37-      25      3 -1.032 6 -7 11 -12
38-      26      3 -1.032 6 -7 -11
39-      27      2 -11.34 7 -8 14 -15
40-      28      0 7 -8 13 -14
41-      29      3 -1.032 7 -8 12 -13
42-      30      3 -1.032 7 -8 11 -12
43-      31      3 -1.032 7 -8 -11
44-      32      2 -11.34 8 -9 14 -15
45-      33      0 8 -9 13 -14
46-      34      3 -1.032 8 -9 12 -13
47-      35      3 -1.032 8 -9 11 -12
48-      36      3 -1.032 8 -9 -11
49-      37      0 -1:15:9          $ Universe outside detector -- kill zone
50-
51-      1      py 0
52-      2      py 1.27
53-      3      py 1.905
54-      4      py 4.022
55-      5      py 6.139
56-      6      py 8.256
57-      7      py 10.373
58-      8      py 12.49
59-      9      py 14.607
60-     10      cy 0.3175
61-     11      cy 1.27
62-     12      cy 3.81
63-     13      cy 6.35
64-     14      cy 6.695
65-     15      cy 8.6
66-
67-      c      **** Volumetric source in the lead sheath ****
68-      c      Based on data from monoenergetic (2.5 MeV) neutron
69-      c      source normal to the face, activating the lead
70-     mode    p
71-     sdef    par=2 erg=d1 axs=0 1 0
72-            rad=d2 pos=frad=d11 ext=frad=d12
73-     si1     L 0.5697 1.0636 $ gamma energies
74-     sp1     d 0.525 0.475 $ weighted branching ratios
75-      c
76-      c      3 = cell 3; 4 = cells 4, 5 & 6; 5 = cell 7;
77-      c      6 = cell 12; 7 = cell 17; 8 = cell 22;
78-      c      9 = cell 27; 10 = cell 32
79-      c
80-     si2     s 3 4 5 6 7 8 9 10
81-      c      %tage of volume of 3, 4, 5 - 10 times a
82-      c      normalized factor based on cells 4, 5, 6:
83-     sp2     0.001589 0.2708 0.090092 0.065564 0.043509 0.031950 0.020250 0.013895
84-     si3     0.3175 1.27 $ dimensions of 3
85-     sp3     -21 1
86-     si4     1.27 8.6          $ dimensions of 4 (Front Face)
87-     sp4     -21 1
88-     si5     6.695 8.6        $ dimensions of 5; cell 7
89-     sp5     -21 1
90-     si6     6.695 8.6        $ dimensions of 6; cell 12
91-     sp6     -21 1
92-     si7     6.695 8.6        $ dimensions of 7; cell 17
93-     sp7     -21 1
94-     si8     6.695 8.6        $ dimensions of 8; cell 22
95-     sp8     -21 1
96-     si9     6.695 8.6        $ dimensions of 9; cell 27
97-     sp9     -21 1
98-     si10    6.695 8.6        $ dimensions of 10; cell 32
99-     sp10    -21 1
100-    ds11    L 0 1.27 0 0 0 0 0 1.905 0 0 4.022 0 0 6.139 0
101-           0 8.256 0 0 10.373 0 0 12.49 0
102-    ds12    s 13 14 15 16 17 18 19 20
103-    si13    0 0.635 $ length of 3
104-    si14    0 1.905 $ length of 4
105-    si15    0 2.117 $ length of 5; cell 7
106-    si16    0 2.117 $ length of 6; cell 12
107-    si17    0 2.117 $ length of 7; cell 17

```



```

108-      si18  0 2.117 $ length of 8; cell 22
109-      si19  0 2.117 $ length of 9; cell 27
110-      si20  0 2.117 $ length of 10; cell 32
111-      c
112-      c      Aluminum G-11
113-      m1     13027 1
114-      c      Lead G-23
115-      m2     82000 1
116-      c      Plastic
117-      m3     1001 1.1 6000 1
118-      imp:p  1 35r 0
119-      cut:n   10000 0
120-      f6:p   9 10 11 14 15 16 19 20 21 24 25 26 29 30
121-          31 34 35 36 t
122-      f8:p   9 10 11 14 15 16 19 20 21 24 25 26 29 30
123-          31 34 35 36 t
124-      e8     0 1e-10 1.1
125-      ctme 3

tally  6      nps = 1022359
          tally type 6      track length estimate of heating.          units      mev/gram
          tally for photons

          masses
          cell:      9          10          11          14          15
16      19
          1.77124E+02  8.85621E+01  1.10703E+01  1.77124E+02  8.85621E+01
1.10703E+01  1.77124E+02
          cell:      20          21          24          25          26
29      30
          8.85621E+01  1.10703E+01  1.77124E+02  8.85621E+01  1.10703E+01
1.77124E+02  8.85621E+01
          cell:      31          34          35          36          total
          1.10703E+01  1.77124E+02  8.85621E+01  1.10703E+01  1.66054E+03

cell  9
          2.24962E-05  0.0046

cell  10
          2.11260E-05  0.0068

cell  11
          1.94816E-05  0.0154

cell  14
          1.72079E-05  0.0052

cell  15
          1.61570E-05  0.0075

cell  16
          1.57686E-05  0.0167

cell  19
          1.29571E-05  0.0060

cell  20
          1.24168E-05  0.0084

cell  21
          1.22486E-05  0.0189

cell  24
          9.64699E-06  0.0069

cell  25
          9.37505E-06  0.0096

cell  26
          8.87250E-06  0.0222

```

Total Mass of Scintillator (grams)

Total Energy Deposited:
(1.21191E-05 MeV/gram) x (1,660.54 grams)
= 0.020124 MeV

Efficiency = 0.020124 MeV/0.8 MeV = 0.0252
→ 2.52%

(Note: 0.8 MeV is weighted average of both gammas)

```

cell 29
7.03477E-06 0.0079

cell 30
6.81473E-06 0.0110

cell 31
6.48803E-06 0.0257

cell 34
4.75525E-06 0.0094

cell 35
4.71852E-06 0.0129

cell 36
4.56518E-06 0.0305

cell union total
1.21191E-05 0.0034
lanalysis of the results in the tally fluctuation chart bin (tfc) for tally 6 with nps
= 1022359 print table 160

tally 8 nps = 1022359
tally type 8 pulse height distribution. units number
tally for photons

cell 9
energy
0.0000E+00 0.00000E+00 0.0000
1.0000E-10 5.72509E-02 0.0040
1.1000E+00 1.36840E-02 0.0084
total 7.09350E-02 0.0036

cell 10
energy
0.0000E+00 0.00000E+00 0.0000
1.0000E-10 2.65484E-02 0.0060
1.1000E+00 6.80974E-03 0.0119
total 3.33581E-02 0.0053

cell 11
energy
0.0000E+00 0.00000E+00 0.0000
1.0000E-10 5.41493E-03 0.0134
1.1000E+00 9.43895E-04 0.0322
total 6.35882E-03 0.0124

cell 14
energy
0.0000E+00 0.00000E+00 0.0000
1.0000E-10 4.54097E-02 0.0045
1.1000E+00 1.17082E-02 0.0091
total 5.71179E-02 0.0040

cell 15
energy
0.0000E+00 0.00000E+00 0.0000
1.0000E-10 2.17614E-02 0.0066
1.1000E+00 5.85900E-03 0.0129
total 2.76204E-02 0.0059

cell 16
energy
0.0000E+00 0.00000E+00 0.0000
1.0000E-10 4.78110E-03 0.0143
1.1000E+00 8.04023E-04 0.0349
total 5.58512E-03 0.0132

cell 19

```

Total MeV/gram

energy			
0.0000E+00	0.00000E+00	0.0000	
1.0000E-10	3.58446E-02	0.0051	
1.1000E+00	9.06727E-03	0.0103	
total	4.49118E-02	0.0046	
cell 20			
energy			
0.0000E+00	0.00000E+00	0.0000	
1.0000E-10	1.78000E-02	0.0073	
1.1000E+00	4.68720E-03	0.0144	
total	2.24872E-02	0.0065	
cell 21			
energy			
0.0000E+00	0.00000E+00	0.0000	
1.0000E-10	3.84699E-03	0.0159	
1.1000E+00	7.21860E-04	0.0368	
total	4.56885E-03	0.0146	
cell 24			
energy			
0.0000E+00	0.00000E+00	0.0000	
1.0000E-10	2.76899E-02	0.0059	
1.1000E+00	7.07090E-03	0.0117	
total	3.47608E-02	0.0052	
cell 25			
energy			
0.0000E+00	0.00000E+00	0.0000	
1.0000E-10	1.39520E-02	0.0083	
1.1000E+00	3.74526E-03	0.0161	
total	1.76973E-02	0.0074	
cell 26			
energy			
0.0000E+00	0.00000E+00	0.0000	
1.0000E-10	2.89918E-03	0.0183	
1.1000E+00	5.23300E-04	0.0432	
total	3.42248E-03	0.0169	
cell 29			
energy			
0.0000E+00	0.00000E+00	0.0000	
1.0000E-10	2.09545E-02	0.0068	
1.1000E+00	5.09117E-03	0.0138	
total	2.60456E-02	0.0060	
cell 30			
energy			
0.0000E+00	0.00000E+00	0.0000	
1.0000E-10	1.06822E-02	0.0095	
1.1000E+00	2.79256E-03	0.0187	
total	1.34747E-02	0.0085	
cell 31			
energy			
0.0000E+00	0.00000E+00	0.0000	
1.0000E-10	2.12450E-03	0.0214	
1.1000E+00	3.80493E-04	0.0507	
total	2.50499E-03	0.0197	
cell 34			
energy			
0.0000E+00	0.00000E+00	0.0000	
1.0000E-10	1.54124E-02	0.0079	
1.1000E+00	3.35205E-03	0.0171	
total	1.87644E-02	0.0072	
cell 35			
energy			

0.0000E+00	0.00000E+00	0.0000
1.0000E-10	7.96785E-03	0.0110
1.1000E+00	1.90638E-03	0.0226
total	9.87422E-03	0.0099

cell 36

energy		
0.0000E+00	0.00000E+00	0.0000
1.0000E-10	1.50534E-03	0.0255
1.1000E+00	2.60183E-04	0.0613
total	1.76552E-03	0.0235

cell union total

energy		
0.0000E+00	0.00000E+00	0.0000
1.0000E-10	6.02098E-02	0.0039
1.1000E+00	5.39175E-02	0.0041
total	1.14127E-01	0.0028

F8 Tally = 0.114127 – 0.0602098
= 0.053917 ← Counts in Scintillator

lanalysis of the results in the tally fluctuation chart bin (tfc) for tally 8 with nps
= 1022359 print table 160

dump no. 2 on file runtpe nps = 1022359 coll = 3776912 ctm =
3.00 nrn = 45365749

3 warning messages so far.

run terminated when it had used 3 minutes of computer time.

computer time = 3.07 minutes

mcnp version 4c 01/20/00 06/04/02 15:23:06
probid = 06/04/02 15:20:02

Figure of Merit Calculation for Original Lead Probe

FOM = F4 Tally (reactions/cm³) x F8 Tally (Counts) x Volume of Lead (cm³)

FOM = (5.1145E-10 reactions/cm³) x (0.053917 counts) x (1,598.69 cm³)

= 4.41E-08 Reactions x Counts

See Table IV, p. 26.

MCNP Code Listing of Optimized Layer Cake

Part 3: F4 Neutron Tally

```
lmcnp      version 4c      ld=01/20/00      12/09/02 15:14:24
*****
probid =   12/09/02 15:14:24
inp=xn9qa2a outp=xn9qa2ao

1-      Pb-207m photons into scintillator
2-      c      ***** XN9QA2A -- POINT SOURCE -- 5 MIN *****
3-      c      ***** 15 CM OUTER RADIUS; 28.28 LBS LEAD *****
4-      c      ***** 8 LAYERS LEAD @ 0.2 CM; 8 PLASTIC @ 1.1 CM *****
5-      c      ***** NO SHEATH ***
6-      c      **** USING SPENCER & JACOBS CROSS SECTIONS FOR PB-207
7-      c      Looking at a monoenergetic point source of DD neutrons
8-      c      striking the lead
9-      1      1 -11.34 1 -2 -18
10-     2      1 -11.34 1 -2 18 -19
11-     3      1 -11.34 3 -4 -18
12-     4      1 -11.34 3 -4 18 -19
13-     5      1 -11.34 5 -6 -18
14-     6      1 -11.34 5 -6 18 -19
15-     7      1 -11.34 7 -8 -18
16-     8      1 -11.34 7 -8 18 -19
17-     9      1 -11.34 9 -10 -18
18-    10      1 -11.34 9 -10 18 -19
19-    11      1 -11.34 11 -12 -18
20-    12      1 -11.34 11 -12 18 -19
21-    13      1 -11.34 13 -14 -18
22-    14      1 -11.34 13 -14 18 -19
23-    15      1 -11.34 15 -16 -18
24-    16      1 -11.34 15 -16 18 -19
25-    17      2 -1.032 2 -3 -18
26-    18      2 -1.032 2 -3 18 -19
27-    19      2 -1.032 4 -5 -18
28-    20      2 -1.032 4 -5 18 -19
29-    21      2 -1.032 6 -7 -18
30-    22      2 -1.032 6 -7 18 -19
31-    23      2 -1.032 8 -9 -18
32-    24      2 -1.032 8 -9 18 -19
33-    25      2 -1.032 10 -11 -18
34-    26      2 -1.032 10 -11 18 -19
35-    27      2 -1.032 12 -13 -18
36-    28      2 -1.032 12 -13 18 -19
37-    29      2 -1.032 14 -15 -18
38-    30      2 -1.032 14 -15 18 -19
39-    31      2 -1.032 16 -17 -18
40-    32      2 -1.032 16 -17 18 -19
41-    33      0 20 -1 -19      $ Cell between neutron source and face
42-    34      0 -20:19:17      $ Universe outside detector -- kill zone
43-
44-      c      **** 0.2 cm Lead; 1.1 cm Plastic ****
45-      1      py 0.0
46-      2      py 0.2
47-      3      py 1.3
48-      4      py 1.5
49-      5      py 2.6
50-      6      py 2.8
51-      7      py 3.9
52-      8      py 4.1
53-      9      py 5.2
54-     10      py 5.4
55-     11      py 6.5
56-     12      py 6.7
57-     13      py 7.8
58-     14      py 8.0
59-     15      py 9.1
```

```

60-      16      py 9.3
61-      17      py 10.4
62-      18      cy 7.5
63-      19      cy 15.0
64-      20      py -300.1      $ Plane near point source
65-
66-      c      **** POINT SOURCE of 2.5 MeV neutrons ****
67-      c      **** 3 meters from face of detector ****
68-      mode n
69-      sdef par=1 erg=2.5 pos=0 -300 0
70-      c      Lead G-23
71-      m1      82000.50c 1      $ <===== NOTE: USING NEUTRON LIBRARY VALUE
72-      c      Plastic
73-      m2      1001 1.1 6000 1
74-      imp:n 1 32r 0
75-      cut:n 10000 0
76-      c      f4 tally
77-      f4:n 1 2 3 4 5 6 7 8 9 10 11 12 13 14 15 16 t
78-      e4      1.6 1.7 1.8 1.9 2.0 2.1 2.2 2.3 2.4 2.5
79-      em4      0 0.0001 3.448 6.055 9.531 13.008 16.4844
80-      19.9605 23.4369 26.9133
81-      c
82-      c      f4 tally -- individual sections
83-      c      *** front face ***
84-      f14:n 1 2 t
85-      e14      1.6 1.7 1.8 1.9 2.0 2.1 2.2 2.3 2.4 2.5
86-      em14      0 0.0001 3.448 6.055 9.531 13.008 16.4844
87-      19.9605 23.4369 26.9133
88-      c      *** Layer "A" ***
89-      f24:n 3 4 t
90-      e24      1.6 1.7 1.8 1.9 2.0 2.1 2.2 2.3 2.4 2.5
91-      em24      0 0.0001 3.448 6.055 9.531 13.008 16.4844
92-      19.9605 23.4369 26.9133
93-      c      *** Layer "B" ***
94-      f34:n 5 6 t
95-      e34      1.6 1.7 1.8 1.9 2.0 2.1 2.2 2.3 2.4 2.5
96-      em34      0 0.0001 3.448 6.055 9.531 13.008 16.4844
97-      19.9605 23.4369 26.9133
98-      c      *** Layer "C" ***
99-      f44:n 7 8 t
100-     e44      1.6 1.7 1.8 1.9 2.0 2.1 2.2 2.3 2.4 2.5
101-     em44      0 0.0001 3.448 6.055 9.531 13.008 16.4844
102-     19.9605 23.4369 26.9133
103-     c      *** Layer "D" ***
104-     f54:n 9 10 t
105-     e54      1.6 1.7 1.8 1.9 2.0 2.1 2.2 2.3 2.4 2.5
106-     em54      0 0.0001 3.448 6.055 9.531 13.008 16.4844
107-     19.9605 23.4369 26.9133
108-     c      *** Layer "E" ***
109-     f64:n 11 12 t
110-     e64      1.6 1.7 1.8 1.9 2.0 2.1 2.2 2.3 2.4 2.5
111-     em64      0 0.0001 3.448 6.055 9.531 13.008 16.4844
112-     19.9605 23.4369 26.9133
113-     c      *** Layer "F" ***
114-     f74:n 13 14 t
115-     e74      1.6 1.7 1.8 1.9 2.0 2.1 2.2 2.3 2.4 2.5
116-     em74      0 0.0001 3.448 6.055 9.531 13.008 16.4844
117-     19.9605 23.4369 26.9133
118-     c      *** Layer "G" ***
119-     f84:n 15 16 t
120-     e84      1.6 1.7 1.8 1.9 2.0 2.1 2.2 2.3 2.4 2.5
121-     em84      0 0.0001 3.448 6.055 9.531 13.008 16.4844
122-     19.9605 23.4369 26.9133
123-     ctme 5

```

```

neutron activity in each cell
print table 126

```

	tracks	population	collisions	collisions	number	flux
average	average					

cell track weight	entering track mfp				* weight (per history)	weighted energy	weighted energy
(relative)	(cm)						
1	1	2239	1907	140	1.2901E-05	4.0754E-03	
1.8945E+00	9.9082E-01	3.9920E+00					
2	2	6202	5223	386	3.5571E-05	8.3654E-03	
2.0370E+00	9.9553E-01	4.0773E+00					
3	3	2469	1810	183	1.6561E-05	1.3067E-03	
1.3389E+00	9.8184E-01	4.0126E+00					
4	4	6298	4847	472	4.2931E-05	2.5226E-03	
1.5706E+00	9.8838E-01	4.0466E+00					
5	5	2354	1672	200	1.8175E-05	1.0955E-03	
1.1930E+00	9.7899E-01	3.8890E+00					
6	6	6111	4424	466	4.2330E-05	1.6376E-03	
1.3748E+00	9.8478E-01	4.0509E+00					
7	7	2354	1552	255	2.2803E-05	7.1693E-04	
1.0003E+00	9.7236E-01	3.9280E+00					
8	8	5698	3968	480	4.3328E-05	1.2262E-03	
1.2085E+00	9.7919E-01	4.0063E+00					
9	9	2208	1418	207	1.8528E-05	7.3541E-04	9.1116E-
01 9.7444E-01	3.9001E+00						
10	10	5014	3488	451	4.0693E-05	1.0123E-03	
1.1173E+00	9.7821E-01	3.9978E+00					
11	11	1904	1222	165	1.4567E-05	5.3984E-04	8.8125E-
01 9.6177E-01	3.8563E+00						
12	12	4359	3050	397	3.5428E-05	1.0093E-03	
1.0798E+00	9.7604E-01	3.9904E+00					
13	13	1555	1052	157	1.4007E-05	4.8885E-04	8.3766E-
01 9.6197E-01	3.8370E+00						
14	14	3597	2617	341	3.0777E-05	8.9386E-04	
1.0026E+00	9.7775E-01	3.9505E+00					
15	15	1201	904	113	1.0094E-05	5.3261E-04	8.8158E-
01 9.6810E-01	3.8752E+00						
16	16	2705	2192	245	2.2172E-05	9.5063E-04	
1.0506E+00	9.8041E-01	3.9626E+00					
17	17	2485	1958	2057	1.8147E-04	1.8489E-03	
1.5543E+00	9.8359E-01	3.3589E+00					
18	18	6484	5236	4527	4.0569E-04	3.4246E-03	
1.7231E+00	9.9036E-01	3.6291E+00					
19	19	2577	1851	2795	2.4446E-04	1.1586E-03	
1.2526E+00	9.7869E-01	2.8917E+00					
20	20	6463	4853	5776	5.1236E-04	1.8546E-03	
1.4431E+00	9.8571E-01	3.2018E+00					
21	21	2526	1731	3291	2.8742E-04	7.7807E-04	
1.0583E+00	9.7364E-01	2.5826E+00					
22	22	6215	4423	6543	5.8044E-04	1.3581E-03	
1.2522E+00	9.8228E-01	2.9062E+00					
23	23	2483	1608	3495	3.0721E-04	6.9504E-04	9.3170E-
01 9.7407E-01	2.3804E+00						
24	24	5647	3970	6700	5.9145E-04	1.0398E-03	
1.1228E+00	9.7946E-01	2.6996E+00					
25	25	2240	1459	3384	2.9597E-04	6.4486E-04	8.7547E-
01 9.6976E-01	2.2974E+00						
26	26	4972	3488	6151	5.4022E-04	9.4888E-04	
1.0688E+00	9.7686E-01	2.6157E+00					
27	27	1896	1265	2956	2.5394E-04	4.7944E-04	8.0432E-
01 9.6127E-01	2.1710E+00						
28	28	4217	3061	5446	4.7930E-04	8.7512E-04	
1.0133E+00	9.7622E-01	2.5307E+00					
29	29	1496	1095	2373	2.0533E-04	5.1008E-04	8.0904E-
01 9.6437E-01	2.1880E+00						
30	30	3320	2596	4157	3.6436E-04	8.2472E-04	
1.0153E+00	9.7546E-01	2.5297E+00					
31	31	1029	920	1404	1.2195E-04	7.1083E-04	9.3406E-
01 9.7244E-01	2.4097E+00						
32	32	2360	2180	2627	2.3227E-04	1.1425E-03	
1.1020E+00	9.8109E-01	2.6872E+00					
33	33	10780161	10778451	0	0.0000E+00	2.1211E+00	
2.4995E+00	1.0000E+00	0.0000E+00					

total 10892839 10861491 68340 6.0247E-03
tally 4 nps = 10778451
tally type 4 track length estimate of particle flux.
tally for neutrons

this tally is modified by cm, em or tm cards.

volumes

	cell:	1	2	3	4	5
6	7					
		3.53429E+01	1.06029E+02	3.53429E+01	1.06029E+02	3.53429E+01
1.06029E+02	3.53429E+01					
	cell:	8	9	10	11	12
13	14					
		1.06029E+02	3.53429E+01	1.06029E+02	3.53429E+01	1.06029E+02
3.53429E+01	1.06029E+02					
	cell:	15	16	total		
		3.53429E+01	1.06029E+02	1.13097E+03		

cell 1
energy

1.6000E+00	0.00000E+00	0.0000
1.7000E+00	7.96758E-13	0.3107
1.8000E+00	3.56337E-08	0.2628
1.9000E+00	2.00625E-07	0.1627
2.0000E+00	2.75395E-07	0.2159
2.1000E+00	1.49410E-07	0.4990
2.2000E+00	1.79824E-08	0.7073
2.3000E+00	6.13742E-08	0.5129
2.4000E+00	5.50582E-08	0.5017
2.5000E+00	2.59639E-05	0.0327
total	2.67594E-05	0.0324

Total Volume of Lead (cm³)

Total Mass of Lead:

1,130.97 cm³ x 11.34 grams/cm³ = 12,825.20 grams
= 12.83 kg
= 28.28 lbs

cell 2
energy

1.6000E+00	0.00000E+00	0.0000
1.7000E+00	1.02775E-12	0.4179
1.8000E+00	4.11907E-08	0.1704
1.9000E+00	1.74769E-07	0.0908
2.0000E+00	3.58269E-07	0.1454
2.1000E+00	1.79455E-07	0.2825
2.2000E+00	6.06392E-08	0.6490
2.3000E+00	2.92439E-08	0.4153
2.4000E+00	4.98592E-08	0.4553
2.5000E+00	2.53935E-05	0.0219
total	2.62870E-05	0.0216

Percentage Volume per Layer:

Percentage Volume = Volume of lead layer/Total Volume
= 141.372 cm³/1,130.97 cm³
= 0.125

Note: All layers have equal volume of lead.

cell 3
energy

1.6000E+00	0.00000E+00	0.0000
1.7000E+00	1.38838E-12	0.2477
1.8000E+00	7.18772E-08	0.2800
1.9000E+00	2.15433E-07	0.1402
2.0000E+00	2.11576E-07	0.2088
2.1000E+00	3.01385E-07	0.3773
2.2000E+00	4.17086E-07	0.2941
2.3000E+00	3.81299E-07	0.2444
2.4000E+00	6.67059E-07	0.1995
2.5000E+00	2.03280E-05	0.0297
total	2.25937E-05	0.0295

cell 4
energy

1.6000E+00	0.00000E+00	0.0000
1.7000E+00	1.21507E-12	0.1622
1.8000E+00	7.13489E-08	0.1850
1.9000E+00	2.32049E-07	0.0894
2.0000E+00	2.93896E-07	0.1867
2.1000E+00	2.70886E-07	0.2037
2.2000E+00	2.32461E-07	0.2013

2.3000E+00	4.31349E-07	0.1365
2.4000E+00	4.95623E-07	0.2344
2.5000E+00	2.00027E-05	0.0177
total	2.20304E-05	0.0181

cell 5

energy		
1.6000E+00	0.00000E+00	0.0000
1.7000E+00	1.20560E-12	0.2398
1.8000E+00	8.85178E-08	0.2279
1.9000E+00	1.96054E-07	0.1667
2.0000E+00	2.05535E-07	0.2738
2.1000E+00	2.45027E-07	0.3156
2.2000E+00	3.39610E-07	0.4573
2.3000E+00	7.32551E-07	0.2005
2.4000E+00	8.80078E-07	0.2591
2.5000E+00	1.64610E-05	0.0396
total	1.91483E-05	0.0394

cell 6

energy		
1.6000E+00	0.00000E+00	0.0000
1.7000E+00	1.35555E-12	0.1614
1.8000E+00	5.88728E-08	0.1562
1.9000E+00	2.28148E-07	0.1195
2.0000E+00	2.82931E-07	0.1429
2.1000E+00	2.54819E-07	0.1526
2.2000E+00	4.24537E-07	0.2091
2.3000E+00	5.38689E-07	0.1345
2.4000E+00	5.80131E-07	0.1087
2.5000E+00	1.60252E-05	0.0236
total	1.83934E-05	0.0225

cell 7

energy		
1.6000E+00	0.00000E+00	0.0000
1.7000E+00	2.09388E-12	0.2225
1.8000E+00	6.70966E-08	0.2206
1.9000E+00	1.84697E-07	0.1643
2.0000E+00	2.05961E-07	0.2115
2.1000E+00	3.86885E-07	0.2472
2.2000E+00	3.40650E-07	0.2610
2.3000E+00	6.41918E-07	0.1905
2.4000E+00	6.24680E-07	0.1907
2.5000E+00	1.32686E-05	0.0457
total	1.57205E-05	0.0417

cell 8

energy		
1.6000E+00	0.00000E+00	0.0000
1.7000E+00	1.86758E-12	0.1499
1.8000E+00	7.24271E-08	0.1616
1.9000E+00	1.82728E-07	0.1046
2.0000E+00	2.47724E-07	0.1202
2.1000E+00	2.07763E-07	0.1535
2.2000E+00	3.33951E-07	0.2017
2.3000E+00	5.50226E-07	0.1256
2.4000E+00	6.05770E-07	0.1015
2.5000E+00	1.27420E-05	0.0324
total	1.49426E-05	0.0291

cell 9

energy		
1.6000E+00	0.00000E+00	0.0000
1.7000E+00	3.24052E-12	0.2297
1.8000E+00	7.54379E-08	0.2469
1.9000E+00	2.08430E-07	0.2324
2.0000E+00	2.08327E-07	0.2148
2.1000E+00	3.03063E-07	0.2018
2.2000E+00	2.11187E-07	0.3153
2.3000E+00	7.27272E-07	0.1777

2.4000E+00	6.17600E-07	0.1828
2.5000E+00	1.01219E-05	0.0473
total	1.24732E-05	0.0430

cell 10

energy		
1.6000E+00	0.00000E+00	0.0000
1.7000E+00	1.44669E-12	0.1524
1.8000E+00	6.07937E-08	0.1359
1.9000E+00	1.82559E-07	0.1020
2.0000E+00	2.03655E-07	0.1697
2.1000E+00	2.23606E-07	0.1936
2.2000E+00	3.39511E-07	0.1902
2.3000E+00	4.66269E-07	0.1224
2.4000E+00	5.78470E-07	0.1042
2.5000E+00	9.80250E-06	0.0260
total	1.18574E-05	0.0245

cell 11

energy		
1.6000E+00	0.00000E+00	0.0000
1.7000E+00	2.66546E-12	0.2052
1.8000E+00	5.84547E-08	0.2723
1.9000E+00	1.43710E-07	0.1783
2.0000E+00	2.71468E-07	0.2614
2.1000E+00	2.98276E-07	0.2292
2.2000E+00	3.81729E-07	0.2737
2.3000E+00	6.24605E-07	0.1912
2.4000E+00	7.20057E-07	0.1622
2.5000E+00	8.06277E-06	0.0688
total	1.05611E-05	0.0572

cell 12

energy		
1.6000E+00	0.00000E+00	0.0000
1.7000E+00	1.31572E-12	0.1677
1.8000E+00	6.63954E-08	0.1295
1.9000E+00	1.52926E-07	0.1142
2.0000E+00	2.59984E-07	0.2696
2.1000E+00	1.70225E-07	0.1588
2.2000E+00	3.59322E-07	0.2077
2.3000E+00	3.65323E-07	0.1564
2.4000E+00	5.69688E-07	0.1342
2.5000E+00	8.02274E-06	0.0364
total	9.96661E-06	0.0333

cell 13

energy		
1.6000E+00	0.00000E+00	0.0000
1.7000E+00	1.42658E-12	0.2597
1.8000E+00	3.62279E-08	0.2525
1.9000E+00	1.33599E-07	0.1856
2.0000E+00	1.74573E-07	0.2606
2.1000E+00	2.99532E-07	0.2861
2.2000E+00	4.17762E-07	0.3899
2.3000E+00	4.77496E-07	0.2254
2.4000E+00	4.82619E-07	0.2013
2.5000E+00	6.25023E-06	0.0889
total	8.27204E-06	0.0740

cell 14

energy		
1.6000E+00	0.00000E+00	0.0000
1.7000E+00	1.24474E-12	0.1896
1.8000E+00	5.72596E-08	0.1320
1.9000E+00	1.01314E-07	0.1241
2.0000E+00	1.30239E-07	0.1479
2.1000E+00	1.94227E-07	0.2208
2.2000E+00	2.25813E-07	0.1895
2.3000E+00	3.80784E-07	0.1797
2.4000E+00	3.84210E-07	0.1270

```

2.5000E+00  6.28080E-06  0.0418
total       7.75465E-06  0.0370

```

```

cell 15
energy
1.6000E+00  0.00000E+00  0.0000
1.7000E+00  9.92286E-13  0.4405
1.8000E+00  2.25024E-08  0.3032
1.9000E+00  9.14423E-08  0.2537
2.0000E+00  1.66361E-07  0.2482
2.1000E+00  2.32458E-07  0.4403
2.2000E+00  1.76953E-07  0.2407
2.3000E+00  3.65103E-07  0.3356
2.4000E+00  6.84297E-07  0.3546
2.5000E+00  4.51014E-06  0.0606
total       6.24926E-06  0.0654

```

```

cell 16
energy
1.6000E+00  0.00000E+00  0.0000
1.7000E+00  8.31628E-13  0.1834
1.8000E+00  3.84842E-08  0.1482
1.9000E+00  8.48031E-08  0.1773
2.0000E+00  1.18717E-07  0.2407
2.1000E+00  1.40239E-07  0.2022
2.2000E+00  2.25609E-07  0.2487
2.3000E+00  2.65715E-07  0.1951
2.4000E+00  3.51274E-07  0.1298
2.5000E+00  4.69070E-06  0.0362
total       5.91554E-06  0.0344

```

```

cell union total
energy
1.6000E+00  0.00000E+00  0.0000
1.7000E+00  1.39761E-12  0.0785
1.8000E+00  5.80020E-08  0.0692
1.9000E+00  1.68496E-07  0.0522
2.0000E+00  2.31420E-07  0.0679
2.1000E+00  2.23116E-07  0.0787
2.2000E+00  2.78390E-07  0.0863
2.3000E+00  4.09200E-07  0.0691
2.4000E+00  4.86766E-07  0.0686
2.5000E+00  1.29327E-05  0.0155
total       1.47881E-05  0.0149

```

lanalysis of the results in the tally fluctuation chart bin (tfc) for tally 4 with nps
= 10778451 print table 160

```

tally 14      nps = 10778451
tally type 4  track length estimate of particle flux.
tally for neutrons

```

this tally is modified by cm, em or tm cards.

```

volumes
cell:      1      2      total
3.53429E+01  1.06029E+02  1.41372E+02

```

```

cell 1
energy
1.6000E+00  0.00000E+00  0.0000
1.7000E+00  7.96758E-13  0.3107
1.8000E+00  3.56337E-08  0.2628
1.9000E+00  2.00625E-07  0.1627
2.0000E+00  2.75395E-07  0.2159
2.1000E+00  1.49410E-07  0.4990
2.2000E+00  1.79824E-08  0.7073
2.3000E+00  6.13742E-08  0.5129
2.4000E+00  5.50582E-08  0.5017
2.5000E+00  2.59639E-05  0.0327
total       2.67594E-05  0.0324

```

**Total F4 Tally, in units of millibarns/cm²
Fluence times cross section**

Converting F4 tally from millibarns/cm² to reactions/cm³:

(1.47881E-05 millibarns/cm²) x (10⁻²⁷ cm²/millibarns) x (3.296 x 10²² atoms/cm³, atomic density of lead)

→ 4.8742E-10 n reactions/cm³

```

cell 2
  energy
    1.6000E+00  0.00000E+00  0.0000
    1.7000E+00  1.02775E-12  0.4179
    1.8000E+00  4.11907E-08  0.1704
    1.9000E+00  1.74769E-07  0.0908
    2.0000E+00  3.58269E-07  0.1454
    2.1000E+00  1.79455E-07  0.2825
    2.2000E+00  6.06392E-08  0.6490
    2.3000E+00  2.92439E-08  0.4153
    2.4000E+00  4.98592E-08  0.4553
    2.5000E+00  2.53935E-05  0.0219
    total      2.62870E-05  0.0216

```

```

cell union total
  energy
    1.6000E+00  0.00000E+00  0.0000
    1.7000E+00  9.69999E-13  0.3383
    1.8000E+00  3.98015E-08  0.1448
    1.9000E+00  1.81233E-07  0.0797
    2.0000E+00  3.37551E-07  0.1239
    2.1000E+00  1.71944E-07  0.2472
    2.2000E+00  4.99750E-08  0.5940
    2.3000E+00  3.72764E-08  0.3229
    2.4000E+00  5.11589E-08  0.3591
    2.5000E+00  2.55361E-05  0.0185
    total      2.64051E-05  0.0184

```

“Front Face” F4 Tally

Note: All F4 tallies for layers in thesis have been converted from millibarns/cm² to neutron reactions/cm³

lanalysis of the results in the tally fluctuation chart bin (tfc) for tally 14 with nps
 = 10778451 print table 160

```

tally 24      nps = 10778451
  tally type 4  track length estimate of particle flux.
  tally for  neutrons

  this tally is modified by cm, em or tm cards.

```

```

volumes
  cell:      3      4      total
            3.53429E+01  1.06029E+02  1.41372E+02

```

```

cell 3
  energy
    1.6000E+00  0.00000E+00  0.0000
    1.7000E+00  1.38838E-12  0.2477
    1.8000E+00  7.18772E-08  0.2800
    1.9000E+00  2.15433E-07  0.1402
    2.0000E+00  2.11576E-07  0.2088
    2.1000E+00  3.01385E-07  0.3773
    2.2000E+00  4.17086E-07  0.2941
    2.3000E+00  3.81299E-07  0.2444
    2.4000E+00  6.67059E-07  0.1995
    2.5000E+00  2.03280E-05  0.0297
    total      2.25937E-05  0.0295

```

```

cell 4
  energy
    1.6000E+00  0.00000E+00  0.0000
    1.7000E+00  1.21507E-12  0.1622
    1.8000E+00  7.13489E-08  0.1850
    1.9000E+00  2.32049E-07  0.0894
    2.0000E+00  2.93896E-07  0.1867
    2.1000E+00  2.70886E-07  0.2037
    2.2000E+00  2.32461E-07  0.2013
    2.3000E+00  4.31349E-07  0.1365
    2.4000E+00  4.95623E-07  0.2344
    2.5000E+00  2.00027E-05  0.0177
    total      2.20304E-05  0.0181

```

```

cell union total

```

energy			
1.6000E+00	0.00000E+00	0.0000	
1.7000E+00	1.25840E-12	0.1359	
1.8000E+00	7.14809E-08	0.1688	
1.9000E+00	2.27895E-07	0.0760	
2.0000E+00	2.73316E-07	0.1560	
2.1000E+00	2.78511E-07	0.1965	
2.2000E+00	2.78617E-07	0.1678	
2.3000E+00	4.18837E-07	0.1192	
2.4000E+00	5.38482E-07	0.1736	
2.5000E+00	2.00841E-05	0.0153	
total	2.21712E-05	0.0156	

analysis of the results in the tally fluctuation chart bin (tfc) for tally 24 with nps
= 10778451 print table 160

Layer "A" F4 Tally

tally 34 nps = 10778451
tally type 4 track length estimate of particle flux.
tally for neutrons

this tally is modified by cm, em or tm cards.

volumes	cell:	5	6	total
		3.53429E+01	1.06029E+02	1.41372E+02

cell 5	energy		
1.6000E+00	0.00000E+00	0.0000	
1.7000E+00	1.20560E-12	0.2398	
1.8000E+00	8.85178E-08	0.2279	
1.9000E+00	1.96054E-07	0.1667	
2.0000E+00	2.05535E-07	0.2738	
2.1000E+00	2.45027E-07	0.3156	
2.2000E+00	3.39610E-07	0.4573	
2.3000E+00	7.32551E-07	0.2005	
2.4000E+00	8.80078E-07	0.2591	
2.5000E+00	1.64610E-05	0.0396	
total	1.91483E-05	0.0394	

cell 6	energy		
1.6000E+00	0.00000E+00	0.0000	
1.7000E+00	1.35555E-12	0.1614	
1.8000E+00	5.88728E-08	0.1562	
1.9000E+00	2.28148E-07	0.1195	
2.0000E+00	2.82931E-07	0.1429	
2.1000E+00	2.54819E-07	0.1526	
2.2000E+00	4.24537E-07	0.2091	
2.3000E+00	5.38689E-07	0.1345	
2.4000E+00	5.80131E-07	0.1087	
2.5000E+00	1.60252E-05	0.0236	
total	1.83934E-05	0.0225	

cell union total	energy		
1.6000E+00	0.00000E+00	0.0000	
1.7000E+00	1.31806E-12	0.1367	
1.8000E+00	6.62840E-08	0.1289	
1.9000E+00	2.20124E-07	0.1001	
2.0000E+00	2.63582E-07	0.1268	
2.1000E+00	2.52371E-07	0.1400	
2.2000E+00	4.03305E-07	0.2326	
2.3000E+00	5.87154E-07	0.1117	
2.4000E+00	6.55118E-07	0.1133	
2.5000E+00	1.61342E-05	0.0204	
total	1.85821E-05	0.0199	

Layer "B" F4 Tally

analysis of the results in the tally fluctuation chart bin (tfc) for tally 34 with nps
= 10778451 print table 160

tally 44 nps = 10778451
 tally type 4 track length estimate of particle flux.
 tally for neutrons

 this tally is modified by cm, em or tm cards.

 volumes
 cell: 7 8 total
 3.53429E+01 1.06029E+02 1.41372E+02

cell 7
 energy
 1.6000E+00 0.00000E+00 0.0000
 1.7000E+00 2.09388E-12 0.2225
 1.8000E+00 6.70966E-08 0.2206
 1.9000E+00 1.84697E-07 0.1643
 2.0000E+00 2.05961E-07 0.2115
 2.1000E+00 3.86885E-07 0.2472
 2.2000E+00 3.40650E-07 0.2610
 2.3000E+00 6.41918E-07 0.1905
 2.4000E+00 6.24680E-07 0.1907
 2.5000E+00 1.32686E-05 0.0457
 total 1.57205E-05 0.0417

cell 8
 energy
 1.6000E+00 0.00000E+00 0.0000
 1.7000E+00 1.86758E-12 0.1499
 1.8000E+00 7.24271E-08 0.1616
 1.9000E+00 1.82728E-07 0.1046
 2.0000E+00 2.47724E-07 0.1202
 2.1000E+00 2.07763E-07 0.1535
 2.2000E+00 3.33951E-07 0.2017
 2.3000E+00 5.50226E-07 0.1256
 2.4000E+00 6.05770E-07 0.1015
 2.5000E+00 1.27420E-05 0.0324
 total 1.49426E-05 0.0291

cell union total
 energy
 1.6000E+00 0.00000E+00 0.0000
 1.7000E+00 1.92416E-12 0.1264
 1.8000E+00 7.10945E-08 0.1340
 1.9000E+00 1.83221E-07 0.0885
 2.0000E+00 2.37283E-07 0.1047
 2.1000E+00 2.52544E-07 0.1421
 2.2000E+00 3.35626E-07 0.1661
 2.3000E+00 5.73149E-07 0.1050
 2.4000E+00 6.10498E-07 0.0900
 2.5000E+00 1.28736E-05 0.0273
 total 1.51371E-05 0.0246

Layer "C" F4 Tally

analysis of the results in the tally fluctuation chart bin (tfc) for tally 44 with nps
 = 10778451 print table 160

tally 54 nps = 10778451
 tally type 4 track length estimate of particle flux.
 tally for neutrons

 this tally is modified by cm, em or tm cards.

 volumes
 cell: 9 10 total
 3.53429E+01 1.06029E+02 1.41372E+02

cell 9
 energy
 1.6000E+00 0.00000E+00 0.0000
 1.7000E+00 3.24052E-12 0.2297
 1.8000E+00 7.54379E-08 0.2469
 1.9000E+00 2.08430E-07 0.2324

2.0000E+00	2.08327E-07	0.2148
2.1000E+00	3.03063E-07	0.2018
2.2000E+00	2.11187E-07	0.3153
2.3000E+00	7.27272E-07	0.1777
2.4000E+00	6.17600E-07	0.1828
2.5000E+00	1.01219E-05	0.0473
total	1.24732E-05	0.0430

```
cell 10
energy
1.6000E+00 0.00000E+00 0.0000
1.7000E+00 1.44669E-12 0.1524
1.8000E+00 6.07937E-08 0.1359
1.9000E+00 1.82559E-07 0.1020
2.0000E+00 2.03655E-07 0.1697
2.1000E+00 2.23606E-07 0.1936
2.2000E+00 3.39511E-07 0.1902
2.3000E+00 4.66269E-07 0.1224
2.4000E+00 5.78470E-07 0.1042
2.5000E+00 9.80250E-06 0.0260
total 1.18574E-05 0.0245
```

```
cell union total
energy
1.6000E+00 0.00000E+00 0.0000
1.7000E+00 1.89515E-12 0.1351
1.8000E+00 6.44547E-08 0.1203
1.9000E+00 1.89026E-07 0.0983
2.0000E+00 2.04823E-07 0.1425
2.1000E+00 2.43470E-07 0.1490
2.2000E+00 3.07430E-07 0.1667
2.3000E+00 5.31519E-07 0.1012
2.4000E+00 5.88252E-07 0.0907
2.5000E+00 9.88235E-06 0.0229
total 1.20113E-05 0.0215
```

Layer "D" F4 Tally

lanalysis of the results in the tally fluctuation chart bin (tfc) for tally 54 with nps
= 10778451 print table 160

```
tally 64 nps = 10778451
tally type 4 track length estimate of particle flux.
tally for neutrons
```

this tally is modified by cm, em or tm cards.

```
volumes
cell: 11 12 total
3.53429E+01 1.06029E+02 1.41372E+02
```

```
cell 11
energy
1.6000E+00 0.00000E+00 0.0000
1.7000E+00 2.66546E-12 0.2052
1.8000E+00 5.84547E-08 0.2723
1.9000E+00 1.43710E-07 0.1783
2.0000E+00 2.71468E-07 0.2614
2.1000E+00 2.98276E-07 0.2292
2.2000E+00 3.81729E-07 0.2737
2.3000E+00 6.24605E-07 0.1912
2.4000E+00 7.20057E-07 0.1622
2.5000E+00 8.06277E-06 0.0688
total 1.05611E-05 0.0572
```

```
cell 12
energy
1.6000E+00 0.00000E+00 0.0000
1.7000E+00 1.31572E-12 0.1677
1.8000E+00 6.63954E-08 0.1295
1.9000E+00 1.52926E-07 0.1142
2.0000E+00 2.59984E-07 0.2696
2.1000E+00 1.70225E-07 0.1588
```

2.2000E+00	3.59322E-07	0.2077
2.3000E+00	3.65323E-07	0.1564
2.4000E+00	5.69688E-07	0.1342
2.5000E+00	8.02274E-06	0.0364
total	9.96661E-06	0.0333

cell union total

energy		
1.6000E+00	0.00000E+00	0.0000
1.7000E+00	1.65315E-12	0.1309
1.8000E+00	6.44103E-08	0.1177
1.9000E+00	1.50622E-07	0.0980
2.0000E+00	2.62855E-07	0.2174
2.1000E+00	2.02237E-07	0.1311
2.2000E+00	3.64924E-07	0.1699
2.3000E+00	4.30144E-07	0.1214
2.4000E+00	6.07280E-07	0.1060
2.5000E+00	8.03275E-06	0.0364
total	<u>1.01152E-05</u>	0.0318

Layer "E" F4 Tally

analysis of the results in the tally fluctuation chart bin (tfc) for tally 64 with nps
= 10778451 print table 160

tally 74 nps = 10778451
tally type 4 track length estimate of particle flux.
tally for neutrons

this tally is modified by cm, em or tm cards.

volumes			
cell:	13	14	total
	3.53429E+01	1.06029E+02	1.41372E+02

cell 13

energy		
1.6000E+00	0.00000E+00	0.0000
1.7000E+00	1.42658E-12	0.2597
1.8000E+00	3.62279E-08	0.2525
1.9000E+00	1.33599E-07	0.1856
2.0000E+00	1.74573E-07	0.2606
2.1000E+00	2.99532E-07	0.2861
2.2000E+00	4.17762E-07	0.3899
2.3000E+00	4.77496E-07	0.2254
2.4000E+00	4.82619E-07	0.2013
2.5000E+00	6.25023E-06	0.0889
total	8.27204E-06	0.0740

cell 14

energy		
1.6000E+00	0.00000E+00	0.0000
1.7000E+00	1.24474E-12	0.1896
1.8000E+00	5.72596E-08	0.1320
1.9000E+00	1.01314E-07	0.1241
2.0000E+00	1.30239E-07	0.1479
2.1000E+00	1.94227E-07	0.2208
2.2000E+00	2.25813E-07	0.1895
2.3000E+00	3.80784E-07	0.1797
2.4000E+00	3.84210E-07	0.1270
2.5000E+00	6.28080E-06	0.0418
total	7.75465E-06	0.0370

cell union total

energy		
1.6000E+00	0.00000E+00	0.0000
1.7000E+00	1.29020E-12	0.1563
1.8000E+00	5.20017E-08	0.1211
1.9000E+00	1.09385E-07	0.1032
2.0000E+00	1.41323E-07	0.1309
2.1000E+00	2.20554E-07	0.1752
2.2000E+00	2.73800E-07	0.1894
2.3000E+00	4.04962E-07	0.1436

Layer "F" F4 Tally

```

2.4000E+00  4.08812E-07  0.1074
2.5000E+00  6.27316E-06  0.0388
total       7.88399E-06  0.0339
lanalysis of the results in the tally fluctuation chart bin (tfc) for tally 74 with nps
= 10778451 print table 160

```

```

tally 84      nps = 10778451
tally type 4  track length estimate of particle flux.
tally for neutrons

```

this tally is modified by cm, em or tm cards.

```

volumes
cell:      15      16      total
3.53429E+01  1.06029E+02  1.41372E+02

```

```

cell 15
energy
1.6000E+00  0.00000E+00  0.0000
1.7000E+00  9.92286E-13  0.4405
1.8000E+00  2.25024E-08  0.3032
1.9000E+00  9.14423E-08  0.2537
2.0000E+00  1.66361E-07  0.2482
2.1000E+00  2.32458E-07  0.4403
2.2000E+00  1.76953E-07  0.2407
2.3000E+00  3.65103E-07  0.3356
2.4000E+00  6.84297E-07  0.3546
2.5000E+00  4.51014E-06  0.0606
total       6.24926E-06  0.0654

```

```

cell 16
energy
1.6000E+00  0.00000E+00  0.0000
1.7000E+00  8.31628E-13  0.1834
1.8000E+00  3.84842E-08  0.1482
1.9000E+00  8.48031E-08  0.1773
2.0000E+00  1.18717E-07  0.2407
2.1000E+00  1.40239E-07  0.2022
2.2000E+00  2.25609E-07  0.2487
2.3000E+00  2.65715E-07  0.1951
2.4000E+00  3.51274E-07  0.1298
2.5000E+00  4.69070E-06  0.0362
total       5.91554E-06  0.0344

```

```

cell union total
energy
1.6000E+00  0.00000E+00  0.0000
1.7000E+00  8.71792E-13  0.1821
1.8000E+00  3.44887E-08  0.1335
1.9000E+00  8.64629E-08  0.1468
2.0000E+00  1.30628E-07  0.1823
2.1000E+00  1.63294E-07  0.2038
2.2000E+00  2.13445E-07  0.2035
2.3000E+00  2.90562E-07  0.1704
2.4000E+00  4.34530E-07  0.1603
2.5000E+00  4.64556E-06  0.0313
total       5.99897E-06  0.0308

```

Layer "G" F4 Tally

```

lanalysis of the results in the tally fluctuation chart bin (tfc) for tally 84 with nps
= 10778451 print table 160
*****
*****
dump no.      2 on file runtpe      nps = 10778451      coll =      68340      ctm =
5.00      nrn =      28571199

```

11 warning messages so far.

run terminated when it had used 5 minutes of computer time.

```

computer time =      5.02 minutes

mcnp      version 4c      01/20/00      12/09/02 15:19:25
probid =    12/09/02 15:14:24

```

MCNP Code Listing of Optimized Layer Cake

Table XIX.

Determination of Volumetric Gamma Source Values for Lead Layers

<u>Layers</u>	<u>F4 Tally (xE-10)</u> (n reactions/cm ³)	<u>Normalized to</u> <u>"Front Face"</u>	<u>Percentage</u> <u>Volume</u> (p. 80 above)	<u>Values input</u> <u>into Part 4</u> (p. 92 below)
Front Face	8.70312	1.0	0.125	0.125
Layer "A"	7.30763	0.839656	"	0.104957
Layer "B"	6.12466	0.703731	"	0.087966
Layer "C"	4.98919	0.573264	"	0.071658
Layer "D"	3.95892	0.454886	"	0.056861
Layer "E"	3.33397	0.383078	"	0.047885
Layer "F"	2.59856	0.298578	"	0.037322
Layer "G"	1.97726	0.227190	"	0.028399

Part 4: F8 Counts Tally and F6 Energy Deposited Tally

```

lmcnpr      version 4c      ld=01/20/00      12/09/02 15:45:46
*****
probid =    12/09/02 15:45:46
inp=xg9qa2a outp=xg9qa2ao

1-      Pb-207m photons into scintillator
2-      c      ***** XG9QA2A -- POINT SOURCE -- 5 MIN *****
3-      c      ***** 15 CM OUTER RADIUS; 28.28 LBS LEAD *****
4-      c      ***** 8 LAYERS LEAD; 8 PLASTIC *****

```

```

5-      c          ***** 0.2 CM LEAD LAYERS; 1.1 CM PLASTIC LAYERS *****
6-      c                      ***** NO SHEATH ***
7-      c          **** USING SPENCER & JACOB CROSS SECTIONS FOR PB-207
8-      c          Looking at Energy Deposited (F6) and Interactions (F8)
9-      c          in Plastic Scintillator
10-     1      1 -11.34 1 -2 -18
11-     2      1 -11.34 1 -2 18 -19
12-     3      1 -11.34 3 -4 -18
13-     4      1 -11.34 3 -4 18 -19
14-     5      1 -11.34 5 -6 -18
15-     6      1 -11.34 5 -6 18 -19
16-     7      1 -11.34 7 -8 -18
17-     8      1 -11.34 7 -8 18 -19
18-     9      1 -11.34 9 -10 -18
19-    10      1 -11.34 9 -10 18 -19
20-    11      1 -11.34 11 -12 -18
21-    12      1 -11.34 11 -12 18 -19
22-    13      1 -11.34 13 -14 -18
23-    14      1 -11.34 13 -14 18 -19
24-    15      1 -11.34 15 -16 -18
25-    16      1 -11.34 15 -16 18 -19
26-    17      2 -1.032 2 -3 -18
27-    18      2 -1.032 2 -3 18 -19
28-    19      2 -1.032 4 -5 -18
29-    20      2 -1.032 4 -5 18 -19
30-    21      2 -1.032 6 -7 -18
31-    22      2 -1.032 6 -7 18 -19
32-    23      2 -1.032 8 -9 -18
33-    24      2 -1.032 8 -9 18 -19
34-    25      2 -1.032 10 -11 -18
35-    26      2 -1.032 10 -11 18 -19
36-    27      2 -1.032 12 -13 -18
37-    28      2 -1.032 12 -13 18 -19
38-    29      2 -1.032 14 -15 -18
39-    30      2 -1.032 14 -15 18 -19
40-    31      2 -1.032 16 -17 -18
41-    32      2 -1.032 16 -17 18 -19
42-    33      0 -1:19:17      $ Universe outside detector -- kill zone
43-
44-     c          **** 0.2 cm Lead; 1.1 cm Plastic
45-     1      py 0.0
46-     2      py 0.2
47-     3      py 1.3
48-     4      py 1.5
49-     5      py 2.6
50-     6      py 2.8
51-     7      py 3.9
52-     8      py 4.1
53-     9      py 5.2
54-    10      py 5.4
55-    11      py 6.5
56-    12      py 6.7
57-    13      py 7.8
58-    14      py 8.0
59-    15      py 9.1
60-    16      py 9.3
61-    17      py 10.4
62-    18      cy 7.5
63-    19      cy 15.0
64-
65-     c          **** Volumetric gamma source in the lead ****
66-     c          **** Based on data from monoenergetic (2.5 MeV) neutron ****
67-     c          **** source normal to the face, activating the lead ****
68-     mode p
69-     sdef par=2 erg=d1 axs=0 1 0
70-          rad=d2 pos=frad=d11 ext=frad=d12
71-     sil L 0.5697 1.0636      $ gamma energies
72-     spl d 0.525 0.475      $ weighted branching ratios
73-     c
74-     c          3 - 10 are Front Face thru Lead Layer "G"
75-     c

```

Volumetric Gamma Source Values listed in Table XIX,
p. 90, input into code here

```

76-      si2   s 3 4 5 6 7 8 9 10
77-      c
78-      c      %tage Volume of 3 - 10 times a normalized factor
79-      c      based on cells 1 - 2 (Front Face):
80-      sp2    0.125 0.104957 0.087966 0.071658 0.056861 0.047885 0.037322
81-      0.028399
82-      si3    15.0      $ Radius of 3 (Front Face)
83-      sp3    -21 1
84-      si4    15.0      $ Radius of "A"
85-      sp4    -21 1
86-      si5    15.0      $ Radius of "B"
87-      sp5    -21 1
88-      si6    15.0      $ Radius of "C"
89-      sp6    -21 1
90-      si7    15.0      $ Radius of "D"
91-      sp7    -21 1
92-      si8    15.0      $ Radius of "E"
93-      sp8    -21 1
94-      si9    15.0      $ Radius of "F"
95-      sp9    -21 1
96-      si10   15.0      $ Radius of "G"
97-      sp10   -21 1
98-      c
99-      c      The following are coordinates of the left side of 3 - 10:
100-     ds11   L 0 0 0 0 1.3 0 0 2.6 0 0 3.9 0 0 5.2 0 0 6.5 0
101-           0 7.8 0 0 9.1 0
102-     ds12   s 13 14 15 16 17 18 19 20
103-     si13   0 0.2      $ Width of 3 (Front Face)
104-     si14   0 0.2      $ Width of 4 (Layer "A")
105-     si15   0 0.2      $ Width of 5 (Layer "B")
106-     si16   0 0.2      $ Width of 6 (Layer "C")
107-     si17   0 0.2      $ Width of 7 (Layer "D")
108-     si18   0 0.2      $ Width of 8 (Layer "E")
109-     si19   0 0.2      $ Width of 9 (Layer "F")
110-     si20   0 0.2      $ Width of 10 (Layer "G")
111-     c      Lead G-23
112-     m1      82000 1
113-     c      Plastic
114-     m2      1001 1.1 6000 1
115-     imp:p   1 31r 0
116-     cut:n   10000 0
117-     c      Total F6 Tally
118-     f6:p    17 18 19 20 21 22 23 24 25 26 27 28 29 30
119-           31 32 t
120-     c      Total F8 Tally
121-     f8:p    17 18 19 20 21 22 23 24 25 26 27 28 29 30
122-           31 32 t
123-     e8      0 1e-10 1.1      $ Counts over all Plastic
124-     ctme 3

```

photon activity in each cell
print table 126

	average	tracks	population	collisions	collisions	number	flux
	cell	average			* weight	weighted	weighted
	track weight	entering					
		track mfp			(per history)	energy	energy
	(relative)	(cm)					
	1	1	86816	105941	83725	9.7851E-02	7.5875E-01
01	1.0000E+00	9.1695E-01					7.5875E-
	2	2	237587	288425	221039	2.5833E-01	7.6054E-01
01	1.0000E+00	9.1945E-01					7.6054E-
	3	3	95877	114925	101633	1.1878E-01	7.4335E-01
01	1.0000E+00	8.9475E-01					7.4335E-
	4	4	257884	307214	261397	3.0550E-01	7.4570E-01
01	1.0000E+00	8.9818E-01					7.4570E-
	5	5	92317	110736	98694	1.1535E-01	7.3829E-01
01	1.0000E+00	8.8769E-01					7.3829E-

	6	6	243620	291088	250735	2.9304E-01	7.4225E-01	7.4225E-
01	1.0000E+00	8.9321E-01						
	7	7	83763	100317	89458	1.0455E-01	7.3719E-01	7.3719E-
01	1.0000E+00	8.8599E-01						
	8	8	218047	260133	222727	2.6031E-01	7.4201E-01	7.4201E-
01	1.0000E+00	8.9283E-01						
	9	9	72951	87597	78398	9.1626E-02	7.3729E-01	7.3729E-
01	1.0000E+00	8.8600E-01						
	10	10	188034	224089	191543	2.2386E-01	7.4060E-01	7.4060E-
01	1.0000E+00	8.9091E-01						
	11	11	62027	74062	65089	7.6071E-02	7.3776E-01	7.3776E-
01	1.0000E+00	8.8669E-01						
	12	12	159467	190133	162197	1.8956E-01	7.4174E-01	7.4174E-
01	1.0000E+00	8.9237E-01						
	13	13	50452	60299	52326	6.1155E-02	7.3816E-01	7.3816E-
01	1.0000E+00	8.8751E-01						
	14	14	128509	152558	127977	1.4957E-01	7.4213E-01	7.4213E-
01	1.0000E+00	8.9304E-01						
	15	15	37805	45436	37714	4.4077E-02	7.4470E-01	7.4470E-
01	1.0000E+00	8.9654E-01						
	16	16	94945	114020	92125	1.0767E-01	7.4823E-01	7.4823E-
01	1.0000E+00	9.0167E-01						
	17	17	70261	67061	13820	1.6152E-02	7.1041E-01	7.1041E-
01	1.0000E+00	1.1755E+01						
	18	18	179779	172025	34207	3.9978E-02	7.1684E-01	7.1684E-
01	1.0000E+00	1.1815E+01						
	19	19	73517	70049	13911	1.6258E-02	7.0706E-01	7.0706E-
01	1.0000E+00	1.1729E+01						
	20	20	186244	178062	34950	4.0847E-02	7.1199E-01	7.1199E-
01	1.0000E+00	1.1775E+01						
	21	21	70252	66913	13328	1.5577E-02	7.0415E-01	7.0415E-
01	1.0000E+00	1.1705E+01						
	22	22	174779	167136	31960	3.7352E-02	7.1282E-01	7.1282E-
01	1.0000E+00	1.1780E+01						
	23	23	63483	60507	11733	1.3713E-02	7.0364E-01	7.0364E-
01	1.0000E+00	1.1699E+01						
	24	24	156918	150168	28386	3.3175E-02	7.1106E-01	7.1106E-
01	1.0000E+00	1.1765E+01						
	25	25	55041	52495	9965	1.1646E-02	7.0409E-01	7.0409E-
01	1.0000E+00	1.1704E+01						
	26	26	135568	129960	24308	2.8409E-02	7.1138E-01	7.1138E-
01	1.0000E+00	1.1768E+01						
	27	27	46166	44111	8162	9.5391E-03	7.0591E-01	7.0591E-
01	1.0000E+00	1.1720E+01						
	28	28	112990	108396	19534	2.2830E-02	7.1400E-01	7.1400E-
01	1.0000E+00	1.1789E+01						
	29	29	36620	35065	6297	7.3594E-03	7.0893E-01	7.0893E-
01	1.0000E+00	1.1746E+01						
	30	30	88494	85014	15199	1.7763E-02	7.1481E-01	7.1481E-
01	1.0000E+00	1.1797E+01						
	31	31	25205	25094	4205	4.9145E-03	7.3118E-01	7.3118E-
01	1.0000E+00	1.1938E+01						
	32	32	59724	59459	9445	1.1039E-02	7.3725E-01	7.3725E-
01	1.0000E+00	1.1995E+01						

total 3645142 3998488 2416187 2.8239E+00
tally 6 nps = 855635
tally type 6 track length estimate of heating. units mev/gram
tally for photons

masses						
cell:						
22	23	17	18	19	20	21
		2.00606E+02	6.01819E+02	2.00606E+02	6.01819E+02	2.00606E+02
6.01819E+02	2.00606E+02					
cell:						
29	30	24	25	26	27	28
		6.01819E+02	2.00606E+02	6.01819E+02	2.00606E+02	6.01819E+02
2.00606E+02	6.01819E+02					
cell:						
		31	32	total		
		2.00606E+02	6.01819E+02	6.41940E+03		

cell 17	1.95157E-05	0.0052
cell 18	1.65483E-05	0.0031
cell 19	1.97346E-05	0.0050
cell 20	1.66342E-05	0.0030
cell 21	1.83763E-05	0.0051
cell 22	1.52682E-05	0.0031
cell 23	1.63470E-05	0.0053
cell 24	1.34634E-05	0.0032
cell 25	1.39843E-05	0.0057
cell 26	1.14290E-05	0.0035
cell 27	1.15854E-05	0.0062
cell 28	9.46601E-06	0.0039
cell 29	9.08965E-06	0.0070
cell 30	7.29713E-06	0.0044
cell 31	5.99111E-06	0.0080
cell 32	4.74579E-06	0.0051

Total Energy Deposited
1.24744E-05 MeV/gram) x (6,419.40 grams)
= 0.080078 MeV

Efficiency = 0.080078 MeV/0.8 MeV = 0.1001
→ 10.01%

(Note: 0.8 MeV is weighted average of both gammas)

cell union total **1.24744E-05** 0.0013
 lanalysis of the results in the tally fluctuation chart bin (tfc) for tally 6 with nps
 = 855635 print table 160

Total MeV/gram

tally 8 nps = 855635
 tally type 8 pulse height distribution. units number
 tally for photons

cell 17		
energy		
0.0000E+00	0.00000E+00	0.0000
1.0000E-10	6.48805E-02	0.0041
1.1000E+00	1.30441E-02	0.0094
total	7.79246E-02	0.0037
cell 18		
energy		
0.0000E+00	0.00000E+00	0.0000
1.0000E-10	1.67485E-01	0.0024
1.1000E+00	3.23760E-02	0.0059

total	1.99861E-01	0.0022
cell 19		
energy		
0.0000E+00	0.00000E+00	0.0000
1.0000E-10	6.82370E-02	0.0040
1.1000E+00	1.31154E-02	0.0094
total	8.13524E-02	0.0036
cell 20		
energy		
0.0000E+00	0.00000E+00	0.0000
1.0000E-10	1.73800E-01	0.0024
1.1000E+00	3.30375E-02	0.0058
total	2.06837E-01	0.0021
cell 21		
energy		
0.0000E+00	0.00000E+00	0.0000
1.0000E-10	6.51317E-02	0.0041
1.1000E+00	1.26479E-02	0.0096
total	7.77797E-02	0.0037
cell 22		
energy		
0.0000E+00	0.00000E+00	0.0000
1.0000E-10	1.63919E-01	0.0024
1.1000E+00	3.03295E-02	0.0061
total	1.94249E-01	0.0022
cell 23		
energy		
0.0000E+00	0.00000E+00	0.0000
1.0000E-10	5.92402E-02	0.0043
1.1000E+00	1.10643E-02	0.0102
total	7.03045E-02	0.0039
cell 24		
energy		
0.0000E+00	0.00000E+00	0.0000
1.0000E-10	1.47552E-01	0.0026
1.1000E+00	2.69063E-02	0.0065
total	1.74459E-01	0.0024
cell 25		
energy		
0.0000E+00	0.00000E+00	0.0000
1.0000E-10	5.15792E-02	0.0046
1.1000E+00	9.45146E-03	0.0111
total	6.10307E-02	0.0042
cell 26		
energy		
0.0000E+00	0.00000E+00	0.0000
1.0000E-10	1.28000E-01	0.0028
1.1000E+00	2.30297E-02	0.0070
total	1.51029E-01	0.0026
cell 27		
energy		
0.0000E+00	0.00000E+00	0.0000
1.0000E-10	4.35443E-02	0.0051
1.1000E+00	7.73344E-03	0.0122
total	5.12777E-02	0.0047
cell 28		
energy		
0.0000E+00	0.00000E+00	0.0000
1.0000E-10	1.07416E-01	0.0031
1.1000E+00	1.85488E-02	0.0079
total	1.25965E-01	0.0028

```

cell 29
  energy
    0.0000E+00  0.00000E+00  0.0000
    1.0000E-10  3.47824E-02  0.0057
    1.1000E+00  5.99087E-03  0.0139
    total      4.07732E-02  0.0052

```

```

cell 30
  energy
    0.0000E+00  0.00000E+00  0.0000
    1.0000E-10  8.43596E-02  0.0036
    1.1000E+00  1.44583E-02  0.0089
    total      9.88178E-02  0.0033

```

```

cell 31
  energy
    0.0000E+00  0.00000E+00  0.0000
    1.0000E-10  2.51544E-02  0.0067
    1.1000E+00  4.04729E-03  0.0170
    total      2.92017E-02  0.0062

```

```

cell 32
  energy
    0.0000E+00  0.00000E+00  0.0000
    1.0000E-10  6.01051E-02  0.0043
    1.1000E+00  9.12071E-03  0.0113
    total      6.92258E-02  0.0040

```

```

cell union total
  energy
    0.0000E+00  0.00000E+00  0.0000
    1.0000E-10  5.02872E-01  0.0011
    1.1000E+00  2.39599E-01  0.0019
    total      7.42471E-01  0.0006

```

F8 Tally = 0.742471 – 0.502872
= 0.239599 ← Counts in Scintillator

```

lanalysis of the results in the tally fluctuation chart bin (tfc) for tally 8 with nps
= 855635 print table 160
*****
*****
*****
dump no. 2 on file runtpe nps = 855635 coll = 2416187 ctm =
3.02 nrn = 33356088

```

2 warning messages so far.

run terminated when it had used 3 minutes of computer time.

computer time = 3.06 minutes

```

mcnp version 4c 01/20/00 12/09/02 15:48:50
probid = 12/09/02 15:45:46

```

Figure of Merit Calculation for Optimized Layer Cake

FOM = F4 Tally (n reactions/cm³) x F8 Tally (Counts) x Volume of Lead (cm³)

FOM = (4.8742E-10 reactions/cm³) x (0.239599 counts) x (1,130.97cm³)

= 13.21E-08 Reactions x Counts

See Table IV, p. 26.

Appendix B

DD Neutron Attenuation in 0.2 cm and 0.3 cm Cases

In an effort to see the effects of DD neutron attenuation due to different widths of scintillator (1.1 cm and 1.25 cm), F4 tallies in lead layers with scintillator removed were compared with F4 tallies in lead layers with scintillator present in each case (0.2 cm and 0.3 cm).

Table XX.

0.2 cm Lead Case: F4 Tallies with Scintillator Removed Compared with F4 Tallies with Scintillator Present

<u>F4 Tallies (x E-10)*</u> (n reactions/cm ³)	<u>0.2 cm with 1.1 cm Scintillator</u>	<u>0.2 cm without Scintillator</u>
Total F4 Tally	4.8742	8.0752 (>66%)
Front Face	8.7031	9.0436 (>3.9%)
Layer “A”	7.3076	8.8126 (>20.6%)
Layer “B”	6.1247	8.5596 (>39.8%)
Layer “C”	4.9892	8.2041 (>64.4%)
Layer “D”	3.9589	7.9988 (>102%)
Layer “E”	3.3340	7.8953 (>137%)
Layer “F”	2.5986	7.2788 (>180%)
Layer “G”	1.9773	6.8086 (>244%)

*Neutrons are DD (2.45 MeV).

As can be seen, the F4 tallies with scintillator removed grow increasingly larger toward the back layers of the detector. The last layer, “G”, has an F4 tally (without

scintillator) which is over 244% greater than its F4 tally with scintillator. These increasingly higher values of F4 tallies in the back layers contribute to the total F4 tally which is over 66% greater (without scintillator) than the total F4 tally with scintillator. The 0.3 cm case is presented in Table XXI below.

Table XXI.

0.3 cm Lead Case: F4 Tallies with Scintillator Removed Compared with F4 Tallies with Scintillator Present

<u>F4 Tallies (x E-10)* (n reactions/cm³)</u>	<u>0.3 cm with 1.25 cm Scintillator</u>	<u>0.3 cm without Scintillator</u>
Total F4 Tally	4.5264	7.9474 (>75.6%)
Front Face	8.9355	9.3726 (>4.9%)
Layer “A”	7.2273	9.0134 (>24.7%)
Layer “B”	5.7639	8.6278 (>49.7%)
Layer “C”	4.5231	8.2342 (>82%)
Layer “D”	3.4297	7.7981 (>127%)
Layer “E”	2.7769	7.4320 (>167%)
Layer “F”	2.0643	6.8441 (>231%)
Layer “G”	1.4907	6.2574 (>319%)

*Neutrons are DD (2.45 MeV).

In examining the 0.3 cm lead layer case, its thicker, 1.25 cm layers of scintillator attenuate even more neutrons throughout the detector. Its back layer, “G”, has an F4 tally (without scintillator) which is over 319% greater than its F4 tally with scintillator. The

greater attenuation throughout all the layers produce a total F4 tally (without scintillator) which is over 75% greater than the total F4 tally with scintillator. Since the detector cannot function without scintillator, this data indicates that thinner layers of scintillator attenuate fewer neutrons. To see if lead has any part to play in DD neutron attenuation, Table XXII below compares the 0.2 cm case without scintillator with the 0.3 cm case without scintillator, and displays the F4 tallies of each.

Table XXII.

0.2 cm Lead Case without Scintillator Compared with 0.3 cm Lead Case without Scintillator

<u>Lead Layers*</u>	<u>0.2 cm w/o Scintillator</u> (n reactions/layer) x 10 ⁻⁸	<u>0.3 cm w/o Scintillator</u> (n reactions/layer) x 10 ⁻⁸
Front Face	12.79 (100%)	19.88 (100%)
Layer "A"	12.45 (97%)	19.11 (96%)
Layer "B"	12.10 (95%)	18.30 (92%)
Layer "C"	11.60 (91%)	17.46 (88%)
Layer "D"	11.31 (88%)	16.54 (83%)
Layer "E"	11.16 (87%)	15.76 (79%)
Layer "F"	10.29 (80%)	14.51 (73%)
Layer "G"	9.62 (75%)	13.27 (67%)

*Note: Neutrons are DD (2.45 MeV).

As was seen in Tables V & X, the 0.3 cm case has more reactions/layer, (it has thicker layers of lead, and hence more volume per layer.) But in looking at the values in parenthesis (which are normalized to the front face value in each case), despite being higher, the neutron reactions/layer for the 0.3 cm case fall off slightly faster from the

front face to the last layer (“G”). Thus, indeed, thicker layers of lead do attenuate neutrons, although not to the degree that thicker layers of scintillator do. Overall, most of the attenuation is due to the thickness of the plastic scintillator, and a small part of it is due to the thickness of the lead. However, to maximize the Figure of Merit, the adage, “thinner is better” holds true here. The thinner the layers of lead are, the thinner the corresponding layers of scintillator will be. This will provide the least amount of neutron attenuation. Also, thinner layers of lead lead to less self attenuation so that the gammas born in the lead from neutron activation can exit the lead and enter the scintillator where they may be counted.

Appendix C

Layer Cake Prototype Sensitivity Data

Table XXIII.

Layer Cake Prototype Sensitivity (in Counts/Incident Neutron) as a Function of
Photomultiplier Tube Bias And Discriminator Setting

	-50 mV	-150 mV	-275 mV	-400 mV
-2000V	3.20E-04*			
-2100V	3.19E-04*	5.60E-05*	1.03E-05*	
-2200V	3.36E-04*			
-2300V	3.63E-04*	9.17E-05*	3.08E-05*	1.45E-05*
-2400V	3.77E-04*			
-2500V	4.62E-04*	2.05E-05*	1.11E-04*	5.03E-05*

*Units of Sensitivity in Counts/incident neutron

Table XXIV.

Layer Cake Prototype Sensitivity (in Incident Neutrons/Count) as a Function of
Photomultiplier Tube Bias And Discriminator Setting

	-50mV	-150mV	-275mV	-400mV
-2000V	3125*			
-2100V	3135*	17,857*	97,087*	
-2200V	2976*			
-2300V	2755*	10,905*	32,468*	68,966*
-2400V	2653*			
-2500V	2165*	4878*	9009*	19,881*

* Units of Sensitivity in Incident Neutrons/Count

Appendix D

Hamamatsu Photomultiplier Tube R1250 Data

HAMAMATSU

PHOTOMULTIPLIER TUBE R1250

**For High Energy Physics, Fast Time Response, High Pulse Linearity
127mm (5 Inch) Diameter, Bialkali Photocathode, 14-Stage, Head-on Type**

GENERAL

Parameter	Description/Value	Unit
Spectral Response	300 to 650	nm
Wavelength of Maximum Response	420	nm
Photocathode	Bialkali	—
Minimum Useful Diameter	120	mm dia.
Window	Borosilicate glass	—
Dynode	Linear focused	—
Number of Stages	14	—
Base	20-pin base	—
Suitable Socket	E678-20A (supplied)	—

MAXIMUM RATINGS (Absolute Maximum Values)

Parameter	Value	Unit
Supply Voltage	Between Anode and Cathode	3000
	Between Anode and Last Dynode	500
Average Anode Current	0.2	mA
Ambient Temperature	-30 to +50	°C

CHARACTERISTICS (at 25°C)

Parameter	Min.	Typ.	Max.	Unit
Cathode Sensitivity	Luminous (2856K)	55	70	—
	Blue (with CS 5-58 filter)	7.0	9.0	—
	Quantum Efficiency at 390nm	—	22	—
Anode Sensitivity	Luminous (2856K)	300	1000	—
	Blue (with CS 5-58 filter)	—	130	—
Gain	—	1.4×10^7	—	—
Anode Dark Current (after 30min. storage in darkness)	—	50	300	nA
Time Response	Anode Pulse Rise Time	—	2.5	—
	Electron Transit Time	—	54	—
	Transit Time Spread	—	1.2	—
Pulse Height Resolution with ¹³⁷ Cs	—	8.3	—	—
Gain Deviation	Long Term	—	1.0	—
	Short Term	—	1.0	—
Pulse Linearity *	2% Deviation	—	160	—
	5% Deviation	—	250	—

* Measured with special voltage distribution ratios shown in the Table 2.

Table 1: VOLTAGE DISTRIBUTION RATIO AND SUPPLY VOLTAGE

Electrode	K	G1	G2	Dy1	Dy2	Dy3	Dy4	Dy5	Dy6	Dy7	Dy8	Dy9	Dy10	Dy11	Dy12	Dy13	Dy14	P
Ratio	2.5	7.5	0	1.2	1.8	1	1	1	1	1	1	1	1	1.5	1.5	3	2.5	

Supply Voltage: 2000Vdc, K: Cathode, Dy: Dynode, P: Anode, G: Grid

**Table 2: SPECIAL VOLTAGE DISTRIBUTION RATIO AND SUPPLY VOLTAGE
FOR PULSE LINEARITY MEASUREMENT**

Electrode	K	G1	G2	Dy1	Dy2	Dy3	Dy4	Dy5	Dy6	Dy7	Dy8	Dy9	Dy10	Dy11	Dy12	Dy13	Dy14	P
Ratio	2.5	7.5	0	1.2	1.8	1	1	1	1	1.2	1.5	2	2.8	4	5.7	8	5	
Capacitors in μ F											0.01	0.01	0.02	0.02	0.02	0.04	0.06	

Supply Voltage: 2500Vdc, K: Cathode, Dy: Dynode, P: Anode, G: Grid

Subject to local technical requirements and regulations, availability of products included in this promotional material may vary. Please consult with our sales office.
Information furnished by HAMAMATSU is believed to be reliable. However, no responsibility is assumed for possible inaccuracies or omissions. Specifications are
subject to change without notice. No patent rights are granted to any of the circuits described herein. © 1999 Hamamatsu Photonics K.K.

PHOTOMULTIPLIER TUBE R1250

Figure 1: Typical Spectral Response

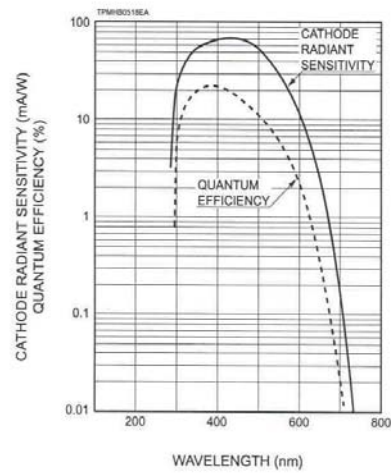


Figure 2: Typical Gain Characteristics

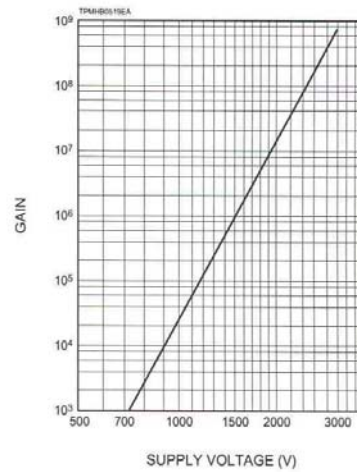
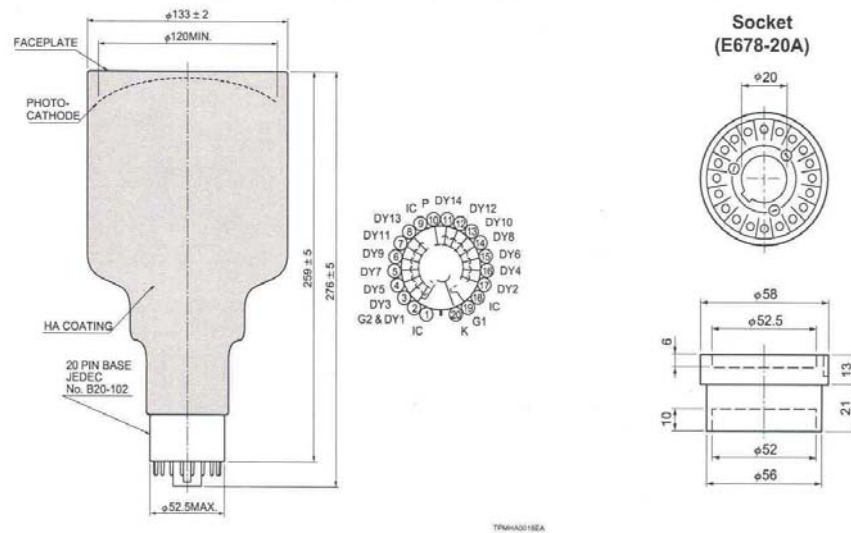


Figure 3: Dimensional Outline and Basing Diagram (Unit: mm)



HAMAMATSU

HOME PAGE URL <http://www.hamamatsu.com>

HAMAMATSU PHOTONICS K.K., Electron Tube Center

314-5, Shimokanzo, Toyooka-village, Iwata-gun, Shizuoka-ken, 438-0193, Japan, Telephone: (81)539/62-5248, Fax: (81)539/62-2205

U.S.A.: Hamamatsu Corporation, 360 Foothill Road, P. O. Box 6910, Bridgewater, N.J. 08807-0910, U.S.A., Telephone: (1)908-231-0960, Fax: (1)908-231-1218

Germany: Hamamatsu Photonics Deutschland GmbH, Arzbergerstr. 10, D-82211 Herrsching am Ammersee, Germany, Telephone: (49)8152-375-0, Fax: (49)8152-2658

France: Hamamatsu Photonics France S.A.R.L., 8, Rue du Saule Trapu, Parc du Moulin de Massy, 91862 Massy Cedex, France, Telephone: (33)1 69 53 71 00, Fax: (33)1 69 53 71 10

United Kingdom: Hamamatsu Photonics UK Limited, Lough Point, 2 Gladbeck Way, Windmill Hill, Enfield, Middlesex EN2 7JA, United Kingdom, Telephone: 44(20)8-367-3560, Fax: 44(20)8-367-6384

North Europe: Hamamatsu Photonics Norden AB, Smidesvägen 12, SE-171-41 SOLNA, Sweden, Telephone: (46)8-509-031-00, Fax: (46)8-509-031-01

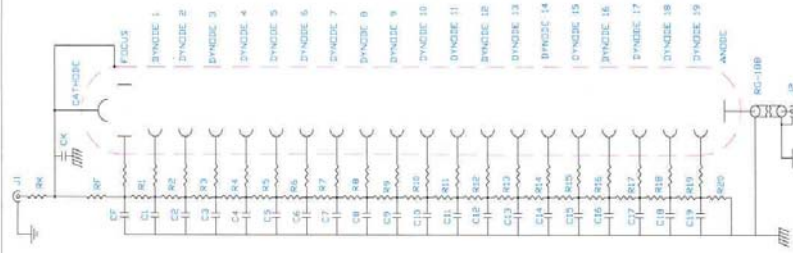
Photomultiplier Tube Information

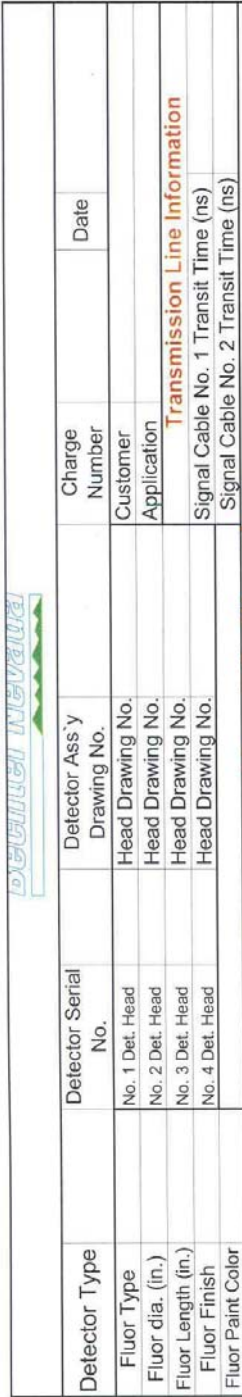
[illegible]

REMARKS:

Technician:

Date _____



[illegible]

Remarks:	
----------	--

	Radiation Calibration by	Date	Detector Technician	Date
	Signature Authorization	Date		

Appendix E

BC-400 Scintillator Data

BC-400,BC-404,BC-408,BC-412,BC-416 Premium Plastic Scintillators

The premium plastic scintillators described in this data sheet include those with the highest light output, as well as the most economical (BC-416). The chart below will direct you to the scintillator suitable for your energy application.

	BC-400	BC-404	BC-408	BC-412	BC-416
Radiation Detected					
<100keV X-rays			X		
100keV to 5MeV gamma rays				X	
>5MeV gamma rays	X				X
Fast neutrons				X	X
Alphas, betas		X	X		
Charged particles, cosmic rays, muons, protons, etc.			X	X	X
Principal Uses/Applications	general purpose	fast counting	TOF large area	large area	large area economy

	BC-400	BC-404	BC-408	BC-412	BC-416
Scintillation Properties –					
Light Output, %Anthracene	65	68	64	60	38
Rise Time, ns	0.9	0.7	0.9	1.0	–
Decay Time (ns)	2.4	1.8	2.1	3.3	4.0
Pulse Width, FWHM, ns	2.7	2.2	~2.5	4.2	5.3
Wavelength of Max. Emission, nm	423	408	425	434	434
Light Attenuation Length, cm*	160	140	210	210	210
Bulk Light Attenuation Length, cm	250	160	380	400	400

	BC-400	BC-404	BC-408	BC-412	BC-416
Atomic Composition –					
No. H Atoms per cc (x10 ²²)	5.23	5.21	5.23	5.23	5.25
No. C Atoms per cc (x10 ²²)	4.74	4.74	4.74	4.74	4.73
Ratio H:C Atoms	1.103	1.100	1.104	1.104	1.110
No. of Electrons per cc (x10 ²¹)	3.37	3.37	3.37	3.37	3.37

*The typical 1/e attenuation length of a 1x20x200cm cast sheet with edges polished as measured with a bialkali photomultiplier tube coupled to one end.

BICRON®

General Technical Data –

Base	Polyvinyltoluene
Density (g/cc)	1.032 g/cc
Refractive Index	1.58
Expansion Coefficient (per°C, <67°C):	7.8X10 ⁻⁵
Softening Point	70°C
Vapor Pressure	May be used in vacuum
Solubility	Soluble in aromatic solvents, chlorinated solvents, acetone, etc. Unaffected by water, dilute acids, lower alcohols, alkalis and pure silicone fluids or grease.
Light Output	At +60°C = 95% of that at +20°C. Independent of temperature from -60°C to +20°C


SAINT-GOBAIN
CRYSTALS & DETECTORS

Scintillation Products
Organic Products



USA

Saint-Gobain Crystals & Detectors
12345 Kinsman Road
Newbury, OH 44065
Tel: (440) 564-2251
Fax: (440) 564-8047

Europe

Saint-Gobain Cristaux & Detecteurs
P.O. Box 3093, 3760 DB Soest
The Netherlands
Tel: 31 (0) 35 60 29 700
Fax: 31 (0) 35 60 29 214

Japan

Saint-Gobain Crystals & Detectors KK
3-7, Kojimachi, Chiyoda-ku,
Tokyo 102-0083 Japan
Tel: 81 (0) 3 3263 0559
Fax: 81 (0) 3 5212 2196

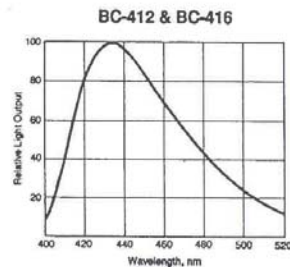
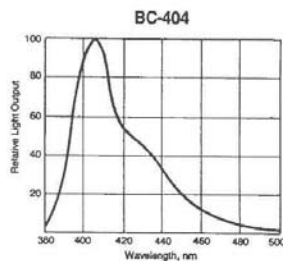
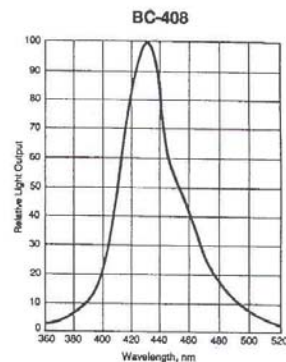
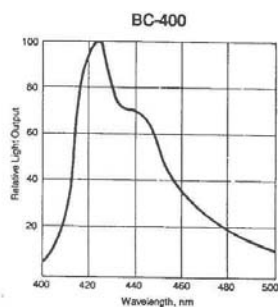
China

Saint-Gobain China Investment Co., Ltd.
24-05 CITIC Building
19 Jianguomenwai Ave.
Beijing 100004 China
Tel: 86 (0) 10 6513 0311
Fax: 86 (0) 10 6512 9843

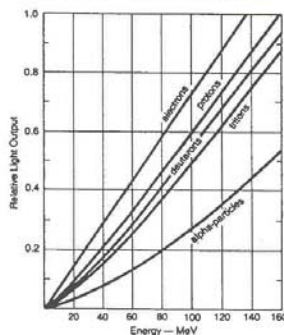
www.detectors.saint-gobain.com

BC-400,BC-404,BC-408,BC-412,BC-416 Premium Plastic Scintillators

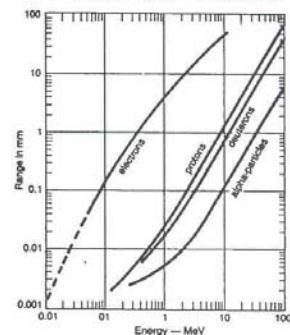
Emission Spectra



Premium Plastic Scintillators Response to Atomic Particles



Range of Atomic Particles in Premium Plastic Scintillators



Manufacturer reserves the right to alter specifications.
©2002 Saint-Gobain Ceramics & Plastics, Inc. All rights reserved.

(06-02)

General Description –

The scintillation emission of a typical plastic scintillator has a maximum around 425 nm. Plastic scintillators are characterized by a relatively large light output — typically 25-30% of NaI(Tl) — and a short decay time of around 2 ns. This makes the material suited for fast timing measurements.

All plastic scintillators are sensitive to X-rays, gamma rays, fast neutrons and charged particles.

Special formulations are available for thermal neutron detection or with improved X-ray efficiency. Plastic scintillators are the most popular scintillation material for use in calorimeters, time of flight detectors, nuclear gauging and large area contamination monitors.

The exact emission wavelength and decay time depend on the type of organic activator and on the host material. A large number of different plastic scintillators are available, each for a specific application. General characteristics of plastic scintillators are presented in another section of this brochure.

Availability –

Our plastic scintillators are produced in a wide variety of shapes and sizes. Cast sheet is the most commonly used form.

You can also obtain precision thin sheets, thin film, rods, annuli, ingots and large rectangular blocks, filaments, powders and beads.

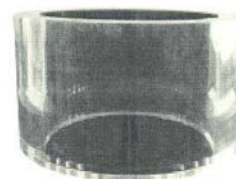
We supply most solid scintillators with their surfaces prepared to optimize light collection. For cast sheets, the cast surfaces are untouched, and the edges are machined and polished or diamond milled.

Rods, annuli and blocks are machined and polished, or coated with a diffuse reflector paint such as BC-620. Such a reflector is used only when there are few reflections of the scintillation light off the scintillator surfaces before the light reaches the PMT. Most applications require finished surfaces.

You can also obtain scintillators as finished detector assemblies. These incorporate light guides, photomultiplier tubes, special radiation entrance windows, and light tight wrappings (or metal housings). Monoline or Multiline assemblies can be made as well.

Plastic Scintillators

A plastic scintillator consists of a solid solution of organic scintillating molecules in a polymerized solvent. The ease with which they can be shaped and fabricated makes plastic scintillators an extremely useful form of organic scintillator.



Plastic Scintillator Applications Guide

Scintillator	Distinguishing Feature	Principal Applications
BC-400	NE-102 equiv.	general purpose
BC-404	1.8 ns time constant	fast counting
BC-408	best general purpose	TOF counters; large area
BC-412	longest attenuation length (NE-110 equiv.)	general purpose; large area; long strips
BC-414		use with BC-484 wavelength shifter
BC-416	lowest cost	"economy" scintillator; large volume
BC-418	1.4 ns time constant	ultra-fast timing; small sizes
BC-420	1.5 ns time constant, low self-absorption	ultra-fast timing; for sheet areas > 100mm ²
BC-422	1.4 ns time constant	very fast timing; small sizes
BC-422Q	quenched; 0.7 ns time constant	ultra-fast timing, ultra-fast counting
BC-428	green emitter	for photodiodes and CCDs; phoswich detectors
BC-430	red emitter	for silicon photodiodes and red-enhanced PMTs
BC-436	deuterated	fast neutron
BC-440	high temperature up to 100°C	general purpose
BC-440M	high temperature up to 100°C	general purpose
BC-444	slow plastic, 285 ns time constant	phoswich detectors for dE/dx studies
BC-444G	285 ns time constant; green emitter	phoswich detectors for dE/dx studies
BC-452	lead loaded (5%)	x-ray dosimetry (<100 keV); Mossbauer spectroscopy
BC-454	boron loaded (5%)	neutron spectrometry; thermal neutrons
BC-470	air equivalent	dosimetry
BC-490	casting resin scintillator	general purpose
BC-498	applied like paint	beta, gamma detection
BC-480	UV to blue waveshifter	Cerenkov detector
BC-482A	green emitter	waveshifter

Distribution

- 2 Bechtel/Nevada
Attn: Lee Ziegler (1)
Attn: Chris Hagen (1)
2621 Loosee Road
Las Vegas, NV 89030
- 1 University of New Mexico
Department of Chemical & Nuclear Engineering
Attn: Gary W. Cooper
209 Farris Engineering Center
Albuquerque, NM 87131
- 1 Texas A&M University
Attn: Bruce Freeman
Department of Nuclear Engineering
3133 TAMU
College Station, TX 77843-3133
- 1 MS 0665 E. J. T. Burns, 2541
- 1 MS 1186 T. A. Mehlhorn, 1674
- 1 MS 1191 K. M. Matzen, 1670
- 1 MS 1196 R. J. Leeper, 1677
- 1 MS 1196 G. A. Chandler, 1677
- 2 MS 1196 C. L. Ruiz, 1677
- 2 MS 1196 G. W. Cooper, 1677
- 1 MS 1196 J. K. Franklin, 1677
- 15 MS 1196 A. J. Nelson, 1677
- 1 MS 9018 Central Technical Files, 8945-1
- 2 MS 0899 Technical Library, 9616